ON THE ROLE OF PHOSPHATIDYLINOSITOL TRANSFER PROTEIN ALPHA IN THE NUCLEAR IMPORT OF PHOSPHATIDYLINOSITOL

Emily Kate Tribble

A dissertation submitted to the faculty of the University of North Carolina at Chapel Hill in partial fulfillment of the requirements for the degree of *Doctor of Philosophy* in the School of Medicine (Molecular, Cell, and Developmental Biology).

Chapel Hill
2011

Approved by:

Vytas A Bankaitis, PhD. (Chairperson)

Patrick J Brennwald, PhD.

Bob Duronio, PhD.

Mohanish P Deshmukh, PhD

Edward D Salmon, PhD

ABSTRACT

Emily Kate Tribble: On the role of phosphatidylinositol transfer protein alpha in the nuclear import of phosphatidylinositol

Lipid metabolism within the nuclear matrix of mammalian cells is robust. Numerous lipid-signaling pathway components are found within purified nuclear fractions, depleted of nuclear envelope and cellular debris using detergents ("endonuclear" fractions). Interestingly, membrane-stripped nuclei also contain measurable quantities of the substrate lipids, notably phospholipids (PLs), despite the absence of detectable bilayer structures. According to published work, these PLs are i) major constituents of the endonuclear space (10-16% by volume), ii) distinct from cytosolic/cellular lipids in molecular species profiles and relative abundance, and iii) generated or consumed in response to physiological cues. The abundance and diversity of PL molecular species in nuclei suggests endonuclear lipids not only signal within the nuclear space, but also impact nuclear structure and function on the whole. That the elements of functional endonuclear phosphoinositide signaling pathways (enzymes and PLs) are found within nuclei has received much attention, as their cytosolic counterparts regulate numerous cellular events. While new evidence suggests that nuclear-generated phosphoinositides participate as cofactors in essential nuclear processes, there are still unanswered questions regarding the regulation, location, and organization of endonuclear phosphoinositides.

Phosphatidylinositol, the PL from which all phosphoinositides are generated, enters the nuclear space via an unknown mechanism. This dissertation originated in testing a candidate

importer protein, the phosphatidylinositol transfer protein alpha, in the nuclear supply of Phosphatidylinositol. Such experiments require envelope-stripped nuclei that meet high purity standards. Initial attempts at purifying nuclei via published protocols were unsuccessful, and a new method for purifying nuclei from mouse embryonic fibroblasts for use in this context is described. Nuclei purified according to the new protocol meet an expanded, quantitative quality control suite. These highly purified nuclei contain several orders of magnitude less PL than previously reported in LC/MS/MS mass analyses. In addition, pulse-labeling and comparative dynamic lipidomic studies of mouse embryonic fibroblast nuclei, either wild type or genetically knocked-out for Phosphatidylinositol transfer protein alpha, purified with this new protocol demonstrated that our candidate shuttle protein was not an obligate requirement in the import of Phosphatidylinositol. Overall, this dissertation demonstrates that proper execution of nuclear preparations is an essential component of studies of endonuclear lipid regulation.

To Mom, Dad, Seth, Ginny, and Auntie Mel: Thanks for putting up with me. You shouldn't have.

To Sasa: Well, we should thank each other. I love you and couldn't have done this without you.

TABLE OF CONTENTS

LIST OF FIGURES

CHAPTER 2

CHAPTER 3

CHAPTER 4

LIST OF TABLES

CHAPTER 3

CHAPTER 3

CHAPTER 1

INTRODUCTION – KEY CONCEPTS OF ENDONUCLEAR LIPID SIGNALING

1.1 Summary

Over 20 years of study has confirmed that the mammalian cell nucleus is an intended site of glycerophospholipid (GPL) metabolism and signaling. Radiolabeling studies repeatedly confirm that numerous phospholipid metabolic enzymes and their metabolites can be found within the confines of but excluding the nuclear envelope. This subcellular region is termed the "endonuclear" compartment. Multiple phospholipid radiolabeling studies performed on highly purified membrane-stripped nuclei demonstrate that the endonuclear compartment is an intended site of nuclear lipid signaling and metabolism. Although the exact physicochemical structure of these signaling and metabolic sites remains unclear, several recent studies have begun to demystify the biology of lipids in the nucleus by discovering that phosphoinositides (PIPs) serve as cofactors in essential nuclear processes. As our understanding of nuclear lipid signaling broadens, it is important that it fit within the context of an expanding view of nuclear architecture and organelle function. Currently, there are some findings regarding endonuclear lipid metabolism and signaling which do not fit with perceptions of nuclear function and organization. This chapter covers what is known about endonuclear lipid signaling, methods for its study, and the physical properties of lipids in the nucleus. In addition, this chapter discusses the methodological limitations that hinder

progress in the endonuclear lipid signaling field and where attentions are best addressed. These discussions serve as a basis and lead to our thesis regarding the physical properties of GPLs in the nucleus and their import into the endonuclear compartment.

1.2 Introduction

1.2.1 The Discovery of Chromatin Associated Lipids and Development of Tools for their Study

The discovery of DNA and its identification as the genetic material spurned great interest in the field of molecular biology and procedures for isolation of Chromatin. Several reports claimed that their most purified chromatin fractions, isolated from rat liver nuclei radiolabeled with [γ-^{32}P] phosphate, contained small quantities of substances that were neither DNA nor protein elements [1-3]. These mystery substances included lipids, leading to the speculation that this lipid pool somehow plays a role in the structure of chromatin and DNA. Among the lipids identified were phospholipids (e.g., Phosphatidylinositol (PtdIns), Phosphatidylcholine (PtdCho), Phosphatidylethanolamine (PtdSer), etc.), Cholesterol, and Sphingomyelin [4-7]. *In vitro* biochemical studies demonstrated the effects of the different lipid types on the behavior and organization of chromatin [8]. The results found that when concentrations of all phospholipid types were less than 10 µM, they raised the melting temperature of DNA and increased the stability of Histone H1 deposition on chromatin. On the other hand, concentrations of phospholipids above 10µM lowered the melting temperature and destabilized Histone H1. Yet another *in vitro* study examining the effect of lipids on stability of chromatin demonstrated that Histone H1 occupation of DNA was destabilized by $PI(4,5)P_2$ [9]. Collectively, the results of these studies implied that lipids have

the potential to alter the biochemical behavior of chromatin. However, the purpose of lipid induced alterations in chromatin behavior was not identified. Moreover, the material being analyzed was no longer recognizable as a nucleus, having undergone extraction in several types of detergents. As a result, these observations carried little weight.

1.2.2 Envelope-free Nuclear Preparations: the Key to Identifying Endonuclear Lipid Metabolic Activities

The advent of the envelope-free nuclear preparation in the late 1970s [10] enabled researchers to address the limitations in the previous studies by characterizing the lipid content of intact nuclear particles that lacked nuclear envelopes. These purified nuclear particles morphologically resemble and are identifiable as nuclei, yet they lack discernable traces of membrane bilayers when viewed using transmission electron microscopy (TEM). Interestingly, the original protocol for preparing envelope-free nuclei was a derivative of a protocol for purification of enveloped-nuclei. The enveloped-nuclei purification protocol which calls for dounce homogenization of cells in a Tris-based buffer containing 3mM calcium and ~10% sucrose (w/v) for nuclear stability [11, 12]. Differential centrifugation of the dounced nuclei through a sucrose cushion pellets the enveloped nuclei. Adding 0.5% Triton-X 100 in the initial extraction buffer lead to the first protocol for preparing envelope-free nuclei, as the modified initial extraction buffer lyses the cells and removes all traces of the nuclear envelope and cellular membranes. Not only did the purified particles lack envelope and membrane traces as visualized by TEM, but they also lacked >99% of cytosolic glucose-6-phosphatase enzyme activity.

Modern day protocols for purifying envelope-free nuclei are cell type specific. Successful cell-type specific protocols have been developed for numerous primary and

immortalized cell types, including Rat and Mouse hepatocytes, chick embryos, a slew of leukemic cell lines, neuroblastoma cell lines, NIH 3T3 and MEF cell lines. The protocols, which can vary widely in procedure, all have one characteristic in common: a brief detergent extraction to remove the envelope and cellular membranes [13-15].

Envelope-free nuclear preparations have been utilized in the discovery of many endonuclear lipid metabolic activities. Regarding phospholipids, the classical applications of the envelope-free nuclear preparation are *in vitro* phospholipid phosphorylation assays. Culturing the cell lines in different conditions prior to extraction has been used to demonstrate differences in regulation of endonuclear phosphoinositide (PIP) signaling enzymes during differentiation, cell growth, the cell cycle, cell stress, and liver regeneration [16]. In addition, quantitative enzymatic and mass spectrometric analyses of envelope-stripped nuclei have been used to identify and measure the amounts of phospholipids within the endonuclear compartment [17]. The use of stable isotopes in soluble GPL precursors also makes possible the study of GPL flux through endonuclear lipid metabolic pathways [17, 18].

Removal of the nuclear envelope from the nuclear particle is not a trivial undertaking. One area where these results are criticized is in the necessary use of detergents (0.5% and higher in concentration), which are used to separate the nuclear particle from cytosolic components. As the extraction procedure typically takes several minutes this has caused concern that the detergent may be introducing some cytosolic lipid deposits to the nuclear space [19]. Also, detergents are more effective at removing some GPLs versus others, and there is also concern that remnants of envelope are not removed by the detergent extraction process. There are several ways to combat this (minimizing detergent exposure, mechanical

shearing of nuclei, etc.) but none of them are perfect. Thus it is likely that what we observe in envelope-stripped nuclei is biased by the use of detergents, but it is possible to minimize these negative effects.

1.2.3 Alternative Methods for Examining Endonuclear Lipid Populations

In addition to the envelop-free nuclei based methods, several independent methods for verifying the endonuclear status of enzymes and phospholipids have been described [20-23]. For instance, the localization of lipid metabolic enzymes within cells and nuclei can be confirmed either by fluorescent-tagging and overexpressing of the enzyme or by using an immunofluorescence approach. Such methods have been used to demonstrate the speckled staining pattern of phosphoinositide kinases (PIPK) and diacylglycerol kinase (DGK) isoforms in the nuclear matrix. This, however, is informative only in indicating where the enzyme accumulates. It does not necessarily indicate that this is the sole, or even primary, site of action.

Independent methods also exist for visualizing PIPs in the endonuclear compartment [24], but they are less reliable than those for verifying the endonuclear status of enzymes. Currently, the most reliable reagents for examining endonuclear PIP pools are protein sensors. Antibodies to PIPs have been used to demonstrate concentration of both $PI(4,5)P_2$ and $PI(3,4)P_2$ in speckled endonuclear domains. Although 100% colocalization is not typical, there is significant overlap with SC-35 endonuclear staining, which is a marker for nuclear speckles. Nuclear speckles are known storage sites for RNA processing enzymes. Unfortunately, these antibodies do not bind cytosolic substrates, which calls into question their specificity. In addition to antibodies, Pleckstrin-Homology (PH) protein domains are a class of PIP-binding domains found in many cellular proteins. They are highly specific and

typically utilized by cellular proteins in tandem with other lipid or protein binding domains to strengthen a protein's association with a membrane. In experimental applications, they are most successfully used when expressed as a tandem construct in cells. PH-domains are very specific, but their affinities for the target lipid are low and they are limited in their ability to detect changes in minor PIP pools.

Specific sensors for unmodified GPLs are not available, but lipophilic dyes and fluorescently labeled lipids are commercially available for general detection of phospholipid pools. Thus far, they have not been developed for regular use in endonuclear lipid signaling experiments, although it is feasible to do so. In fact, lipid sensors are in short supply, and development of alternative methods for lipid detection has become necessary.

Alternative protein or nucleic acid readouts are also becoming viable alternatives to endonuclear lipid study. This does require knowledge of biological functions of GPLs in the endonuclear compartment, and this has been a slow door to open. From a functional aspect, we still know very little but are beginning to know more of the nuclear processes in which phospholipids participate [20, 25].

These types of studies have been used to outline several metabolic pathways found within nuclei and demonstrate their responsiveness to growth factor stimulation, apoptotic stimuli, differentiation, cellular stresses, and changes in the cell cycle [Reviewed in 26]. The sheer number and diversity of documented enzymatic activities in the endonuclear compartment and the presence of their substrates strongly suggest that lipids are active participants in endonuclear biology. In addition, the reported amount of phospholipid produced by some of these pathways indicates that lipids might also play structural roles in the nucleus. In the next section, we cover these findings and discuss what they mean for the

nuclear compartment. We limit the findings we present to discussion of phospholipids, as they are the focus of this dissertation.

1.3 Accommodating Bulk Phospholipid in the Nucleus: PtdCho Endonuclear Synthesis and Implications for Nuclear Function

The answer to the question "how much lipid is in the endonuclear compartment" is important in that it will indicate what biological functions GPLs could fulfill. Several reports have measured GPLs, Sphingomyelin, and Cholesterol, in envelope-free nuclear preparations from a variety of tissues [17, 27-29]. Although they adhered to different quality control standards, these reports unanimously indicate that the distribution of endonuclear lipid constituents is different from that found in the whole cell. Some of them indicate that cell signaling events change the endonuclear lipid profile, and the manner in which the cellular profile changes is not necessarily mirrored in the endonuclear profile and vice versa [27]. In this section, we describe the findings that characterize the lipid mass in the endonuclear compartment, focusing specifically on one major report claiming that PtdCho mass far outweighs the other GPL molecules and is a major constituent of the endonuclear compartment. We also discuss possible organizations of the purported endonuclear lipid mass.

1.3.1 Endonuclear Phosphatidylcholine Metabolism

Of all the phospholipids recorded as components of the endonuclear compartment, Phosphatidylcholine is unique in its ability to be synthesized in the nucleus without additional help from cytosolic components. Isoforms of enzymes responsible for PtdCho synthesis permanently reside within the nucleus, as documented by their transient expression

in cells as fluorescently-tagged proteins [22, 24]. Cells primarily synthesize PtdCho from Choline and Diacylglycerol via the three step CDP-choline pathway. These activities are present within nuclei that have been stripped of cellular membranes and nuclear envelope using detergents, as demonstrated by *in vitro* biochemical assays performed on the purified nuclei. The endonuclear region is not the only intended target of nuclear PtdCho biosynthetic enzymes, as it has been shown that stimulation of the rate limiting enzyme in PtdCho synthesis, CCTα, via treatment with oleic acid produces massive extensions of the inner nuclear membrane (INM) that protrude into the endonuclear space [30, 31]. Whether the source of PtdCho in the endonuclear compartment is the INM invaginations or independent endonuclear lipid structures is unknown.

PtdCho can also be recycled in the endonuclear compartment by endonuclear enzymatic isoforms. In the nucleus, PtdCho is cleaved by a nuclear D-type Phospholipase (PLD) isoform to generate PtdOH and Choline (thus, PtdOH can also be generated as a byproduct in the nuclear space). PtdOH is dephosphorylated by a Phosphatidic Acid Phosphatase (PAP) activity to make DAG. Incidentally, nuclear diacylglycerol kinase (DGK) isoforms also resides in the nuclear matrix for conversion of DAG to PtdOH [reviewed in 32]. Both PtdOH and DAG are signaling molecules and their balance is tightly regulated in endonuclear compartments [33]. DAG and Choline are funneled back into the CDP-choline pathway for PtdCho synthesis. Thus, endonuclear PtdCho metabolism requires no external aid from cytosolic components.

1.3.2 Saturated PtdCho Species as Major Constituents of the Nuclear Matrix

The fact that PtdCho can be synthesized in the nuclear compartment while others are not translates to mass measurements of endonuclear GPLs in tissue culture cells. The

development of mass spectrometry techniques for measurement of phospholipids has enabled species-specific mass calculations of phospholipids from subcellular fractions. There is one major study on the subject, and it indicates that about 90% of endonuclear GPLs extracted from purified, envelope-stripped IMR-32 nuclei are PtdCho species [17]. ESI/MS/MS analyses also detected significant amounts of PtdOH and PtdEtn species and near baseline contributions from the other classes of GPLs, which were not quantified. While PtdCho is typically the most abundant GPL in animal cells, its strong enrichment in the nucleus indicates that it is somehow important for nuclear function.

The ESI/MS/MS analysis of GPL mass IMR-32 nuclei indicate that there is a lot of lipid in the nuclear matrix. Conversion of total detected GPL mass / nucleus to a value expressed in GPL molecules / nucleus reports over 4 billion GPL molecules / endonuclear particle (primarily PtdCho species). The authors' conservative reported estimate of nuclear volume occupied by endonuclear GPL was approximately 10% (in comparison, the genome occupies 39%). The other reported unique feature of endonuclear PtdCho is the saturated nature of the acyl chains. Only saturated / monounsaturated acyl chains were found in the PtdCho species reported in the nuclear matrix, properties that cause lipids to assume a solid state. This phenomenon was unique to the PtdCho species. PtdEtn and PtdOH profiles were similar in terms of fatty acyl chain composition to that found in the whole cell. Overall, the collective physical properties of the lipids described would indicate that the GPL mass imparts a gel-like quality to the endonuclear compartment.

1.3.3 Physical Form of Endonuclear Lipids: Where's the Beef?

The sheer quantity of GPL reported within the nuclear space of IMR-32 nuclei suggests that visible lipid structures should be present in the endonuclear space.

Unfortunately, transmission electron microscopy of purified envelope-free nuclei or of nuclei within whole cells has failed to obviate such structures. That familiar lipid structures (lipid droplets and membrane bilayers) are not visible within purified nuclei and the nuclei of whole cells raises issues of detergent artifacts. It is possible that the atypical endonuclear GPL assumes a form we do not recognize by standard methods but given the mass amounts described by Hunt *et al.* [17], this is not likely the case.

Several independent methods have identified invaginations of the nuclear envelope that project into the endonuclear space. While invaginations could account for some of the phospholipid mass reported in the IMR-32 Neuroblastoma nuclei, they cannot explain how lipid mass occupies 10% of the endonuclear volume. PIP imaging experiments would suggest that some of the nuclear compartments, such as speckles, have lipid scaffolds as a core. Dynamic imaging studies have confirmed in a number of cases that these nuclear protein bodies do not behave as solid particles [reviewed in 34].

The ability to organize the nuclear space into discrete subdomains without the aid of bilayer structures is actually a hallmark of the endonuclear compartment. *In vitro* experiments performed on purified nuclei have demonstrated that, using artificial buffer conditions, nuclei in the process of falling apart can be rescued to a normal morphology and execute nuclear functions. This happens within the time frame of a few minutes and in the absence of additional cellular assistance. Such a scenario hardly seems possible if the consistency of the nuclear matrix is a semi-solid. However, these results do not eliminate the possibility that particular subnuclear domains are enriched in saturated GPL. Specifically, chromosome territories are excellent candidates for endonuclear lipid deposits. They are defined as the endonuclear space occupied by individual chromosomes that overlap only in

their peripheral regions where active genes meet. Recent dynamics studies performed on chromosome territories have demonstrated that other that saltatory motion, chromosome territories undergo little movement in live cells [35]. In addition, different regions of individual chromosome territories have little movement with respect to each other, indicating that under static growth conditions the chromosome territory functions as a solid. In this regard, saturated GPLs might have some use in solidifying chromosome territories. However, the question of how much lipid can be accommodated in this fashion is again brought to the forefront.

1.3.4 Needed Improvements in Quality Control Measures for Generating Envelope-Stripped Nuclei

Currently, the ESI/MS/MS data from purified IMR-32 nuclei is a source of controversy in the endonuclear lipid signaling field. Others have measured endonuclear lipid mass in purified envelope-stripped nuclei by enzymatic methods to report lower (sometimes much lower) GPL content [27-29]. Different cell types and different nuclear purification procedures were used in each instance, possibly leading to sizeable discrepancies in the endonuclear GPL mass measurements. Clearly, repetition in other cell types will indicate which reports are likely to be the general trend. We ourselves have repeated endonuclear GPL mass measurements in immortalized MEF nuclei using LC/MS/MS. Our preliminary results suggest that the endonuclear compartment is likely to be a GPL-poor environment, but that there is consistently detectable GPL within highly purified nuclei [manuscript in preparation].

These types of discrepancies highlight the need for standardization and more probative, quantitative quality control measures in nuclear preparations. While envelope-removal

requirements are cell-type dependent, criteria for purity are independent of cell type. Thus, it is important to standardize quantitative criteria that can be used to compare purities across cell types in absolute terms. Most current purity validation protocols utilize TEM to demonstrate the envelope-free status of the purified particles and western blot for cytosolic and nuclear markers to demonstrate absence of unwanted cellular membranes. Removal of cellular membranes and envelope is never 100%, and we strongly think the degree of purity should be stated as a percentage so that data can be properly interpreted. We take steps to address these issues in chapters 2 and 3.

1.4 Phosphoinositide Signaling in the Endonuclear Compartment

Our discussion so far has focused on the presence of GPLs in the endonuclear compartment and how much of that space they consume. What function GPLs serve in the endonuclear space is also a major question in the endonuclear lipid signaling field. Where the answer to this question is the most obvious is in the presence of PIPs and their metabolic enzymes in the endonuclear space. The majority of studies examining endonuclear phospholipids concern the synthesis and regulation of PIP molecules. PIPs have many roles in the cytosol, including regulation of membrane trafficking, cytoskeletal formation, and plasma membrane receptor signaling [Reviewed in 16]. Many proteins utilize PIPs in cellular membranes to add additional affinity to other protein-protein reactions[36]. For PIP metabolism in the endonuclear compartment, one of the major questions is, again, how much and to what extent is PIP signaling a part of biological processes in the endonuclear compartment. Much of the interest in measuring GPLs is in gaining perspective as to how

much of the signaling GPL metabolites (such as PIPs) are present in the endonuclear space. In this section, we discuss some of the major findings in endonuclear PIP signaling.

1.4.1 Basic Principles of Phosphoinositide Signaling

Phosphatidylinositol is only one of the many biologically active inositol containing compounds in mammalian cells [Reviewed in 37]. This GPL is synthesized in the smooth Endoplasmic Reticulum by the enzyme PtdIns synthase (substitution reaction from CDP-Diacylglycerol and L-*myo*-inositol). In addition, mammalian cells can generate 7 different PIPs, with phosphorylations possible at any or all of the 3, 4, and 5 positions of the myo-inositol ring of PtdIns. Also, many cellular membranes contain phosphoinositides, and their phosphorylation is conducted by specific kinases sensitive to the already phosphorylated state of the substrate (i.e., PIPs phosphorylated at a given position are only valid substrates for certain PIPKs; Reviewed in 38).

The canonical phosphoinositide signaling pathway involves plasma membrane phosphorylation of PtdIns by a PtdIns-kinase (PIK) to generate phosphatidylinositol-4-phosphate (PI(4)P). This lipid is then subject to phosphorylation by a PtdIns-(4)-phosphatase (5) kinase to generate PI(4,5)P_2. PI(4,5)P_2 is commonly referred to only as PIP_2 because of its participation in an overwhelming number of cellular events including membrane trafficking, receptor signaling, and cytoskeletal regulation. Thus, it is this molecule we refer to when positional phosphorylation information is not given. Importantly, PIP_2 is cleaved by C-type Phospholipases (PLCs) to generate the cell-essential second messengers IP_3, which gates calcium, and DAG, which is responsible for Protein Kinase C (PKC) activation and phosphorylation of numerous downstream cellular targets. IP_3 also serves as a precursor for higher order inositol phosphates, which can be singly phosphorylated on every position, and

doubly phosphorylated on some ring positions. Inositol phosphate signaling regulates an expanding number of nuclear processes, although it is unclear whether nuclear PIP_2 is necessary for their generation. It is now appreciated that the other phosphoinositides have key signaling roles in endocytosis and endosome maturation, lipid storage, and receptor signaling [also reviewed in 38].

1.4.2 Discovery of Phosphoinositide Signaling Activities in the Nuclear Matrix

In the early 1980's, two reports from Smith and Wells emerged that found phospholipid kinase activities in the nuclear envelope [39, 40]. The specific products of these activities were PIPs, and those who had observed lipids within nuclear matrix fractions took note. A pioneering set of *in vitro* experiments performed on differentiating Friend Erythroleukemia (MEL) nuclei, washed with Triton to remove the envelope, found similar activities within the nuclear compartment [41]. Purified MEL cell nuclei were incubated with [γ-^{32}P] Phosphate, and phospholipids were extracted for analysis. The result was a pool of radiolabeled phospholipids generated in the absence of envelope. The pool included Phosphatidic Acid (PA), Phosphatidylinositol Phosphate (PIP) and PIP_2, the latter of which was observed in only trace amounts in the absence of differentiating conditions. The substrate lipids within the endonuclear compartment were Diacylglycerol (DAG), Phosphatidylinositol (PtdIns), and Phosphatidylinositol phosphate (PIP). All of these are metabolites of phosphoinositide signaling pathways. The corresponding enzyme activities include a Diacylglycerol Kinase (DGK) activity (to produce PA), Phosphatidylinositol kinase (PIK) activity (to produce PIP), and a phosphatidylinositol phosphate kinase (PIPK) activity (to produce PI (4, 5) P_2). Also exciting was the implication that PI(4,5)P_2 accumulates in response to differentiation cues, indicating that endonuclear lipids change in response to

extracellular signals. It is now appreciated that PIP_2 levels in nuclei correspond to cell cycle progression [42], growth factor signaling [43], cell and tissue stress [20], and differentiation cues [41, 44].

Since the discovery of these activities in the nucleus, nuclear DAG, PIK, and PIPK enzymatic isoforms have been identified. DGKs θ, ζ, ε, and ν localize to the endonuclear compartment as shown by immunofluorescence and biochemical assays [Reviewed in 54]. The PI 4-Kinase β isoform has been demonstrated to localize to the nucleus of NIH-3T3 cells and is responsive to treatment with the nuclear export inhibitor, Leptomycin B [45]. PIP_2 synthesis can occur one of two ways in the endonuclear compartment. PIPK1α can synthesize PIP_2 from PI(4)P, and PIPKIIβ phosphorylates PI(5)P in nuclei in the 4 position to generate PIP_2. What is interesting about the localization of these metabolic enzymes is that they (a) cluster within the nucleus in speckle-like domains and (b) colocalize somewhat with the splicing factor / speckle marker, SC-35 [24]. While nuclear speckles are currently thought to function as storage compartments for unused RNA processing machinery, it is tempting to speculate that regulation of endonuclear PIP synthesis could influence the stored and active transcription machinery.

The spike in $PI(4,5)P_2$ levels in response to signals that effectively halted cell growth led to speculation about downregulation of PLC activity. Evidence in favor of differential PLC regulation in response to growth or differentiation cues came from a study performed on Swiss 3T3 fibroblast nuclei [42]. This study demonstrated stimulation of quiescent 3T3 cells with IGF-1 caused the nuclei to decrease PI(4)P synthesis in favor of $PI(4,5)P_2$ and Diacylglycerol. This would suggest that nuclear PLC activity is decreased when cells are quiescent, and that activity is either turned on or up-regulated when cells re-enter the cell

cycle. This same study also identified a Phosphatidic Acid Phosphatase (PAP) activity within nuclei as well, which would lead to increased nuclear DAG content.

Overlap of PIP signaling pathways with other GPL metabolic pathways can complicate interpretation of enzymatic activity data. For instance, DAG is a byproduct of PIP_2 cleavage and also an essential substrate for PtdCho biosynthesis via the CDP-choline pathway (see earlier section). Initial examination of nuclear DAG species found that the majority of the endonuclear DAG pool is structurally similar to the endonuclear PtdCho pool, highly saturated. PtdIns species, however, are typically polyunsaturated, leading to questions of whether nuclear PIP_2 is metabolized to DAG at all. Further analyses of the DAG pool indicate that about 10% of the endonuclear DAG is polyunsaturated. Identification of DAG species in MEL cell nuclei after release from a Nocodazole induced cell cycle arrest demonstrated that G1 DAG synthesis produces primarily polyunsaturated species. Thus, there is differential regulation of DAG in the endonuclear compartment [46].

1.4.3 Translocation of PLC Isoforms in Response to Cellular Cues

Although activation of phospholipase C isoforms occurs in the cytosol in response to growth signaling, several PLC isoforms respond by translocating to the nuclear compartment [Reviewed in 47]. PLC activation and translocation are viewed as the regulatory points of endonuclear PIP_2 metabolism and seems to be a growth factor specific response. For example, the PI-PLCβ1a isoform translocates to the nucleus when MEL cells are stimulated by IGF-1 but not PDGF. The PLCβ1a splice variant is the most heavily studied of the PLC isoforms demonstrated to translocate to the nucleus, although the γ1 and δ1 isoforms are also studied in this context. This occurs through phosphorylation of the C-terminal tail, which is incidentally unique among PLC-β1 isoforms. The consistently reported consequence of PLC

translocation to the nuclear compartment is a decrease in nuclear PIP_2. As mentioned in the previous section, polyunsaturated DAG species increase under these conditions [47].

1.4.4 Phosphoinositide Accommodation in the Endonuclear Compartment

Nuclear phosphatidylinositol and its derivatives are minor components of the endonuclear lipid mass [17, 42, 43]. Unlike in the case of the endonuclear PtdCho mass, we have some visual indications of where the signaling lipids might reside in the nuclear space. Apart from the biochemical detection of PIPs and phosphoinositide pathway intermediates, the primary mode of detection for PIPs has been through the use of monoclonal antibodies to $PI(4,5)P_2$. As with the PI(4)K and PIPK isoforms, endonuclear $PI(4,5)P_2$ localizes to speckle like compartments. These foci also stain positively for SC-35, the marker for nuclear speckles. ImmunoEM experiments have demonstrated the presence of PIP_2 at the tip of nuclear envelope projections into the nuclear matrix. It is currently unclear whether the PIP_2 observed at the end of envelope invaginations is always associated with nuclear PIP_2 foci, but it is known that speckle domains are not necessarily associated with nuclear envelope invaginations. What is odd is that an antibody to PI(4)P does not recognize an endonuclear substrate, but does recognize cytosolic lipids (our unpublished data). One possible explanation for this is that PI(4)P generated in the endonuclear space is immediately funneled to PIPKs for synthesis of PIP_2; however, antibodies to PIP_2 do not recognize cytosolic PIP pools where PH-domains do, raising issues of specificity regarding the antibodies. Fortunately, an independent analysis of cellular PIP_2 using a PIP_2-binding tandem PDZ2 protein domain detects pools of PIP_2 in both the cytosol and endonuclear compartment. Thus, it is likely that PIP foci are a bona fide feature of the endonuclear space. Regardless of subcellular localization, underdetection of cellular PIP pools is a concern for a two reasons.

First, PIPs are typically observed, in both biochemical and immunofluorescence assays, when cells have been extracted in detergents that could easily interfere with the usefulness of some reagents while leaving others unaffected. Second, as the analyzed material is not always fixed, or even immediately fixed, the time needed for processing is also a time when the material being detected can be metabolized to other molecules. Thus, a variety of factors complicate detection of endonuclear phospholipids (and cellular phospholipids for that matter).

1.4.5 Phosphoinositides as Cofactors in Endonuclear Processes

Within the last decade, several reports of nuclear processes that utilize PIPs as cofactors have emerged. ING2, the Plant Homeodomain (PHD) finger containing protein, is a stress activated protein which induces cell cycle arrest alongside p53 domains. The PHD domains of ING2, and of many other proteins found in nature, were shown to have *in vitro* PIP binding activity. The PHD fingers of ING2 were shown to be specific for PI(5)P *in vivo*. Overexpression of the kinase that phosphorylates only PI(5)P and no other PIPs disrupted nuclear localization of ING2. The PIP-binding activity of ING2 was deemed necessary for function, as the lipid binding portion inhibited apoptosis when overexpressed [25].

Using the speckle-binding portion of the protein as bait, a recent screen for proteins that bind PIPK1α identified a non-canonical PolyA-polymerase assigned the name (STAR-PAP) which is responsible for polyadenylating a subset of the transcriptome. *In vitro* experiments verified the polyadenylase activity of the protein and that polyadenylation was specifically stimulated by the inclusion of PIP_2 in the reaction mixture. Substitution of PIP_2 with any of the other PIPs did not similarly stimulate PAP activity. Interestingly, knockdowns of both STAR-PAP and PIPK1α identified a shared pool of genes which were

affected by the loss of either STAR-PAP or the kinase. There are several overlapping classes of genes affected under both knockdown conditions, a subset of the negatively affected transcripts are participants in the oxidative stress response. In response to treatment with the oxidative stress agents, such as tButylhydroquinone (tBHQ) these genes are transcribed and processed for translation. The loss of either PIPK1α or STAR PAP inhibits processing of the oxidative stress transcripts. Also, the kinase activity of PIPK1α was needed for STAR-PAP activity indicating an *in vivo* role for PIP_2 production in HEK293 nuclei [20].

1.4.6 Phosphatidylinositol and its Import into the Nuclear Compartment

The localization of PIKs and PIPKs suggests that compartmentalization of these signaling molecules has conferred to them specialized endonuclear signaling roles. Given this, it is striking that PtdIns is among GPLs that cannot be synthesized in the nuclear compartment *de novo*. Currently, there is no experimental evidence to suggest how PtdIns arrives in the endonuclear space. Given the information we have regarding PIP organization in the nuclear compartment, it seems likely that lipids are organized in discrete foci. A soluble PtdIns-transporter that shuttles PtdIns into the nuclear matrix for nuclear PIP signaling is ideally suited to supply endonuclear lipid pools. The most attractive candidate for this activity is the phosphatidylinositol transfer protein alpha (PITPα), a soluble, nucleocytoplasmic PtdIns/PtdCho transfer protein that is found in most mammalian cell types [48]. Alternate theories exist for how PtdIns enters the endonuclear compartment, but these involve temporary association of intranuclear sites with the nuclear envelope, a mechanism which does not afford the temporal efficiency associated with signaling events. Thus, it seems likely that a protein shuttle is best suited for rapid control of discrete PtdIns pools.

1.5 Summary and Thesis Statement

From mass spectrometric analyses of endonuclear GPL mass to biochemical experiments detailing the generation of PIPs from purified envelope-free nuclei, we have a developing picture of the nuclear matrix as a major site of phospholipid signaling and biosynthesis. One issue slowing our understanding in this matter is that prior studies have reported different amounts of GPL in the nuclear matrix [17, 42, 43]. Unfortunately, no prior work has experimentally confirmed the biochemical mass results with a visualization of endonuclear lipid structures.

Given discrepancies in the amount of GPL reported to be in the nuclear matrix, it is important to reproduce these results in a number of cell types. As prior studies use different procedures and adhere to varying quality control standards regarding nuclear preparations, it is likely that the source of discrepancy in biochemical experiments arises from these differences. For instance, as with any experimental method, an important concern in studies involving nuclear preparation is artifacts introduced by the experimental protocol. A main source of artifacts is the use of detergents in nuclear preparations. While the use of detergents in nuclear preparations cannot be avoided, the use of detergents across protocols is not consistent and neither is the treatment of resulting artifacts in the measured results. Nevertheless, there are means by which one can increase confidence in the result in the presence of artifacts. Unfortunately, the art of nuclear preparation is a poorly documented subject. Nuances in generating successful envelope-free nuclear preparations are not appreciated, mostly because the sensitivities are not discussed in detail and the quality of the product is similarly lacking in description. The focus of this work is tripartite:

1. To generate a nuclear preparation method for embryonic fibroblasts that is well documented in description and is more quantitative in practice. (Chapter 2)
2. To apply this method to the biological problem of endonuclear GPL mass. (Chapter 3)
3. To assess whether the nuclear role of PITPα is to import PtdIns into the nuclear matrix in a dynamic lipidomics assay requiring envelope-free nuclear preparations.

What has been generated is a well-documented preparation method that, when applied with the appropriate quality control standards: (1) demonstrates the GPL-poor quality of the nuclear matrix in MEF cell lines and (2) disproves the hypothesis that PITPα supplies the nuclear matrix with PtdIns for endonuclear lipid signaling.

CHAPTER 2

BASIC ELEMENTS OF A SUCCESSFUL ENVELOPE-FREE NUCLEAR PREPARATION METHOD

2.1 Summary

The previous chapter has shown that the ability to purify nuclei without their envelopes is an invaluable investigative technique to the study of endonuclear lipid metabolism. Preparations of envelope-free nuclei produce intact nuclear particles that retain their "nuclear" morphology but contain only trace amounts of visible organellar and heterogeneous membrane debris. The latter is important for experiments that employ envelope-free nuclei as a substrate because their results can be biased by membrane contaminants.

This chapter describes a method that we have generated in collaboration with the Cocco Lab in Bologna, Italy for purification of high quality envelope-free nuclei from immortalized and primary mouse embryonic fibroblast (MEF) cell lines which offer genetic tractability. The protocol statement provides minimal descriptions of the steps in envelope-free nuclear preparation, which is discussed within. To this, we have added additional detailed instruction for addressing practical issues in optimizing and standardizing the practice of envelope-free nuclear preparation. This highly detailed version of the protocol is effective for reproducible purification of envelope-free nuclei from 1×10^7 MEF cells. We note that nuclear preparations are sensitive to small variations in procedure. To combat this

sensitivity, the protocol includes visual checkpoints during the purification as essential steps. With the use of these visual cues, the preparation yields stable intact particles and consistent yields in terms of protein (10%). The purified envelope-free nuclei are suitable for use in mass spectrometric applications, enzyme assays, and immunostaining.

2.2 Introduction

The ability to use detergents to purify the endonuclear compartment from cellular membranes and nuclear envelope contaminants is an essential tool in the study of endonuclear lipid metabolism. At face value, published envelope-free nuclear preparation protocols appear relatively uncomplicated. General principles of nuclear preparations include lysis of cells, extraction of cells in high detergent concentrations to solubilize cellular membranes; cytosolic components, and the nuclear envelope; and differential centrifugation to isolate nuclei from debris and enveloped nuclei. Ideally, the purification technique should also preserve the endonuclear compartment as an intact particle that is still recognizable as a nucleus, with minimal loss of nucleoplasm, nuclear matrix, and chromatin. Maintenance of these properties in the endonuclear compartment after purification is the source of complexity in envelope-free nuclear preparation protocols.

Consider the removal of the nuclear envelope, which provides not only a boundary but structural support for the organelle. Conditions within the nuclear compartment are overcrowded, a fact which some speculate is responsible for hastening biological interactions in this compartment. In addition, the nucleus is a sizeable organelle, occupying ~$1/10^{th}$ of cellular volume in most cell types. In undifferentiated cell types, nuclei are commonly even larger and occupy a greater amount of cell volume. Observation of the nuclear matrix by

TEM would indicate that the nucleus lacks obvious internal structural components for support (i.e., protein scaffolding, or internalized membrane systems). Therefore, one might think that under lysis conditions, the nuclear particle would naturally expand and eventually disintegrate.

Several properties of the nucleus prevent dissolution of the nucleus in the absence of the nuclear envelope. First, the nuclear lamina, which lays immediately beneath the nuclear envelope, provides structural support for the nucleus and contributes to the shape of the organelle. Detergents used to purify the envelope-free nuclei largely leave the lamina intact while dissolving the lipid bilayers attached to it. Second, the nucleus is sturdy. High concentrations of detergents are used in envelope-free nuclear preparations, yet a nuclear particle survives the extraction. While yield of both nuclear material and nuclear particles is not 100%, the final product is easily recognized as a nucleus.

The selection of cell type for envelope-free nuclear preparation is important. One helpful attribute of cell lines in any cellular study is genetic tractability. We selected mouse embryonic fibroblasts (MEFs), which not only offer genetic tractability, but also offer fewer degrees of separation from the animal than many commonly used cell lines and simultaneous generation of wild-type and mutant cell lines from a single litter. Another beneficial attribute of a nuclear preparations is that it is applicable to multiple cell types. A single nuclear preparation protocol for wild-type MEF cells should be applicable to MEFs generated from transgenic, knockout, or knock-in animals. If modifications in the protocol are needed for isolation of mutant envelope-free nuclei, this can be recorded as a biochemical defect caused by the mutant condition. The disadvantage of preparing envelope-free nuclei from MEFs is that their membranes are more slightly more resistant to detergent extraction.

Currently, there is one other protocol available for purification of envelope-free nuclei from MEF cells. Both primary and immortalized MEF cell nuclei purified via this method are resistant to separation from heterogenous cellular debris (see Figure 1). This protocol was equally ineffective in both primary and immortalized MEF cell lines. With the aid of Lucio Cocco's lab in Bologna, Italy, we adapted a more stringent nuclear preparation style for use in MEF cells (see Figure 2). The 1x protocol, which purifies intact envelope-free nuclei from 1 x 10^7 cells, utilizes sufficiently pure from heterogenous membrane debris in visual analyses. Also, the purified material easily meets quality control standards for purity.

The protocol elements we describe are very straightforward on paper, but sensitive to several variables in practice. First, all manipulations are performed on ice to slow undesirable enzymatic activities that could affect the integrity or yield of nuclei. Solutions are either autoclaved sterilized or DEPC-treated to eliminate exogenous nuclease activity. For example, sharp temperature shifts that happen when heat transfers from fingertips to the solution can destabilize nuclei. Second, the density of the cell lysate in all steps influences the final yield of the nuclei and the success of envelope removal. Thus, accurate cell counts and consistency in pipetting is very important. Third, it is important to monitor the preparation because the protocol will likely need to be adjusted based on visual analysis of the membrane-removal process. We provide detailed instructions for these considerations and have provided them as additional guides through the protocol.

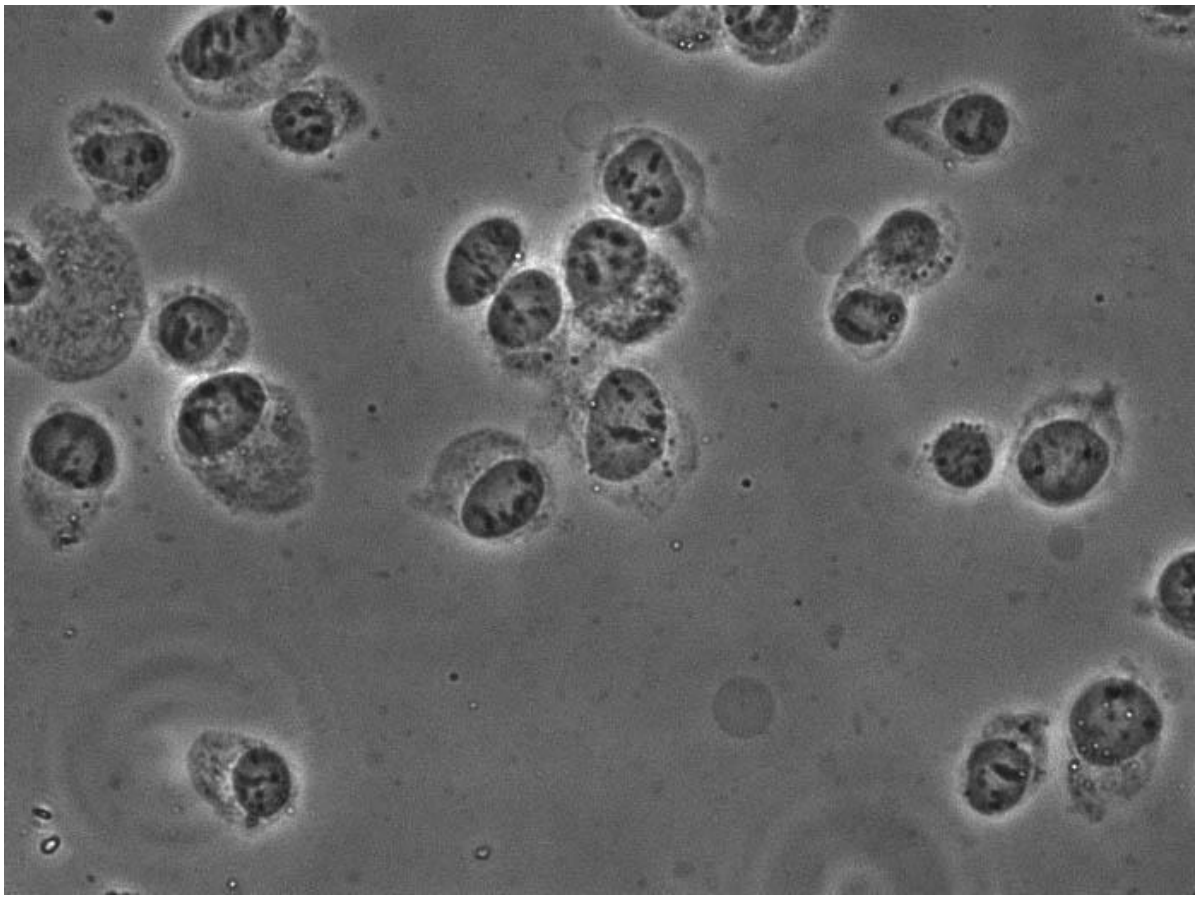

Figure 1. Preparation of envelope-free nuclei from iMEF cells via the protocol published by A. Hunt (2006). Phase contrast image of highly purified nuclei surrounded by insolubilized cellular debris. The nucleus is visible as the phase dark center of each extracted particle. The image was taken at 40x magnification. This protocol calls for extraction of pelleted cells in 0.5% Triton-X 100 to remove the nuclear envelope. Isolation of the purified nuclei follows without a mechanical shearing step; nuclei are instead pelleted through a 30% sucrose cushion.

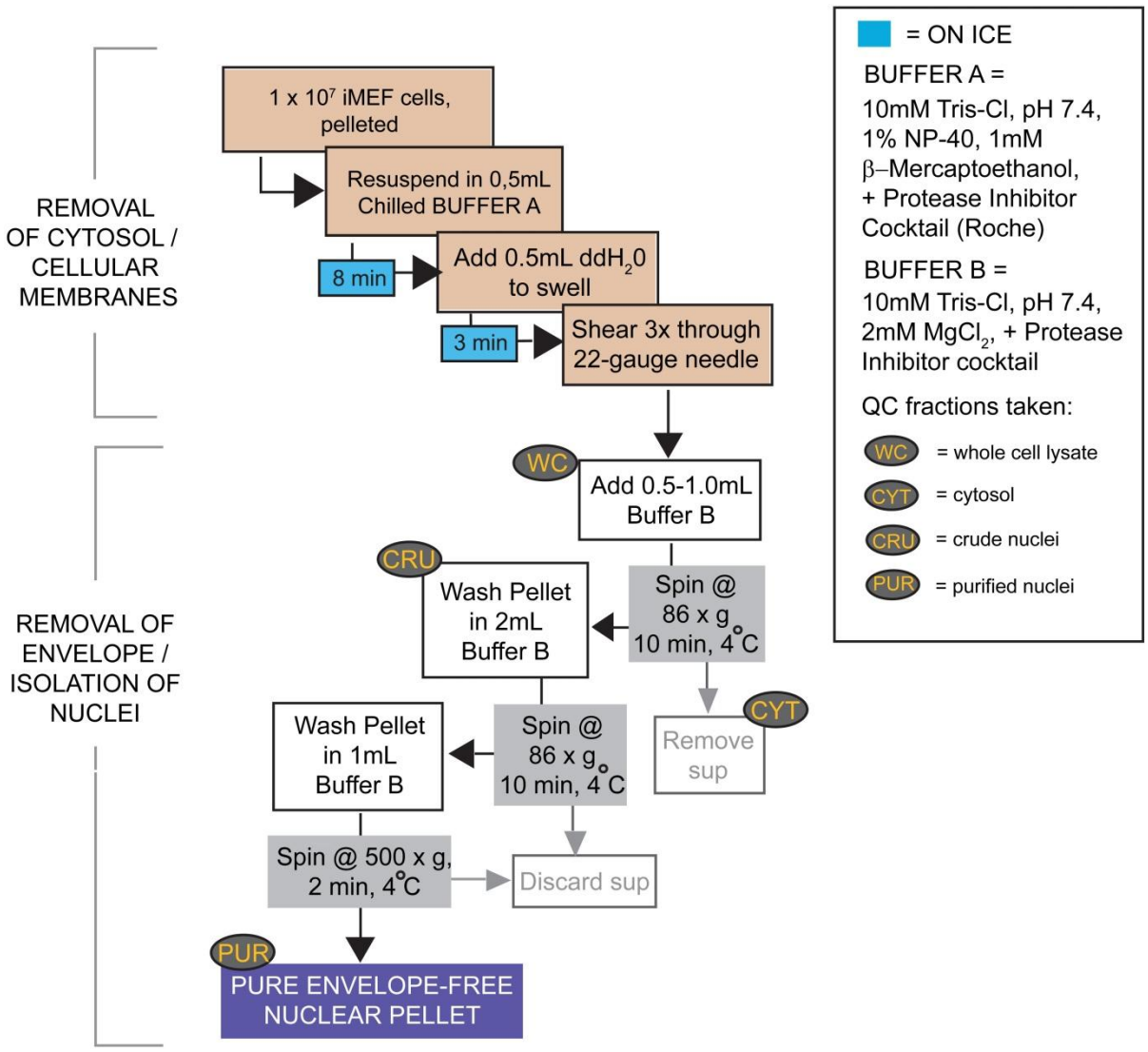

Fraction	WC	CYT	CRU	PUR
Total Protein (mg)	3.11 ± 0.45	2.55 ± 0.56	0.51 ± 0.09	0.34 ± 0.10

Figure 2. Nuclear purification scheme. A schematic flow diagram for rapid purification of envelope-stripped iMEF nuclei is illustrated. Total protein in individual fractions generated during the nuclear purification process is shown in mg.

2.3 Materials Needed

2.3.1 Tissue Culture / Cell counting / Isolation of Cells for Envelope-free Nuclear Preparation

1. PBS
2. Dulbecco's Modified Eagle Medium (DMEM; Gibco, prod. No 11995)
3. Fetal Bovine Serum (FBS; Gemini Biotechnology)
4. 100x Penicillin / Streptomycin solution (P/S; Cellgro)
5. 0.25% Trypsin/EDTA (Cellgro)
6. Case of 150mm coated tissue culture dishes (you can use flasks but they are deeper and fewer will fit in a given incubator space)
7. Laminar flow hood for tissue culture and assorted sterile culture reagents (pipets, tips, vacuum pump for aspiration, etc.)
8. Small inverted phase contrast microscope fitted with 10x and 40x dry objectives.
9. 15 and 50mL sterile disposable conical tubes
10. Hemacytometer
11. Ice bucket
12. Table-top centrifuge for 15mL conical tubes

2.3.2 Envelope-free Nuclear Preparation

1. 0.1 M Tris-Cl, pH 4.4, sterilized by autoclaving
2. NP-40 detergent
3. B-Mercaptoethanol
4. PMSF
5. Complete Protease Inhibitor Cocktail Tablets, EDTA-free (Roche)
6. 0.1M $MgCl_2$, sterilized by autoclaving
7. Sterile, RNase/DNase free ddH_2O
8. Low retention sterile barrier tips for p1000, p200, and p20 pipetmen and matching pipettes.

9. Scissors to blunt pipette tips
10. Timer
11. Glass slides and coverslips
12. Inverted microscope with 40x phase contrast dry objective and Camera (for documentation)
13. Sterile 15mL conical tubes.
14. Sterile eppendorf tubes
15. Luer-lock syringes in 1 or 5mL volumes
16. 1.5 inch, sterile, 22-gauge needles.
17. Balancer tubes for centrifugation
18. Beckman tabletop refrigerated centrifuge fitted with a JS-400 swinging bucket rotor

2.3.3 Homogenization of Nuclei and Protein Analyses

1. M-PER lysis reagent (Pierce Biopharmaceuticals)
2. 1mL syringes
3. 22-, 25-, and 27-gauge needles (ideally ½" to 2/3" in length)
4. BCA Assay for Microplate Reader (Pierce)
5. BSA 2mg/mL standards
6. Clear, flat-bottomed 96 well plates
7. SDS-PAGE Clean up kit (Thermo Scientific)
8. Eppendorf tubes and eppendorf centrifuge
9. n Blotting Reagents

2.3.4 Fixation of Nuclei and Staining

1. Ice cold methanol
2. chilled HBSS
3. ice bucket
4. Diaminophenylindol (DAPI; Invitrogen)
5. Hoescht Nuclear Dye (Invitrogen)
6. Nile Red Lipid Dye

2.4 Buffer List

2.4.1 Nuclear Preparation Buffers

Buffer A (Extraction - 100mL total volume):

- 10 mM Tris-Cl, pH 7.4 (10mL of a sterilized 0.1M Tris-Cl stock solution, pH 7.4)
- 1% NP-40 (v/v ; 1mL)
- 10 mM β-Mercaptoethanol (74µL)
- *0.5 mM PMSF
- * 1x Complete Protease Inhibitor Cocktail, EDTA-free (Roche)
- Sterile ddH_2O to 100mL
- Aliquot and freeze at -20ºC. Thaw and complete with the starred items just before use.

Buffer B (Wash - 100mL total volume):

- 10mM Tris-Cl, pH 7.4 (10mL of a sterilized 0.1M Tris-Cl stock solution, pH 7.4)
- 2mM $MgCl_2$ (2 mL of a sterile 0.1M MgCl2 stock solution)
- *1x Complete Protease Inhibitor Cocktail, EDTA-free (Roche)
- Sterile ddH_2O to 100mL.
- Store at 4ºC for up to 2 weeks or freeze in aliquots at -20ºC and thaw and complete with the starred reagent as needed.

2.5 Protocol

2.5.1 Seeding Cells for Nuclear Preparation

Nuclei are much more likely to release their envelopes when cells are grown at subconfluence for several passages. It is important to make sure that cells do not reach confluence for several passages before attempting a nuclear preparation. When plating cells for experimentation, cells should be plated so that they reach 60-80% confluence in 24 to 48 hours. At this point cells should be well spread and have typical fibroblast morphologies. The conditions for a 1x preparation of iMEF cells are shown below. All steps are taken under sterile conditions.

1. Culture iMEF cells for several passages in complete DMEM in a 10% CO2 incubator. At no point should cells should reach extreme confluence. The desired confluency of iMEF/MEF cells 1-2 days before the nuclear preparation should be about 70-80% confluence in two 15cm coated tissue culture dishes.
2. In preparation for plating, aliquot 20mL of pre-warmed complete DMEM to 6 -15cm coated tissue culture dishes in a sterile tissue culture hood.;
3. Wash cells in an excess of sterile PBS and trypsinize iMEF cells from both of the subconfluent (~80% confluent) 15cm tissue culture plates by adding 1.5mL Trypsin/EDTA (0.25% Trypsin) to each plate. This process should be very rapid (1-2 minutes) at room temperature.
4. Collect trypsinized cells in complete DMEM to a sterile 50mL conical tube using 13.5mL media per plate. Divide the suspension between two 15 mL conical tubes and pellet in a tabletop centrifuge at 500 x *g* for 3 minutes.

5. Discard supernatant and resuspend each pellet well in 8mL of DMEM. Recombine suspensions to a sterile 50mL conical tube. Count 10µL of the cell suspension on a hemacytometer. Under these conditions, final counts should yield cell densities of 200,000-300,000 cells per mL suspension.

   In practice, cell counting with such large volumes of cells can be problematic. We suggest the following guidelines:

   - Take a 10µL aliquot for counting as soon as possible after resuspending. Allowing too much time to pass after resuspension causes the solution to settle. Set a 20µL pipetman to 10µL and equip with a sterile tip before resuspending so that the cells do not settle before they are counted.
   - The 10µL aliquot should be taken from at least 1" below the surface of the suspension. Cells will settle very quickly into the lower part of the suspension, and thus the very top of the solution should be avoided to prevent undercounting.
   - The most accurate counts are obtained when the density of cells in the suspension being counted is such that the total count from the four large squares on the hemacytometer is around 100. If counts are too low (less than 50) or too high (over 200), accuracy in counting suffers. If the cell suspension is too dense, add more sterile complete DMEM to dilute the cells as needed. If the cell suspension is too dilute, then the cells have not reached the proper density.
   - When applying the 10µL of suspension to the hemacytometer, make sure that the hemacytometer is clean, that the glass coverslip is centered and that the

solution washes evenly over the entire gridded platform. Avoid adding more cell suspension than enough to cover the gridded area, and do not bump the glass coverslip after loading with cell sample.

- Cell suspensions should be counted several times to ensure that the counts are accurate. This is needed particularly in larger experiments. This is more crucial when counting cells for the actual nuclear preparation. Small errors in counts can lead to significantly under/overplating cells. The suspension should also be triturated several times in between counts.

6. For cells at 60-80% confluence in 24 hours, seed 800,000 cells to each of the six 150mm tissue culture dishes containing the pre-warmed complete DMEM.

   In practice, we suggest the following additional steps:

   - Cells should settle evenly on the whole surface of the plate to avoid areas of the plate growing faster than the others. The best strategy for plating is to add the cell suspension dropwise to the medium and then gently slide the dish in a cruciform pattern (back, forth, side to side, repeat…) along the hood surface to spread the cells. Make sure the surface on which you are working is level. If the hood surface is not level, move cells to the incubator as soon after plating as possible. Also, it is best to avoid stacking large numbers of dishes on a single shelf as the shelf will sag slightly towards the center of the incubator and the cells will settle towards the sagging side.
   - It is important to make sure that cells are seeded to all plates equally, as a single plate will be counted as a representative of the other plates.

- To seed cells for experimentation closer to the 48 hour time point, plate 200,000-300,000 cells per 150mm tissue culture dish.

2.5.2 Counting Cells and Isolating Cells for Envelope-Free Nuclear Preparation

The envelope-free nuclear preparation we describe is very sensitive to cell numbers. It is important to accurately count cells before beginning the preparation (see notes 2 through 6). Also, complete nuclear preparation solutions and chill on ice before beginning the isolation procedure.

1. Pre-warm complete DMEM, PBS, Trypsin/EDTA in a 37ºC water bath.
2. Remove a single 150mm dish containing the iMEF cells plated 24-28 hours prior and confirm that the cells are 70-80% confluent.
3. Wash the cells in prewarmed PBS, trypsinize them in 1.5 mL Trypsin/EDTA (0.25% Trypsin) and collect the cells to a single 15mL conical tube with 13.5mL of pre-warmed complete DMEM. Tilt the dish and let the last few hundred µL of media collect to the bottom rim.
4. Pellet the cells in a table top centrifuge at 500 x *g* and replace the supernatant with 8mL of complete DMEM.
5. Thoroughly resuspend the cells in the medium and record the total volume of suspension. Count the cells from 10µL of suspension to obtain the density of the cell suspension (in cells/mL).

   In practice, we have found it **CRITICAL** to count cells 8-10 times (i.e., count 8 to 10 individual 10µL samples of cell suspension) and take the average. This will be helpful with reproducibility. For help with counting, we have already listed several steps in the previous section.

6. Calculate the number of cells per plate using the total volume of suspension (in mL/150mm dish) and the density of the cells (in cells/mL). This number can be used to calculate the number of plates needed for 1 x 107 cells (a 1x preparation). This is typically 4-5 150mm tissue culture dishes.

   In practice, we have found it critical to **STOP** at this point and make sure that you have 50-60mL of chilled complete DMEM, and about 50mL of chilled PBS or HBSS. In addition you should prepare reagents for the nuclear preparation on ice and fully supplemented with the relevant inhibitors. You should also reserve centrifuges or microscopes for experimentation.
7. If the number of plates needed is not an integer, round up to the nearest integer. Remove that many plates from the incubator and wash the cells in PBS.
8. Remove the wash and trypsinize cells thoroughly with 1.5mL of Trypsin/EDTA per plate. It is preferable that no clumps remain. Ideally, all cells should be individual, although small clusters of cells (2-4 cells) are acceptable.
9. Collect the trypsinized cells in an excess of chilled complete DMEM, using partial plates if necessary. Then collect the cells from each plates individually in 13.5 mL medium and add suspensions to an equivalent number of sterile 15mL conical tubes.
10. Pellet the cells in a table top centrifuge for 3 minutes at 500 x *g*.
11. Wash the cells once in 10mL chilled DMEM to completely neutralize any remaining Trypsin.
12. Wash cells in 15mL of chilled PBS or HBSS, collecting all cells to a single tube. Pellet cells for 3 minutes at 500 x *g*.
13. Repeat wash 2 times and discard the supernatant.

14. Proceed immediately to detergent extraction.

2.5.3 Detergent Extraction/Hypotonic Lysis of iMEF Nuclei

The initial resuspension of the iMEF cells in detergent containing buffers begins the membrane stripping / nuclear isolation process. Buffers needed at this point should be thoroughly chilled. All steps should be conducted on ice. We include protease inhibitors, use DNase/RNase free ddH_20 for solutions and sterile filter tips in the procedure; additional inhibitors (Nuclease inhibitors) can be added if necessary. These steps are time sensitive, and it is important to keep an eye on the nuclei as they are undergoing extraction.

1. Completely remove any remaining supernatant from the cell pellet using a 200µL pipette tip.
2. Using a p1000 pipetman equipped with a sterile barrier tip, add 500µL of chilled Buffer A supplemented with protease inhibitors to the pellet. Start the timer for 8 minutes and gently but thoroughly resuspend the pellet. Keep the tube on ice during these manipulations.

    In practice, there are three additional important recommendations:

    - Make sure to thoroughly mix Buffer A immediately prior to using, as detergent containing solutions can settle.
    - Just as nuclear preparations are sensitive to cell number, they are also sensitive to buffer volumes. We suggest checking the accuracy of your pipettes using a weigh scale, as well as, the precision with which you pipette. Wipe loaded tips with a kimwipe to remove excess solution.
    - We recommend using low retention tips during each portion of the procedure. Nuclei without their envelopes are very sticky.

3. Remove 3-5µL of suspension using a p20 pipetman and transfer to a glass slide. Top the suspension using a coverslip and examine the extracting nuclei on a phase contrast microscope at 10x magnification. Ensure that the cells are completely separated from one another. If they are not completely separated from one another, then continue pipetting very gently with a p1000 pipetman, this time equipped with a blunted, sterile barrier tip.
4. Once the suspension contains no clumps, examine another 3-5µL aliquot on a phase contrast microscope using a 40x objective. The nucleus at this point should be observed as the phase dense center of the extracting particles, surrounded by cellular debris which appears as less dense (see Figure 3).
5. Occasionally agitate the extracting solution (every few minutes) by flicking, inverting, or swirling the cells. It is important in practice, to keep fingers out of contact with the bottom of the tube.
6. Visually monitor the nuclei at the 5 or 6 minute mark to make sure that the nuclei are not swelling too much or that extranuclear debris has not already been completely removed. If they appear clean earlier than expected (see Figure 3), proceed to the next step (swelling).

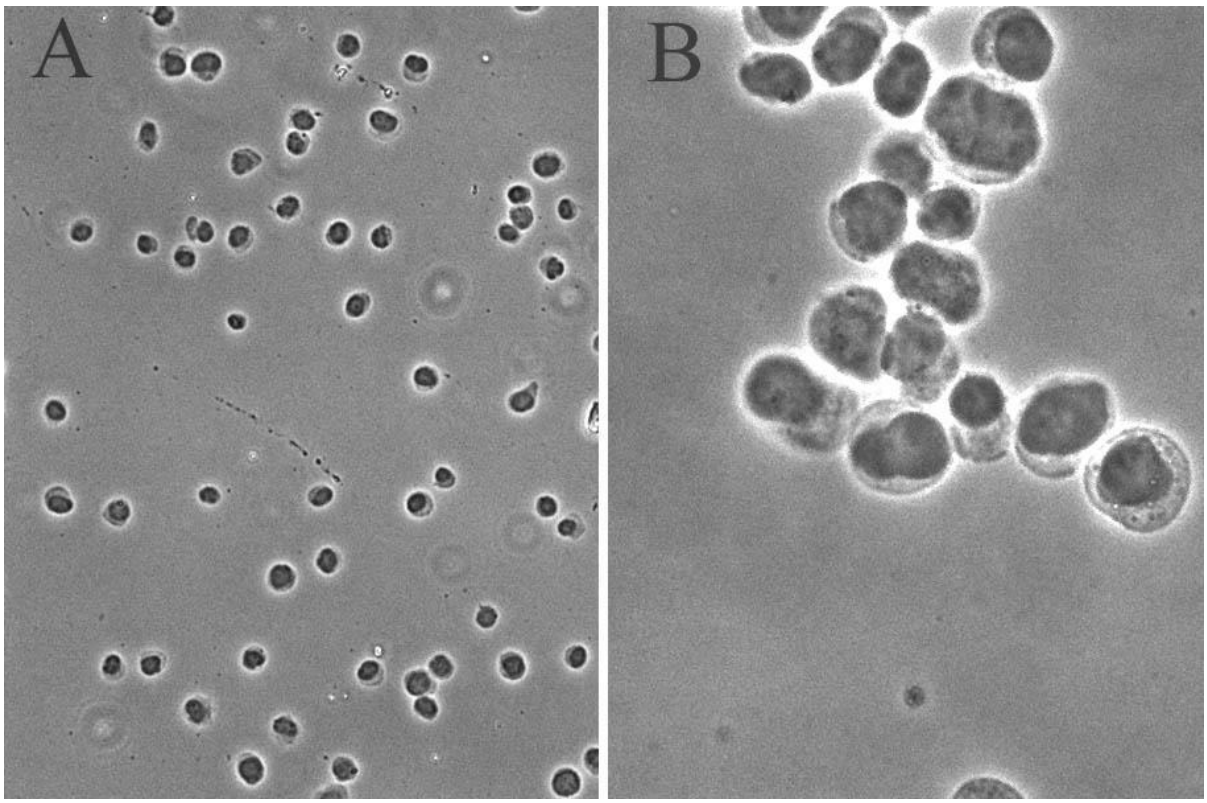

Figure 3. Phase contrast images of nuclei undergoing detergent extraction. (A) iMEF cells after detergent extraction in Prep Buffer A. 10x magnification. (B) iMEF cells after a few minutes of extraction in buffer A. 40x magnification. The nucleus appears as the phase dense center of the particle (i.e. the yolk to the fried egg). The extraction process does not proceed at the same rate for all nuclei. Some nuclei still have visible debris attached while some do not.

In practice, there are two important guidelines for applying the force:

- Part of successful nuclear preparation is the application of force at the correct times. After the initial resuspension of the cells in buffer A, nuclei become very sensitive to shearing forces. Overpipetting or being too forceful with nuclei during steps will lower the yield. While we employ force during the shearing portion of the procedure, it is the only stage where some force is needed to remove the nuclear envelope. When it is necessary to mix the nuclei, favor swirling or flicking the tube over pipetting and always use blunted pipette tips.
- Again avoid contact with the very bottom of the tube. The heat from fingertips is easily transmitted to the extracting solution and can cause the extraction to proceed more rapidly than desired.

7. When the 8 minute timer sounds, add 500µL of ice cold sterile ddH2O to the suspension using a p1000 pipetman equipped with a blunted, sterile barrier tip. Start the timer for 3 minutes. Pipette slowly and briefly (2-3 passages), keeping the tube on ice.
8. Monitor a small (3-5µL) aliquot of the swelling nuclei via phase contrast microscopy at 40x magnification (see Figure 4). They should appear slightly larger than in previous observations. If nuclei appear hyper-swollen, then proceed to the shearing step immediately. Agitate once during the incubation by swirling or flicking the tube. Use this incubation to assemble the syringe and needle for the shearing steps to follow.

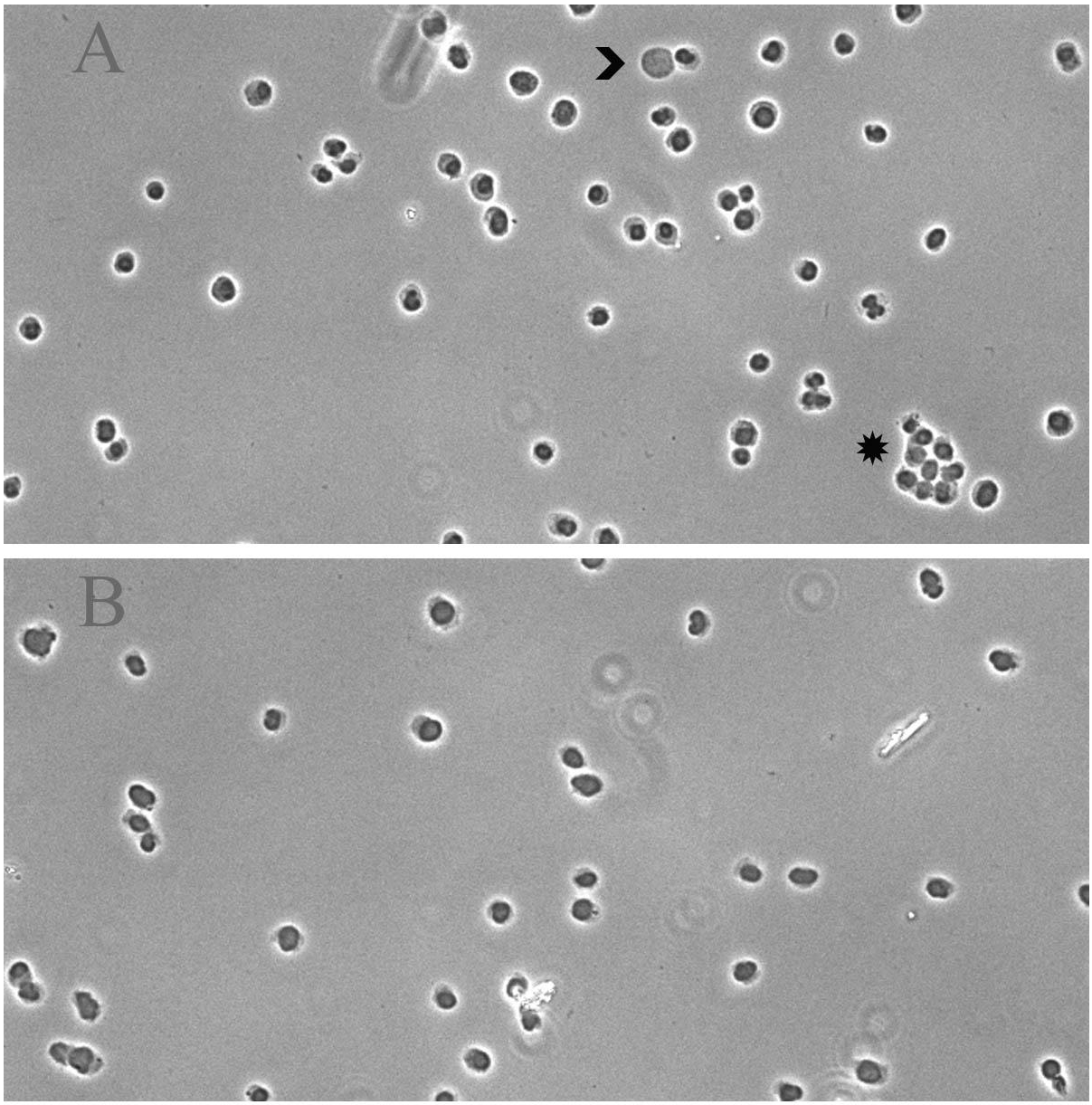

Figure 4. Comparison of extracting nuclei and swelling nuclei. (A) Nuclei again undergoing extraction in buffer A. Magnification is 10x. The chevron indicates a nucleus which has swollen too quickly in the extraction buffer. The star indicates an insufficiently separated clump of cells. Clusters should be separated in the first few minutes of extraction, because the extraction process will not be as efficient for clumped cells. (B) Addition of 500µL ddH2O to the extracting nuclei causes the particles to swell slightly. This is a very subtle change, but notice that the nuclear portion of the extracting particles is consistently larger in *(B)* than in *(A).*

In practice, the degree of swelling can be difficult to control and gauge. If these problems persist, we found the following insight helpful:

- The degree to which the nuclei and cells swell during the extraction process is dependent on the density of extracting cells in the suspension. Hyperswelling is an indicator that too few cells are being extracted. No perceptible swelling may be a sign that the starting pellet contained too many cells, but this is often difficult to observe because the necessary amount of swelling is subtle. Neither situation is without remedy. To prevent this from happening in future preparations, revisit cell counting techniques.

2.5.4 Shearing Nuclei and Nuclear Envelope release

The passage of nuclei through an appropriately gauged needle promotes release of the majority of the nuclear envelope. MEF cell lines require a 1.5 inch 22-gauge needle for shearing the nuclei. The addition of a buffer containing Mg2+ encourages release of envelope remnants. After the release, an envelope-free endonuclear particle is ready for differential sedimentation.

1. At the end of the 3 minute swelling step, insert a 22-guage needle attached to a sterile 5mL luer-lock syringe into the nuclear suspension. Keep the tube on ice.
2. Passage the nuclei through the needle 3 times using considerable force.

   In practice, proper application of force can be problematic to learn. We provide three helpful learning tips:

   - When shearing nuclei, there should be considerable resistance in the syringe for nuclear envelope removal. The amount of time consumed by an upstroke or a downstroke of the needle is about 7 seconds under normal conditions. In

the event that nuclei are hyper-swollen, either increase amount of time for each passage through the needle (10-15 seconds on each upstroke or down stroke) or decrease the number of passages.

- If nuclei appear resistant to shearing, more forceful passaging through the needle may be necessary. However, under the conditions described above, not more than 4 passages should be necessary for successful removal of debris. In fact, adding additional passages is equally harmful as it is cleansing.
- We recommend the use of a luer-lock syringe over a syringe with a slip-tip. In the event that the nuclei are resisting envelope release, the seal between the needle and the syringe in a standard needle syringe is not tight enough to generate the necessary force.

3. Pipet 3-5µL of triturate onto a glass slide. Top with a coverslip and examine at 40x magnification on a phase contrast microscope.
4. Examine the nuclei and ensure that the majority of nuclei have lost any associated debris (see Figure 5). We recommend examining as many nuclei as possible, but at least 50 should be examined. Of those 50, at least 40 should exhibit minimal associated debris. If fewer than 40 of the 50 nuclei examined have no associated debris then add an additional passage through the needle.

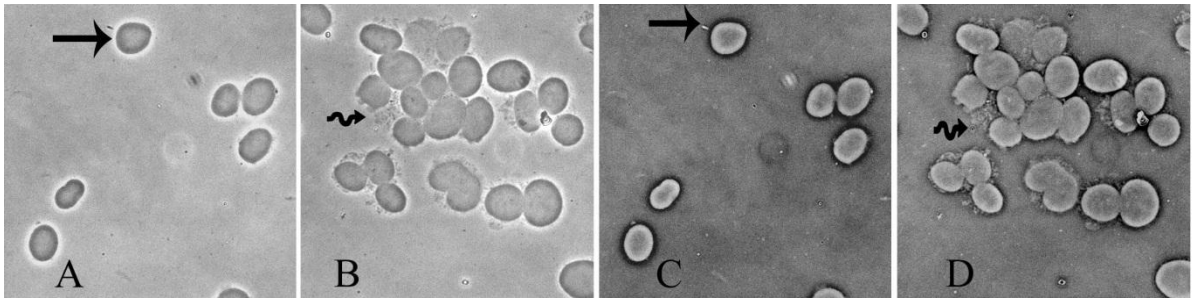

Figure 5. Successfully sheared vs. unsuccessfully sheared nuclei. All images are taken at 40x magnification. (A) Loss of extranuclear debris after shearing the swollen particles 3x through a 22-gauge needle. Note that the phase dense center of each particle remains (arrow), but the lighter surrounding material has been effectively removed. (B) Insufficiently sheared nuclei remain decorated with material that does not resemble a nuclear particle (squiggly arrow). An extra passage is needed here to remove the remaining cytosolic debris. (C-D) Negative images of A and B (respectively) to contrast the smoothness of successfully sheared nuclei with the unsuccessfully sheared product.

In practice, we find that any additional passages through the needle are an indicator of too many cells undergoing extraction.

5. Using a p1000 pipetman equipped with a blunted, sterile barrier tip, add 500µL of chilled Buffer B to the sheared nuclei. Pipet up and down slowly a few times to mix. Avoid excessive trituration.
6. Examine 3-5µL of triturate again on a glass slide using a phase contrast microscope. The addition of buffer B causes a visible change in the appearance of the nuclei which we have termed "unveiling". Unveiled nuclei have greater contrast, and the lamin boundary and nucleoli become more pronounced (see Figure 6). At this stage, more than 45 of 50 nuclei should appear as such, with little to no associated debris.
7. Remove 100µL of the suspension containing the unveiled nuclei and cellular debris. Save in an eppendorf tube as the whole cell fraction for quality controls.
8. Cap the stripped nuclei and proceed immediately to the pelleting steps.

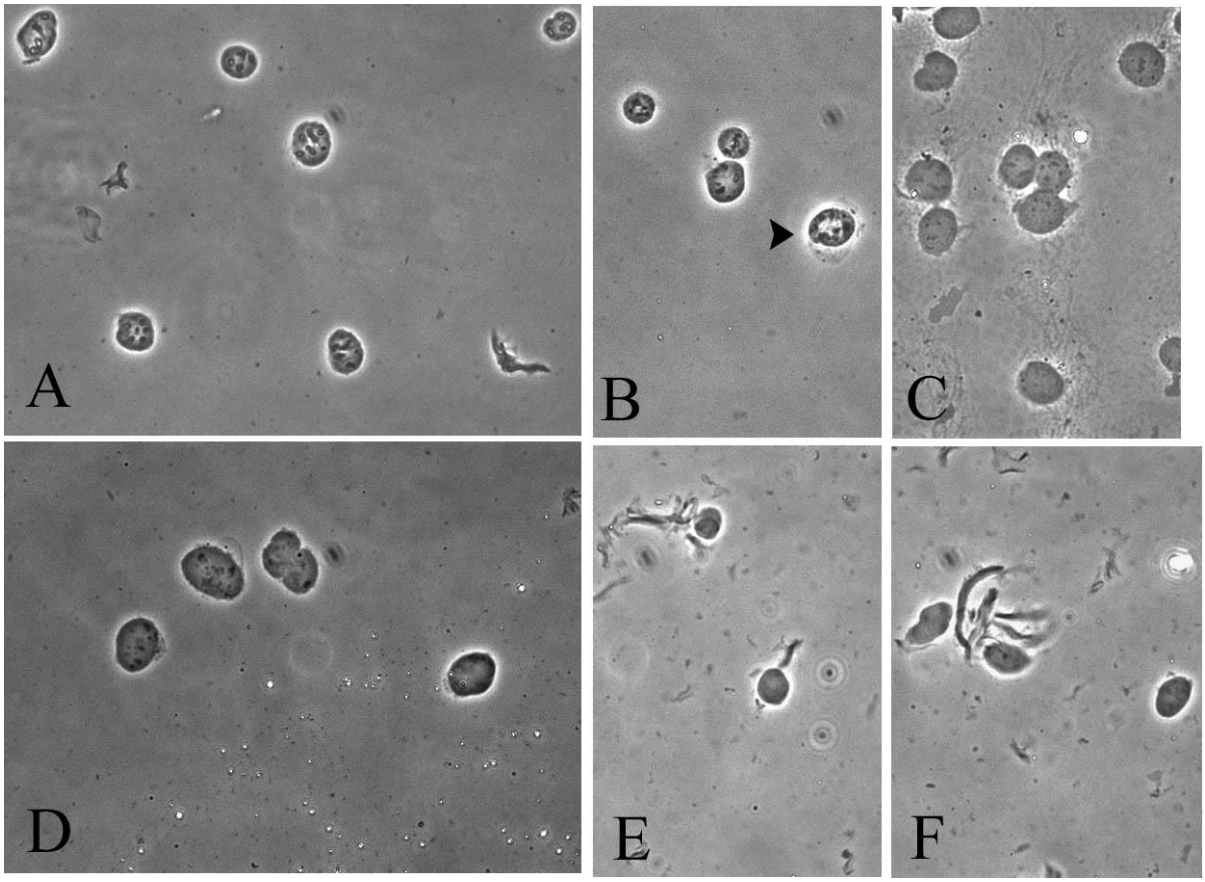

Figure 6. Unveiling of sheared nuclei. All phase contrast images are taken at 40x magnification. (A) Extracted, sheared nuclei supplemented with 500µL of Buffer B. Each of the nuclei has been sufficiently unveiled. Note the increased contrast of the nuclear borders and nucleoli. (B) As in *(A)*, except that the arrowhead indicates a nucleus which has unwanted attachments (C) Removal of $MgCl_2$ from the buffer causes causes the nuclei to swell further, and the nuclei do not become unveiled. (D) Nuclei isolated from overgrown cells. Under these growth conditions, the nuclear envelope is resistant to removal. (E-F) Substitution of 2mM KCl (E) or 10mM KCl (F) for the 2mM MgCl2 in Buffer B causes nuclei to become destabilized. Most nuclei under these conditions disintegrate, but the few that remain do not resemble those treated with the normal buffer B.

2.5.5 Sedimentation of Envelope-Stripped Nuclei

We use very slow speeds to sediment envelope-free nuclei and not their enveloped, more buoyant counterparts. Because the nuclei are in detergents, it is important to proceed with haste through each step including the centrifugation. Reserve and thoroughly chill centrifuges prior to beginning the preparation. The addition of a few minutes to the prep time before the nuclei are centrifuged will affect the integrity and yield of the nuclei.

1. After examining the unveiled state of the nuclei, place them with a balancer in a table top centrifuge chilled at 4ºC. As we use very slow speeds to sediment nuclei, it is important to have a centrifuge with precise control.
2. Set the centrifuge to spin for 10 minutes at a speed of 86 x *g*. In the interim, chill a sterile 15mL conical tube and three eppendorf tubes in the ice bucket for the upcoming washes and taking fractions for quality controls.
3. Proceed quickly through this and the next 2 steps. Remove the tube from the centrifuge once the spin has ended and place immediately on ice taking care not to disturb the pellet. The pellet should appear glassy and bluish.
4. Using a p1000 pipetman equipped with a barrier tip, remove the supernatant (cytosolic fraction). If performing quality control or protein analysis, then save 100µL of cytosol to a chilled eppendorf tube; otherwise, discard. Make sure to remove as much of the supernatant as possible to avoid transferring membranous debris to the purified nuclei.
5. Blunt a 1mL sterile barrier tip, and gently overlay the pellet with 500µL of Buffer B. Do not triturate just yet, but remove the pellet as a plug and transfer to the new chilled 15mL conical tube.

6. Keeping the tube on ice, pipette gently a few times to partially disrupt the pellet. Do not pipet too much or this will destabilize the nuclei. Remove the tube from the ice only briefly to check the behavior of the nuclei. Visible clumps should remain in the suspension.

    In practice, we made two helpful observations:

    - Nuclei naturally aggregate when the envelope is removed successfully. This is not a problem. In fact, it is an indicator that the envelope has been removed well. If nuclei are snowy and easily dissociated from one another, this is a sign that envelope-removal was ineffective.
    - If nuclei are consistently prone to extreme aggregation, the wash can be changed from Buffer B to HBSS without Calcium or Magnesium. This is less preferable when the nuclear pellets are going to be analyzed by mass spectrometry.

7. Add an additional 1.5mL Buffer B to the pellet and swirl to mix. Return nuclei to the chilled centrifuge for a second 10 minute spin at 86 x *g*.
8. The pellet at this point should be white. Remove and discard the wash.
9. If intending to use nuclei for assays that are less sensitive to detergents, then remove the wash and proceed as needed. If intending to use nuclei for mass spectrometry, then a second wash is preferred. Blunt a sterile 1mL barrier tip and pipette 1mL of buffer B onto the pellet. Remove the pellet as a plug and transfer to the second chilled eppendorf tube.
10. Triturate slowly and gently using the blunted tip. Break up clumps as much as possible but avoid over-triturating the purified particles.

In practice, we have found that it is nearly impossible to separate purified nuclei from one another without suffering large decreases in yield.

11. Blunt a 200µL barrier tip and remove 150µL of the purified nuclei to the third eppendorf tube for quality control analyses. Store on ice. Pipet a few µL onto a slide, avoiding clumps, and again examine the purified product to ensure that the nuclei have not changed dramatically in their morphology (see Figure 7).
12. In a chilled eppendorf centrifuge, pellet the nuclei at 500 x *g* for 2 minutes.
13. Remove the supernatant as thoroughly as possible. If the nuclei are intended for later use, flash freeze the pellet in liquid nitrogen and store long term at -80ºC. Also store quality control fractions at -80ºC if not processing immediately.

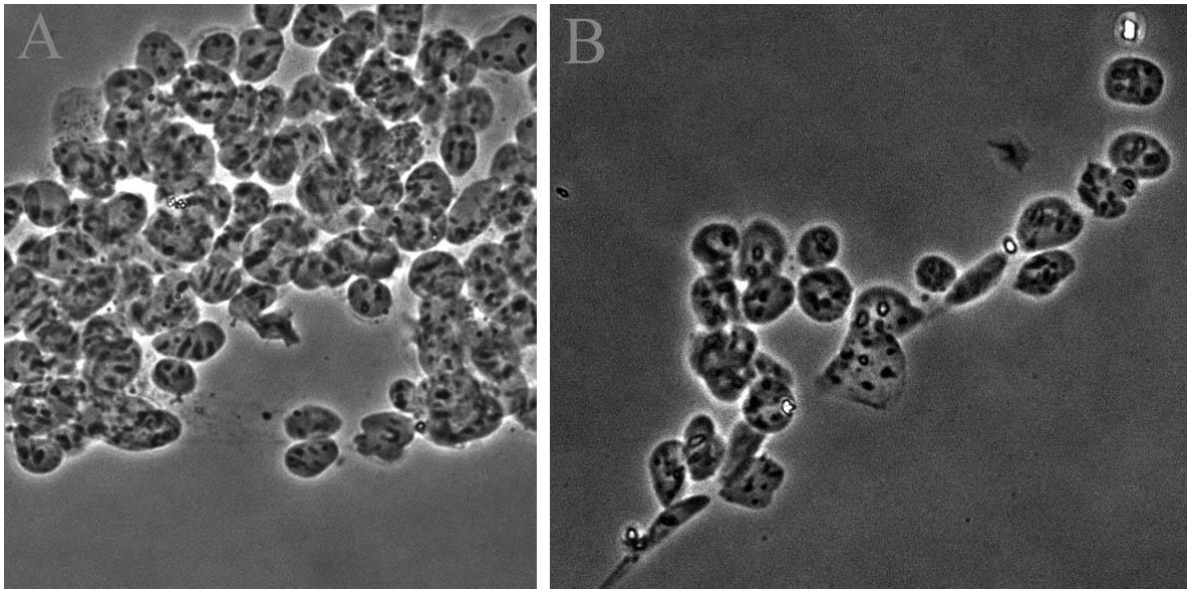

Figure 7. Highly purified envelope-free nuclei aggregate but maintain their nuclear morphology. All phase contrast images are taken at 40x. (A) Highly purified nuclei – large aggregate. (B) Highly purified nuclei – smaller aggregate. Breaking up the purified pellet deforms some of the nuclei, but they remain visibly similar in density to their non-deformed neighbors.

2.5.6 Manipulation of Envelope-Free Nuclei for Total Protein Content

It is important to break up the nuclear and cellular pellets to recover as much protein as possible. Nuclei are particularly resistant to destruction and require extensive trituration through a needle to break them apart.

1. Thaw whole cell, cytosolic, and purified nuclear quality control fractions (if necessary) in an ice bucket.
2. Meanwhile, add 40µL of fresh protease inhibitor cocktail (Roche Biopharmaceuticals) to 960µL of M-PER lysis reagent (Roche Biopharmaceuticals). Keep the solution on ice.
3. Once the purified nuclear fractions have been thawed, pellet the nuclei briefly in a 4ºC table-top eppendorf centrifuge (2 minutes at 500 x *g*). Remove the supernatant from the nuclear fraction.
4. Add 200µL of M-PER supplemented with protease inhibitors to the nuclear pellet. Blunt a low-retention pipet tip and triturate the nuclei briefly to break up the pellet. This is not to protect the nuclei. Instead, it is intended to prevent any clumps from sticking to the walls of the pipette tip.
5. Add an additional 100µL of M-PER reagent to the whole cell and cytosolic fractions. Pipette up and down slowly to mix.
6. Vigorously passage purified nuclear fractions at least 20x through a 22-gauge needle attached to a 1mL syringe. Take care to avoid excess bubbles. If there is considerable resistance, then continue to triturate until the resistance lessens.

In practice, we have one suggestion:

- Try to use short length needles (less than 1"). This will guard against loss of material. Also, the resistance in the syringe will increase as nuclei disintegrate. Continue triturating with this gauge needle until the resistance begins to lessen. Otherwise, subsequent trituration with smaller needles will be very difficult.

7. Using separate needles/syringes, repeat disruption with whole cell and cytosolic fractions. These fractions should require significantly less trituration.
8. Vigorously triturate purified nuclei again through a 25-gauge needle at least 30 times.
9. Examine a few µL of triturate on a phase contrast microscope using at least a 40x objective. If no intact or even partially destroyed nuclei are observed, proceed to the next step. If there are intact nuclei, continue triturating until nuclei are completely disrupted.

   In practice, *if* nuclei are resistant to disruption, continue with a 27-gauge needle or triturate more vigorously.

10. Repeat with whole cell and cytosolic fractions. Make certain that any nuclei are destroyed in these fractions as well.
11. Spin fractions at max speed for 10 minutes to pellet any DNA. Remove supernatant to fresh eppendorf tubes. If the DNA pellet is needed for additional manipulations, then keep it on ice or store at -20ºC.

    In practice, some proteins will remain bound to the DNA even after extensive trituration because they require acidic conditions to be separated from DNA. To extract these proteins from the DNA pellets, completely resuspend pellets in 200µL of 0.4 H_2SO_4 and rotate on a platform for at least 30 min. Pellet debris at max speed

and save the supernatant containing the acid extracted proteins. These proteins will require precipitation for use in protein analysis (BCA or Western).

12. Dilute whole cell and cytosolic fractions 1:10 in ddH20. Dilute the purified nuclear fractions either 1:5 or 1:10 in ddH20.
13. Analyze protein content according to the protocol for BCA assay for microplate reader (Thermo Scientific). The recommended linear range for BSA standards is from 25µg/mL to 1mg/mL, with emphasis placed on the lower half of the curve. All standards should contain similar concentrations of the buffers in the cellular fractions.
14. For Western analysis of cellular fractions, we recommend precipitating the triturate and resuspending in a smaller volume. We do this using the SDS-PAGE clean-up kit.

    In practice, Western analyses of the Histone content should include the acid extracts from the DNA pellets. Some histone proteins will be released using M-PER, but a considerable portion of Histone proteins, particularly those which are modified and in lower abundance, remain in the acid extract. Precipitate these and the M-PER extract, combining them into a single aliquot with resuspension.

In terms of protein yield, we find that the yield of nuclear protein is between 3 and 15 percent of whole cell protein. The average amount of protein found in a 1x nuclear preparation (1 x 10^7 cells) is between 100-400µg nuclear protein.

2.5.7 Fixing and Fluorescent Staining of Nuclear Particles

The use of fluorescent dyes or molecules in nuclear preparations can be useful in confirming that purified nuclei are indeed nuclei. Immunofluorescence and staining can also be used to confirm that the purified nuclear particles do not contain unwanted elements, such as membranes or cytosolic proteins. Because nuclei are sensitive to handling, we

recommend fixation prior to most staining procedures. However, some dyes (such as Hoescht and DAPI) can be incorporated into buffers during the extraction process. This type of "multitasking" to combine purification and staining prevents additional manipulations that might damage the purified nuclei. Expression of fluorescent proteins in intact cells prior to nuclear isolation is also particularly useful as a quality control measure.

Use of DNA Stains During Nuclear Extraction:

1. Incorporate DAPI or Hoescht into the nuclear preparation buffers at least 1 step prior to the fixation point. For example, if you wish to fix nuclei after the first pelleting step, incorporate DAPI or Hoescht into Buffer A or Buffer B at a concentration of 1:1000. Alternatively, mounting media containing Hoescht or DAPI are available for purchase, and can eliminate the need to stain nuclei during the procedure entirely. If nuclei are stained during the nuclear isolation procedure, we still recommend fixation of nuclei for longer term storage, as we explain in the next section.

Fixation of Nuclear Particles:

1. After envelope-free nuclei undergo their final wash, pellet the nuclei for 2 minutes at 500 x *g*. Completely remove the supernatant.

   In practice, if nuclei are only intended for staining experiments, it is best to make HBSS the final wash buffer before fixation.

2. Keeping the tube on ice, resuspend nuclei in 1mL of ice cold Methanol (stored at -20ºC) using a blunted, low retention barrier pipette tip.
3. Place tubes in the freezer for 20 minutes, inverting once or twice during the incubations.

4. In the freezer, allow nuclei to settle to the bottom of the tube after the last inversion. If nuclei are not easily sedimenting in the tube, then pellet gently at 500 x *g* for 2 minutes at 4ºC.
5. Remove the supernatant carefully, keeping the tube on ice.
6. Gently add 1mL of chilled HBSS to the tube. Cap the tube and invert several times to wash nuclei. Return the tube to ice. Wait 5 minutes and again invert the tube to mix.
7. Allow the nuclei to settle and remove the wash.
8. If nuclei are to be additionally stained, proceed immediately to blocking or staining with dyes. If mounting without additional staining, then add 50µL or 1 drop of mounting media to the tube.
9. Blunt a 200µL tip and gently triturate. Avoiding clumps if possible, pipette 10-20µL onto a glass slide. Top gently with a coverslip and seal the edges with nail polish. (see Figure 8)

Staining Purified Envelope-free Nuclei with Nile Red:

1. To protect the Nile Red solutions which are light sensitive from over exposure, find an area that has poor or minimal lighting or work out of amber tubes.
2. In a light sensitive tube, make a working solution of Nile Red that is 10µg/mL in acetone.
3. Add 1000µL of HBSS to purified and fixed envelope-free nuclei that have been washed once to remove trace MeOH.
4. Pipette 10µL of Nile Red into the Nuclei resuspended in HBSS. This is a 1:100 dilution. Avoid pipetting up and down if possible.

5. Cap the tube and invert several times to mix. Allow nuclei to stain in the dark for at least 5 min at room temperature. Do not invert again. Instead, allow nuclei to settle to avoid future centrifugation.
6. Wash nuclei 2x in 1mL HBSS, avoiding unnecessary pipetting or centrifugation.
7. Mount nuclei as described in the previous section.

Examples of the Hoescht and Nile Red Staining of purified envelope-free nuclei are provided in Figure 9. We have examined the Nile Red staining in the long red range (580-610) which examines phospholipids in the purified nuclei. Any detectable lipid attached to these nuclei is peripheral to the nuclear particle and is not abundant. We have chosen to show this in a cell line that overexpresses Histone H2B covalently linked to GFP (generous gift from Ted Salmon). Neutral lipids stained with Nile Red absorb and fluoresce in the same wavelength range as GFP fluorescence. Thus, under these circumstances we did not examine the neutral lipid population which includes sterols, diacylglycerol, and triglycerides.

Although we have not attempted to stain nuclei with antibodies using this procedure, we are convinced that the fixed purified nuclei can withstand several rounds of washing, which would be necessary during an immunostaining procedure. Without fixation, considerable loss of endonuclear material would occur.

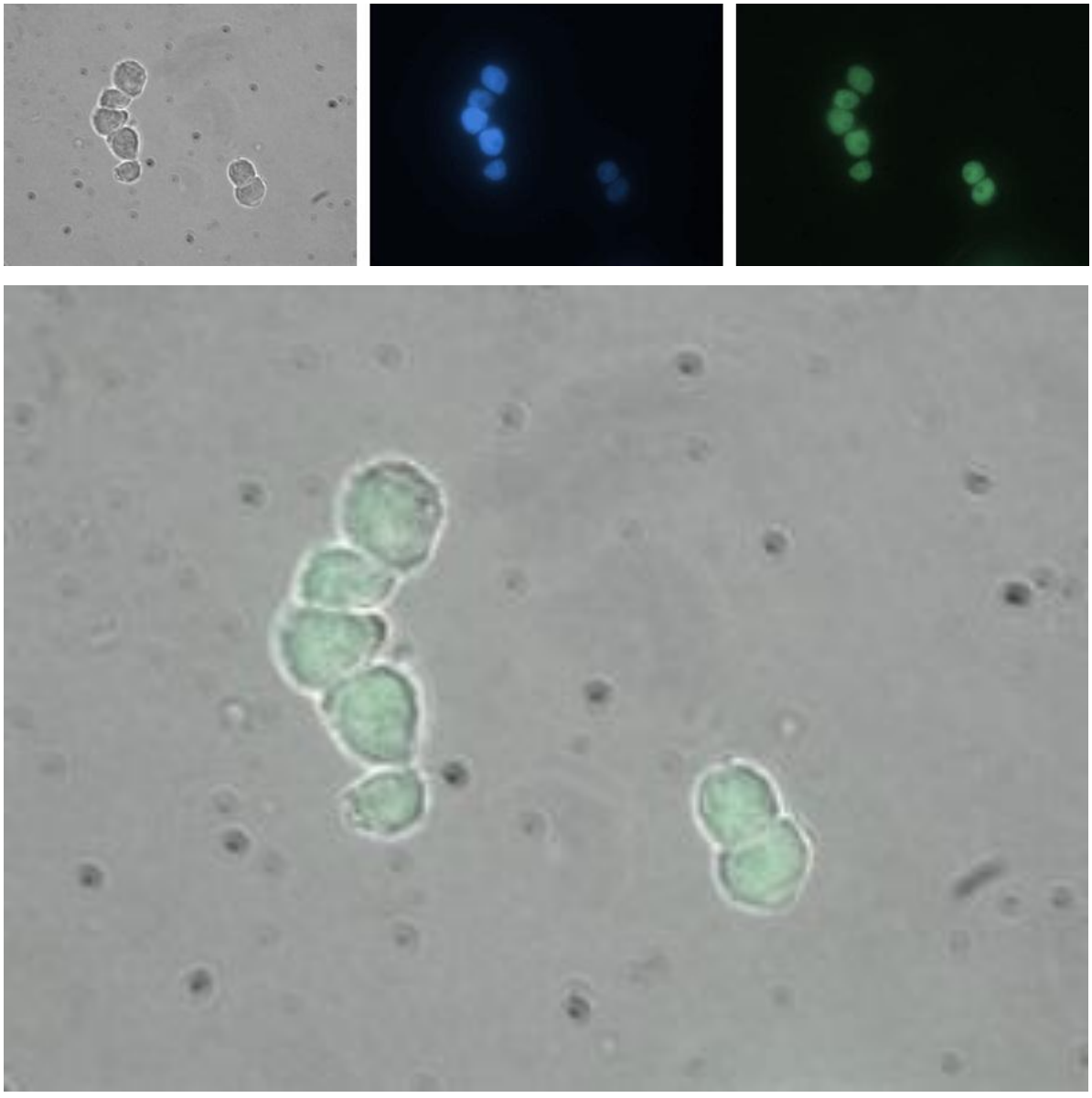

Figure 8. Hoescht staining of envelope-stripped nuclei. Images are at 63x magnification. Envelope stripping procedures were used on HeLa tissue culture cells stably expressing H2B-GFP (generous gift of Ted Salmon). HeLa cell nuclei were extracted as with iMEF nuclei to remove the nuclear envelope. A 25-gauge needle was used to shear the nuclei, which are smaller than MEF nuclei. Hoescht was included at 1:1000 in the extraction buffer. Purified nuclear particles were fixed in Methanol, mounted on slides and imaged on an inverted TC microscope (A) Brightfield image, (B) Hoescht staining, and (C) H2B-GFP fluorescence.

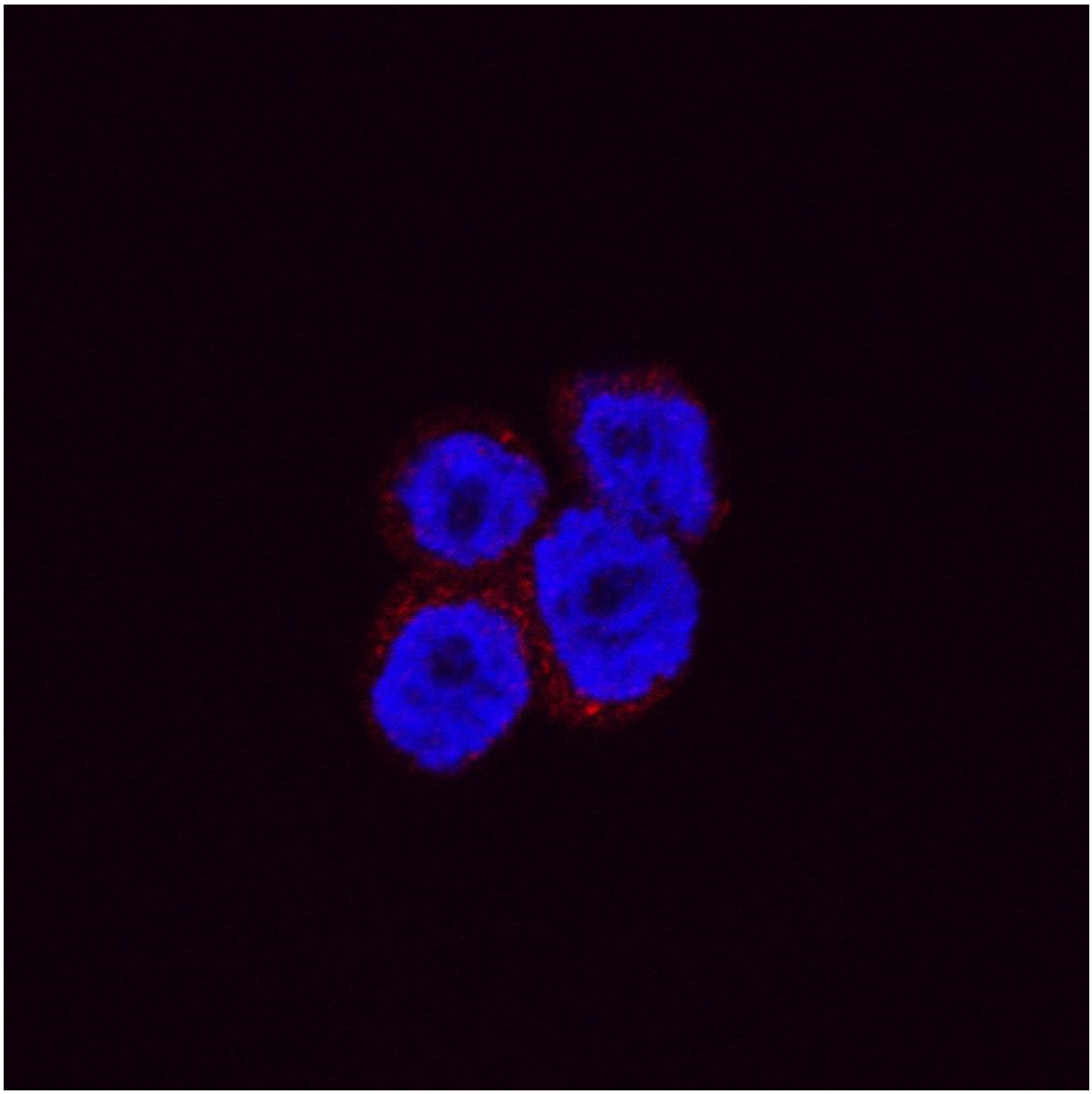

Figure 9. HeLa H2b-GFP nuclei stained with Nile Red and Hoescht. The nuclei are not well stripped by this protocol and we see phospholipids (in red) surrounding the nuclear material (in blue).

2.6 Discussion

In this chapter, we have described in detail a protocol for the purification of envelope-free nuclei from immortalized MEF cells and primary MEF cells. This protocol, however, has not been similarly proven in other cell types. In the evolution of the method, we have discovered that harsh physical manipulations are necessary for removal of the inner nuclear envelope in MEF cell types (both immortalized and primary). In comparison, commonly used cancer cell lines and primary liver cells typically require less time in detergent and less manipulation for nuclear envelope release [41, 50]; however, we note that if subjected to the same purification criteria, others' protocols may require adjustment.

All of the steps in our protocol are necessary for true removal of the inner nuclear envelope and avoiding measurement of contaminants as bona fide endonuclear components. Thus, nuclear integrity is sacrificed slightly for purity. Substantial resistance to envelope release has been documented in another fibroblastic cell line [42], which also requires high concentrations of detergents to remove the envelope. This explains why fibroblastic cell lines are not frequently used in the generation of envelope-free nuclei, despite their usefulness.

Currently, the published methods to separate nuclei from their envelopes exclusively involve detergent extraction. This is beneficial in that detergents are very efficient in removing membranes and are currently the best way to separate the nuclear particle from the envelope. Unfortunately, enzymatic methods that would encourage the release of the envelope also have significant effects on the overall biology and morphology of the nuclear particle.

One possible alternative method that will decrease exposure to detergents is to purify nuclei with envelopes and then remove the envelope afterwards. Classical approaches to nuclear purifications involve high salt concentrations which disrupt morphology. Recently, a report of a nuclear purification technique emerged that uses concentrated inert polymers or molecules (e.g., Polyethylene glycol or Dextran) to mimic cytosolic pressures on the nuclear envelope. This method does not require detergents, and thus detergents could be used very briefly to remove the inner and outer nuclear envelope from isolated nuclei.

Regardless of the purification protocol, visual cues are invaluable in creating purified nuclear particles with minimal unwanted cytosolic debris, and will certainly be useful tools for creating new envelope-removing, nuclear purification protocols for other cell types. The use of phase contrast microscopy is invaluable for preparing nuclei with consistently high quality as it enables real-time adjustments to the time of incubations, the force needed to remove the envelope, and/or the volumes of buffers as the nuclei progress through the purification. In addition, the use of microscopy helps in the selection of buffer elements for the preparation. The unveiling of nuclei observed with the addition of Magnesium ions is a hallmark of the purification process and cannot be replaced by Potassium (a monovalent cation). This is important, as several have criticized the use of Magnesium in nuclear preparations for its ability to "destabilize" nuclei [18]. While the use of Magnesium indeed causes some loss of nuclear material, the loss of this material is accompanied by the loss of the inner nuclear envelope which is more critical for measuring matrix associated lipids. This is confirmed by the behavior of the final nuclear product, which behaves in a particulate manner in spite of forming aggregates.

Even though it is a useful protocol tool, the ability to visualize nuclei during the envelope removal process has been underused in formulating quality controls that interrogate membrane-free status . The classically employed quality control measures that serve this purpose include western blot for nuclear and cytoplasmic markers and transmission electron microscopy (TEM) of purified nuclear particles [41, 51]. These quality controls (and our expanded, more quantitative suite of quality controls discussed at length in the next chapter) are more informative in probing the success of envelope stripping than prior methods. However, they have a few drawbacks that make development of fluorescent assays to assess membrane status very attractive. For instance, TEM is a direct interrogation of the membrane bilayer content of envelope-free nuclear preparations, but does not easily identify non-classical lipid structures. Moreover, Western blot is a great bulk assay that examines the absence of cellular membrane markers, but it is at its core an indirect assay. Both of these techniques require a significant quantity of nuclei (which are often precious) and considerable time for processing.

Fluorescence assays that label lipids and/or proteins could nicely complement the drawbacks of classical quality controls used in purifying envelope-free nuclei. Many of the critical steps could be performed prior to nuclear extraction. Commercially available lipid dyes (e.g., Nile Red, DiI, etc.) and fluorescently labeled lipids (e.g., Bodipy-conjugated PtdCho) can be used to label living whole cells [52, 53]. Extraction of nuclei from these labeled cells would allow a before and after comparison of the whole cell and the purified, envelope-free nucleus. As the purified nuclei fix easily in methanol, a small amount of purified product could be simply fixed, mounted on a slide, and examined on a confocal microscope. Other advantages to such an experiment include: i) examining or identifying

non-classical lipid structures, ii) identifying contaminants preserved or introduced during purification, iii) examining the intactness of the purified nuclear particle, iv) rapid processing times, and v) minimal manipulations of the purified substances that could inadvertently destroy the true morphology of the particle or remove purified elements. However, the use of detergents during nuclear preparations could be problematic in retention of some lipid labels that have high partition coefficients and are easily extracted by detergents. This would not prevent the use of lipid dyes, as they may still be used to quickly stain nuclei after the purification as well. It would be best to confirm that fluorescent labeling of nuclei before purification produces a similar result to nuclei fluorescently stained after purification.

CHAPTER 3

QUANTITATIVE PROFILING OF THE ENDONUCLEAR GLYCERO-PHOSPHOLIPIDOME OF MURINE EMBRYONIC FIBROBLASTS

3.1 Summary

A rapid and reliable method for purifying quality envelope-stripped nuclei from immortalized murine embryonic fibroblasts (iMEFs) was established. The method integrates an expanded suite of quality control criteria that are essential for confident assessments of purity. Quantitative profiling of the glycero-phospholipids (GPLs) in envelope-free iMEF nuclei prepared by this method yield several major conclusions. First, we find the endonuclear glycero-phospholipidome differs from that of bulk membranes, and phosphatidylcholine (PtdCho) and phosphatidylethanolamine (PtdEtn) species are the most abundant endonuclear GPLs by mass. By contrast, phosphatidylinositol (PtdIns) represents a minor species. Contrary to the prevailing view, we find only a slight enrichment of saturated versus unsaturated GPL species in iMEF endonuclear fractions. Moreover, much lower values for GPL mass were measured in the iMEF nuclear matrix than those reported for envelope-stripped IRB-32 nuclei. The collective results indicate that the nuclear matrix is a GPL -poor environment where GPL occupies only ca. 0.1% of the total nuclear matrix volume. This value suggests GPL accommodation in this compartment can be satisfied by binding to resident proteins.

3.2 Introduction

The mammalian nuclear matrix is a recognized site of lipid biosynthesis and signaling [reviewed in 18, 19, 49, 54-56]. Radioisotope and stable isotope tracer studies consistently identify GPLs, and the enzymatic activities that metabolize them, within purified nuclear fractions purportedly devoid of nuclear envelope and other cellular membrane contaminants [17, 28, 33, 41, 57, 58, 59]. These findings suggest the existence of an independently-regulated GPL pool within the nuclear matrix -- one distinct from the nuclear envelope and from bulk cellular membranes. In support of this interpretation, nuclear isoforms of a number of GPL metabolic enzymes have been described [21, 22, 24, 57, 58, 39, 40, 60, 61]. The STAR-PAP RNA poly-A polymerase provides a compelling example of a GPL-regulated enzyme which discharges its function within the nuclear matrix [20, 62]. At issue, however, is the scale of nuclear GPL metabolism and nuclear glycerol-PL load. Quantitative mass spectrometric methods have made address of these issues feasible. The one major study on this topic estimates that GPL occupies 10- 16% of the nuclear matrix of IRB-32 cells by volume [17]. This value is quite high considering that the genome is estimated to occupy some 39% of the nuclear volume in the IRB-32 cell line. Furthermore, the endonuclear GPL pool is reported to be unusual in that it is dominated by saturated PtdCho molecular species. The abundance of endonuclear GPLs, when coupled with their predominantly saturated nature, motivates speculation that PLs significantly influence the chemical properties of the nuclear matrix – i.e., by contributing to the formation of gel-like regions within the nuclear matrix [17, 19]. This concept raises a fundamental question of how the nuclear matrix accommodates such a large PL load? That is, how are lipids organized within the nuclear matrix?

Given the mounting evidence for endonuclear lipid signaling, and the lingering questions regarding how lipids are organized in nuclear matrix, we re-investigated the problem of endonuclear lipidomics. To this end, we developed a reliable and reproducible method for purification of envelope-free nuclei from immortalized murine embryonic fibroblasts (iMEFs). This method adheres to a stringent quality-control regime for assessing purity of isolated endonuclear compartments.

Quantitative GPL profiling of these highly purified fractions describes an endonuclear GPL composition which is distinct from that of bulk cellular membrane. Contrary to previous reports, however, the profile shows no particular enrichment of saturated GPL molecular species. Moreover, the mass measurements record considerably lower GPL content in endonuclear compartments than those previously reported. The collective data confirm the nuclear matrix harbors a GPL pool of distinct composition from that of bulk membrane. The data further indicate the MEF nuclear matrix to be a PL-poor environment that requires no unusual provisions for PL accommodation other than binding to resident proteins.

3.3 Materials and Methods

3.3.1 Reagents and General Notes

Chemicals and reagents were purchased from Fisher Scientific (Pittsburg, PA) or from Sigma-Aldrich (St. Louis, MO), unless otherwise stated. All lipid standards were purchased from Avanti Polar Lipids (Alabaster, AL). Organic solvents and supplies used to prepare samples for electron microscopy were obtained from Electron Microscopy Sciences (Hatfield, PA).

3.3.2 Media and Antibodies

Dulbecco's Modified Eagle Medium (DMEM) and antibiotics were obtained from Gibco/Invitrogen (Carlsbad, CA). Fetal bovine serum was obtained from Gemini Bio-products (Sacramento, CA). A mouse monoclonal antibody directed toward β-tubulin (product no. T5293) and rabbit polyclonal antibody directed toward lamin A (product no. L1293) were obtained from Sigma Aldrich. A mouse monoclonal antibody towards α-tubulin was obtained from Neomarkers Inc. (Fremont, CA; product no. MS-581-P). Other rabbit polyclonal antibodies utilized in this study include: an anti-calnexin antibody (from Stressgen Assay Designs; Ann Arbor, Michigan; product no. SPA-860), an anti-histone H3 antibody (generous gift of Brian Strahl, UNC-Chapel Hill), an anti-NURIM antibody (Santa Cruz Biotechnology, Santa Cruz, CA; product no. sc-133260) and an anti-fibrillarin antibody (Abcam Inc., Cambridge, Massachusetts; product no. ab5821). Goat-anti-mouse or goat-anti-rabbit horseradish peroxidase (HRP)-conjugated secondary antibodies (BioRad, Hercules, CA) were used for development in enhanced chemi-luminescent (ECL) assays. Donkey-anti-rabbit secondary antibody, conjugated to IR Dye 800 was purchased from Rockland Immunochemicals Inc. (Gilbertsville, PA; product no. 611-731-127) for use in Odyssey immunoblotting experiments.

3.3.3 Cell Culture and Transfection

Murine embryonic fibroblasts (MEFs) were derived from E14-E16 embryos, and immortalized MEF lines were generated using the SV40 large T-antigen method [63]. Unless otherwise specified, all primary and immortalized cell lines were cultured in complete Dulbecco's Modified Eagle Medium containing 4.5 g/L glucose and supplemented with 10%

FBS, 1 U/mL penicillin G, and 100 μg/mL streptomycin (complete DMEM). All cell culture was performed at 37°C in a 10% CO_2 incubator.

3.3.4 Initial Steps in Purifying Envelope-Stripped MEF Nuclei

Envelope-stripped nuclei were prepared using the method of Martelli *et al*. [57] with essential modifications: iMEF cells were seeded to 150 mm tissue culture dishes and grown for 24-48 hours. Approximately 10^7 iMEFs were pelleted (for a 1x preparation) and washed three times in Dulbecco's Phosphate Buffered Saline solution. After complete removal of PBS, the cell pellet was resuspended thoroughly in 500 μL of chilled Buffer A (10 mM Tris-HCl pH 7.4, 1% NP-40, 10 mM β-mercaptoethanol, 0.5 mM PMSF) supplemented with Complete Protease Inhibitor cocktail (Roche Biopharmaceuticals). Cells were incubated on ice for 8 minutes with occasional agitation. An equal volume of ice cold ddH_2O was added to swell the cells. Following a 3 min incubation, swollen cells were subsequently subjected to three passages through a 22-gauge needle. Removal of cellular debris was monitored by examination of several μL of triturate by phase contrast microscopy. In sufficiently sheared samples, minimally 40 of 50 nuclei examined lacked significant cytosolic or membranous debris. After addition of 0.5 mL of chilled buffer B (10 mM Tris-HCl pH 7.4, 2 mM $MgCl_2$) supplemented with protease inhibitors, the nuclei were gently triturated and again examined by microscopy. Nuclei were returned to ice for 1 min in preparation for centrifugation, during which a portion of lysate (representing the whole cell fraction) was saved for immunoblot analysis of cellular markers and total protein quantification.

3.3.5 Ultimate Steps in Purifying Envelope-Stripped MEF Nuclei

Nuclei were sedimented at 86 x *g* for 10 minutes at 4°C. The supernatant (cytosolic fraction) was either discarded or saved for quality control analysis as needed. The crude pellets were washed once with an excess of Buffer B and sedimented again at 86 x *g* for 10 minutes at 4°C. During an unscaled preparation, the purified nuclei were resuspended in buffer B and distributed as necessary for quality control protein analyses. When generating 3x purified nuclear pellets for analysis of phospholipids by ESI LC-MS, the purified pellet was instead resuspended in 1 mL total of Buffer B. Of this suspension, 85% of the final material was pelleted at 500 x *g* for 2 min at 4ºC. Following complete removal of the supernatant, the pellet was snap frozen in liquid nitrogen and stored at -80ºC in preparation for phospholipid analysis by ESI LC-MS. Aliquots (150 µL) were collected for protein measurements and quality controls before the final pelleting step.

3.3.6 Immunoblot Analyses of Envelope-Free Nuclei

In preparation for immunoblot analysis, whole cell lysates, wash fractions, and nuclear pellets were homogenized in M-Per lysis buffer (Thermo Scientific) supplemented with Complete Protease Inhibitor Cocktail (Roche Biopharmaceuticals). Samples were triturated vigorously through a 25-gauge needle until complete sample disruption was achieved (as confirmed by phase contrast microscopy). Samples were clarified by centrifugation, and the supernatant was separated to a fresh tube for protein precipitation. Proteins were precipitated using the SDS-PAGE Clean-up kit (GE Life Sciences; Piscataway, NJ) according to the manufacturer's directions. Precipitates were resuspended in CHAPS buffer (8M urea, 2% CHAPS, and 50 mM DTT). These samples were reconstituted in 1x Laemmli Sample Buffer and analyzed by SDS page (10% gels) and immunoblotting for

nuclear and contaminant membrane markers. Gel loading was normalized by "cell equivalents". When loading gels for Odyssey westerns, the range of signal linearity was determined for each fraction with each antibody.

Resolved proteins were transferred to nitrocellulose membranes by standard methods. Membranes were blocked in the appropriate blocking reagent (as recommended by the manufacturer) for 1 hour at room temperature and probed with primary antibody overnight at 4ºC. Decorated membranes were washed three times for 10 minutes in TTBS and incubated for an additional 1-2 hrs. with the corresponding HRP-conjugated secondary antibody diluted in 2% BSA in TTBS. Blots were again washed 3x in TTBS and once in PBS before development using the enhanced chemiluminescence method (Amersham Biosciences). We define the threshold for acceptable purity as lack of detectable calnexin immunoreactivity in a nuclear preparation of 2.4×10^5 cell equivalents.

In preparation for detection of blotted proteins, using the Odyssey platform, transferred membranes were blocked for 1 hr at room temperature in Odyssey Blocking Buffer (LI-COR Biotechnology; Lincoln, NE). The appropriate primary and secondary antibodies were diluted in a 1:1 solution of Odyssey Blocking Buffer and PBS. Secondary incubations and terminal wash steps were performed in the dark. Decorated membranes were analyzed on the Odyssey® Infrared Imaging system using Odyssey® 2.0 software (LI-COR biotechnology). Scan settings were high image quality, resolution was set to 169 µm, and the intensity of the scan was 5.0. Antibody signals were quantified as integrated intensities of the areas above and below the bands of interest.

3.3.7 Quantification of Cellular Protein

Prior to protein quantification, cellular fractions were reconstituted in 1% SDS and incubated at 95ºC for 10 minutes. Cooled samples were homogenized by at least 30 passages through a 25-gauge needle. Satisfactory sample disruption was confirmed by phase microscopy and samples were subsequently clarified by centrifugation. In preparation for BCA analysis (Thermo Scientific; Rockland, IL), samples were diluted 1:10 or 1:20. Diluted fractions were analyzed in triplicate according to the protocol for BCA assay for microplate reader.

3.3.8 Electron Microscopy of Envelope-Free Nuclei

Purified nuclei were pelleted and fixed in 2% glutaraldehyde, 1% tannic acid in 0.1 M sodium cacodylate, 2 mM $CaCl_2$, and post-fixed in 2% OsO_4 in 0.1 M sodium cacodylate, 2 mM $CaCl_2$. Samples were stained in 4% uranyl acetate in 50% EtOH, dehydrated in a 50-100% EtOH/H_2O series, cleared with propylene oxide and embedded in Embed-812 resin (Electron Microscopy Sciences). Ultrathin sections (50 µm) were prepared using a Leica UCT ultramicrotome, and images were acquired with a Tecnai 12 transmission electron microscope (FEI, Hillsboro, OR), equipped with a Gatan model 794 multiscan digital camera.

To examine nuclei at different stages of purification, samples were fixed during extraction, shearing, and "unveiling" stages (see results section) of separate 1x preparations. Nuclei undergoing the initial extraction in Buffer A (500 µL total volume) were diluted to 10mL with an excess of fixative (2% glutaraldehyde, 1% tannic acid, 2 mM $CaCl_2$ in 0.1 M sodium cacodylate, pH 7.4). Nuclei were fixed at the 6 minute time point. Sheared nuclei (1 mL) and "unveiled" nuclei (1.5 mL) were also diluted to the same final volume in fixative.

1mL of each dilution was pelleted at 100 x *g* for 10 min at 4ºC. Fixed samples were washed 2x for 10 min in 1 mL fixative. After washing thoroughly in 2 mM CaCl2 in 0.1 M sodium cacodylate, pH 7.4, samples were processed for EM as described above.

3.3.9 Profiling of Bulk iMEF Phospholipid

To generate iMEF pellets for bulk cellular GPL analysis, 1.2 x 10^6 cells were seeded onto 150 mm tissue culture dishes and grown for 24 hours to 60-70% confluence. Some 10^7 cells were harvested by trypsinization, pelleted, and washed 2x in HBSS without Ca^{++} or Mg^{++}. Cells were then transferred to microfuge tubes in 1 mL of the same buffer and pelleted at 1000 x *g* for 5 min. Following complete removal of the supernatant, pellets were frozen in liquid nitrogen and stored at -80°C prior to lipid extraction and global phospholipid quantification by ESI LC/MS.

3.3.10 Glycerophospholipid Extraction and Analyses

Glycerophospholipids from whole cells or nuclear pellets were extracted using a modified Bligh and Dyer procedure [64]. Approximately 1 x 10^7 iMEF cells or 3 x 10^7 nuclei per pellet in cold 1.5-ml microfuge tubes (Laboratory Product Sales, Rochester, NY) were vortexed with 800 µl of cold 0.1 N HCl:CH_3OH (1:1) and 400 µl of cold $CHCl_3$ was added. The extraction proceeded with vortexing (1 min) and centrifugation (5 min, 4^{o}C, 18,000 x *g*). Quantification of GPLs was achieved by the use of ESI LC/MS employing synthetic (non-naturally occurring) diacyl and lysophospholipid standards as communicated elsewhere [65]. Typically, 200 ng of each odd-carbon standard was added to each sample. Identification of the individual phospholipids was accomplished by tandem mass spectrometry (LC/MS/MS) using an MDS SCIEX 4000 QTRAP hybrid triple quadrupole/linear ion trap mass

spectrometer and a Shimadzu HPLC system with a normal phase Luna Silica column (2 x 250 mm, 5 µm) using a gradient elution [65]. Identification of the individual species was based on their chromatographic and mass spectral characteristics and comparison to these of chemically defined standards [65,66]. This analysis allows identification of both fatty acid moieties but does not determine position on the glycerol backbone (*sn-1* vs. *sn-2*).

3.3.11 Statistical Analyses

Data are presented as means plus standard errors. Differences between percentages of the total GPL pool represented by different classes for whole cells versus nuclei were determined by Student's *t*-test.

3.4 Results

3.4.1 Purification of Envelope-Free iMEF Nuclei

Purification of quality envelope free nuclei requires comprehensive removal of contaminating cellular membranes and nuclear envelope with minimal compromise of nuclear integrity or of the biochemical character of the nuclear matrix. Because of the experimental advantages offered by the genetically tractable MEF system for addressing questions related to nuclear signaling, we developed a method for preparing highly purified envelope-free nuclei from these cells. The method generates purified endonuclear compartments suitable for quantitative lipidomic analyses and yields reproducible data. The procedure employs serial manipulations of detergent solubilization, hypotonic swelling and mechanical shearing to arrive at envelope-free nuclear preparations.

As a general comment, the protocol we use for purification of envelope free nuclei works optimally when 1 x 10^7 primary or iMEF cells are used as starting material (termed a 1x scale). The efficacy of the method is sensitive to scale and applications that require larger mass quantities of nuclei are best served by generating several smaller nuclear preparations in parallel and pooling the corresponding PL extracts. We recommend processing no more than 3 x 10^7 cells during a single purification. Buffer volumes used in preparing larger samples should be scaled accordingly. A methodological flowchart is depicted in Figure 1. From nine independent 1x preparations of envelope-free nuclei, an average of 0.34 ± 0.10 mg of endonuclear protein was recovered. As the averaged 1x quantity of total cellular starting material was 3.11 ± 0.45 mg of total cellular protein, the final protein yield in the purified endonuclear fractions is ca. 10% of total.

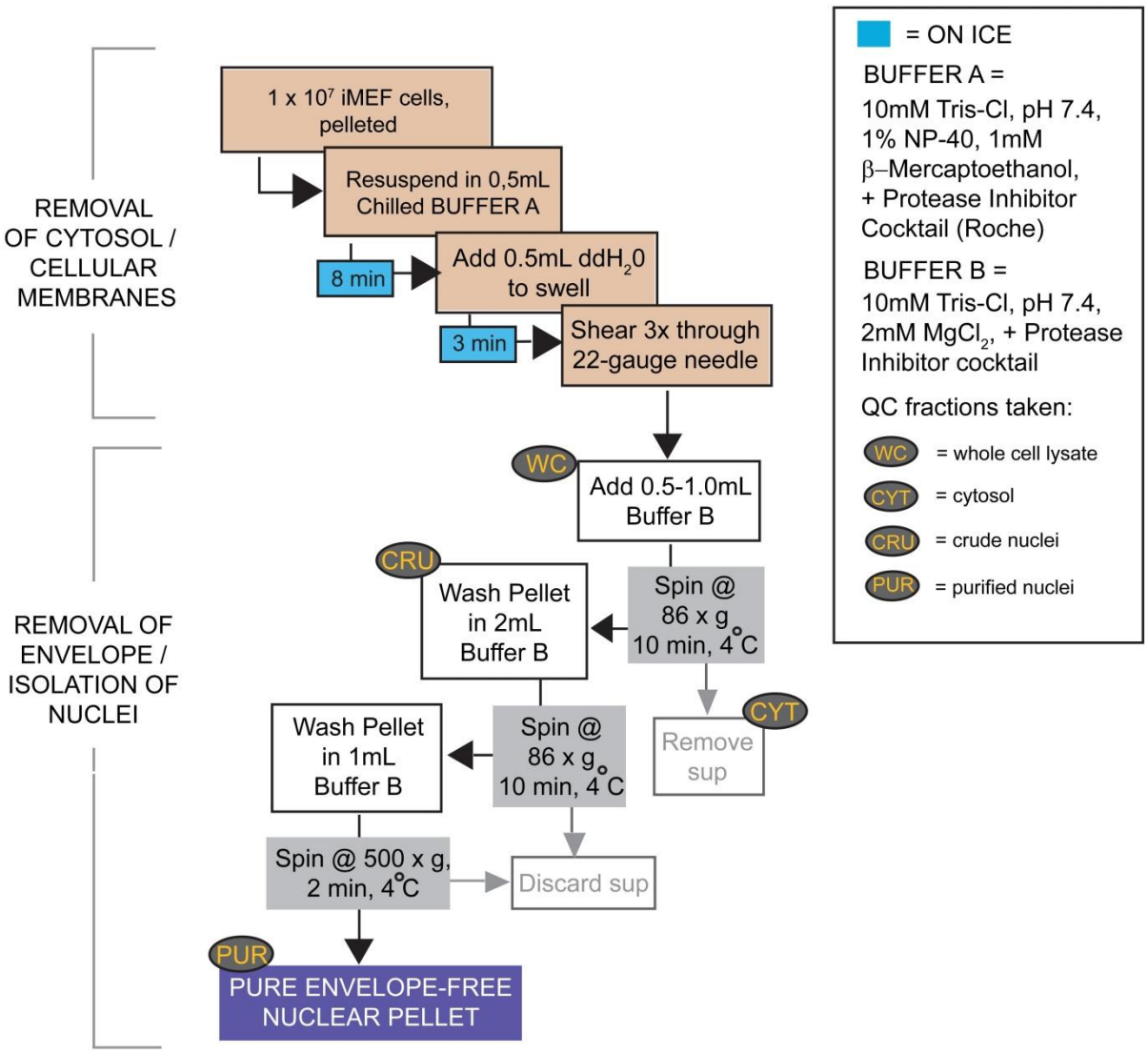

Fraction	WC	CYT	CRU	PUR
Total Protein (mg)	3.11 ± 0.45	2.55 ± 0.56	0.51 ± 0.09	0.34 ± 0.10

Figure 1. Nuclear purification scheme. A schematic flow diagram for rapid purification of envelope-stripped iMEF nuclei is illustrated. Total protein in individual fractions generated during the nuclear purification process is shown in mg.

3.4.2 Visual Landmarks for Monitoring Purification Quality

Several physical transformations accompany separation of the nuclear particle from contaminating cellular membranes and nuclear envelope. These physical transformations are readily observed during the purification and reliably diagnose quality of the final preparation. As such, these morphological landmarks serve as facile real-time reporters of processing efficacy. The stages of processing at which these transformations are monitored are highlighted in Figures 2 and 3. Typical nuclear morphologies observed during the initial detergent extraction are shown in Figure 2B. The nuclear particles are readily distinguished from assorted cytosolic and organelle debris by light microscopic examination at 40x magnification. The efficacy of the hypotonic swelling step is similarly interpretable as nuclei increase slightly in diameter (Figure 2C).

An effective shearing step is an essential component of the purification. Rapid and vigorous trituration of crude nuclear fractions through a 22-gauge needle liberates nuclei of associated debris and leaves the sheared nuclei as oblate particles. Satisfactory outcomes at this stage are defined by lack of associated large debris in at least 40 of 50 nuclear particles examined. Examples of typical nuclear morphologies at this stage are shown in Figures 2D and 2E. Electron microscopic analyses demonstrate that cellular debris attached to the detergent-extracted nuclear particle (Figure 2F) is mostly removed by the shearing step (Figure 2G). Although a small amount of debris remains attached to nuclei at this stage, closer examination of nuclear borders reveals that shearing removes the majority of the nuclear envelope (Figure 2H).

Upon dilution of suitably sheared nuclei into buffer B, the nuclear envelope is effectively removed. This stripping event is monitored via phase contrast microscopy by

what we term an ‘unveiling’ process. ‘Unveiling’ is characterized by the nuclei becoming less opaque, and the nucleoli assuming much sharper contrast relative to nucleoplasm (Figure 3B). The loss of nuclear envelope is visible in electron micrographs of nuclei fixed immediately after addition of buffer B (Figure 3C, left two panels). Borders of stripped nuclei appear fuzzy and without discernable traces of nuclear envelope (Figure 3C, right two panels). Subsequent pelleting and washing steps complete the envelope stripping process (Figure 4). Purified nuclei retain their morphology and appearance throughout the purification process.

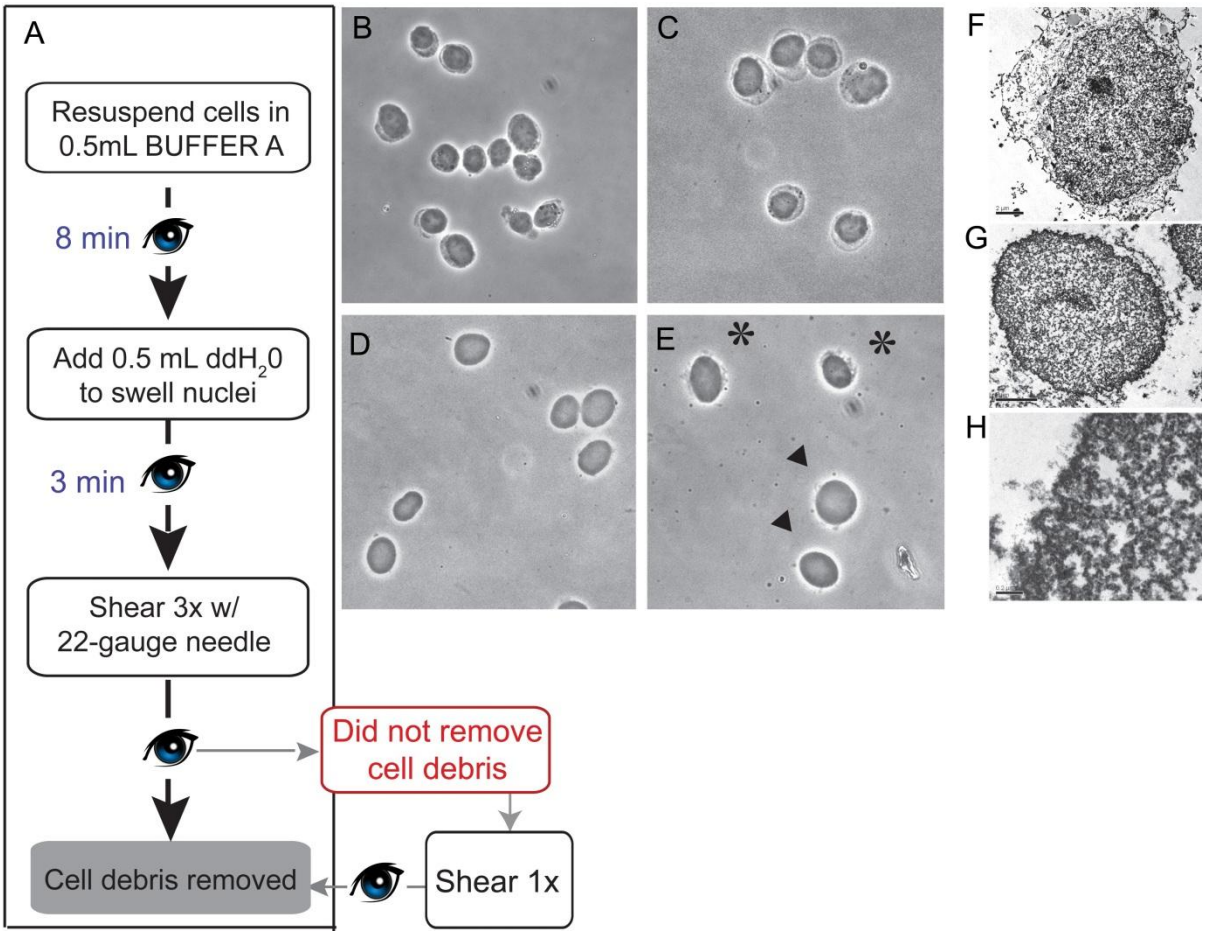

Figure 2. Phase contrast monitoring of nuclear particles. (A) Flow chart of the critical steps for removing extranuclear debris is indicated. All steps are executed on ice using chilled solutions and tubes. Eye symbols identify points where extraction efficacy is monitored by phase contrast microscopy. (B-E) Phase contrast images of extracting nuclei at various steps during the purification. All images were taken using a 40x objective, and 3-5µL of sample were typically viewed under a coverslip. (B) Cells are resuspended in the buffer A to initiate the extraction process. At this stage, nuclei are visible as the phase dense center of each cellular particle. Partially solubilized cytoplasm/plasma membrane contaminants are discerned as the less dense material surrounding the nuclear particle. (C) Addition of an equal volume of chilled ddH2O swells the nuclei and further enhances contaminating material. (D-E) Images of swollen nuclei sheared 3x through a 22-gauge needle. (D) Successfully sheared nuclei exhibit little to no visible debris attached. (E)Nuclei marked with an asterisk retain attached debris. Nuclei marked with arrowheads are scored as at a suitable stage of purification. (F-H) Electron micrographs of nuclear prep stages. (F) Electron micrograph of nucleus (1100x) fixed after 6 minutes of extraction in buffer A. Scale bar = 2 µm. (G) Sheared nucleus (1100x). Minor amounts of debris are still attached to the lamin boundary, which is clearly visible. Scale bar = 2 µm. (H) Higher magnification (15,000x) image of a nuclear border which has been successfully stripped of envelope. Scale bar = 0.2 µm.

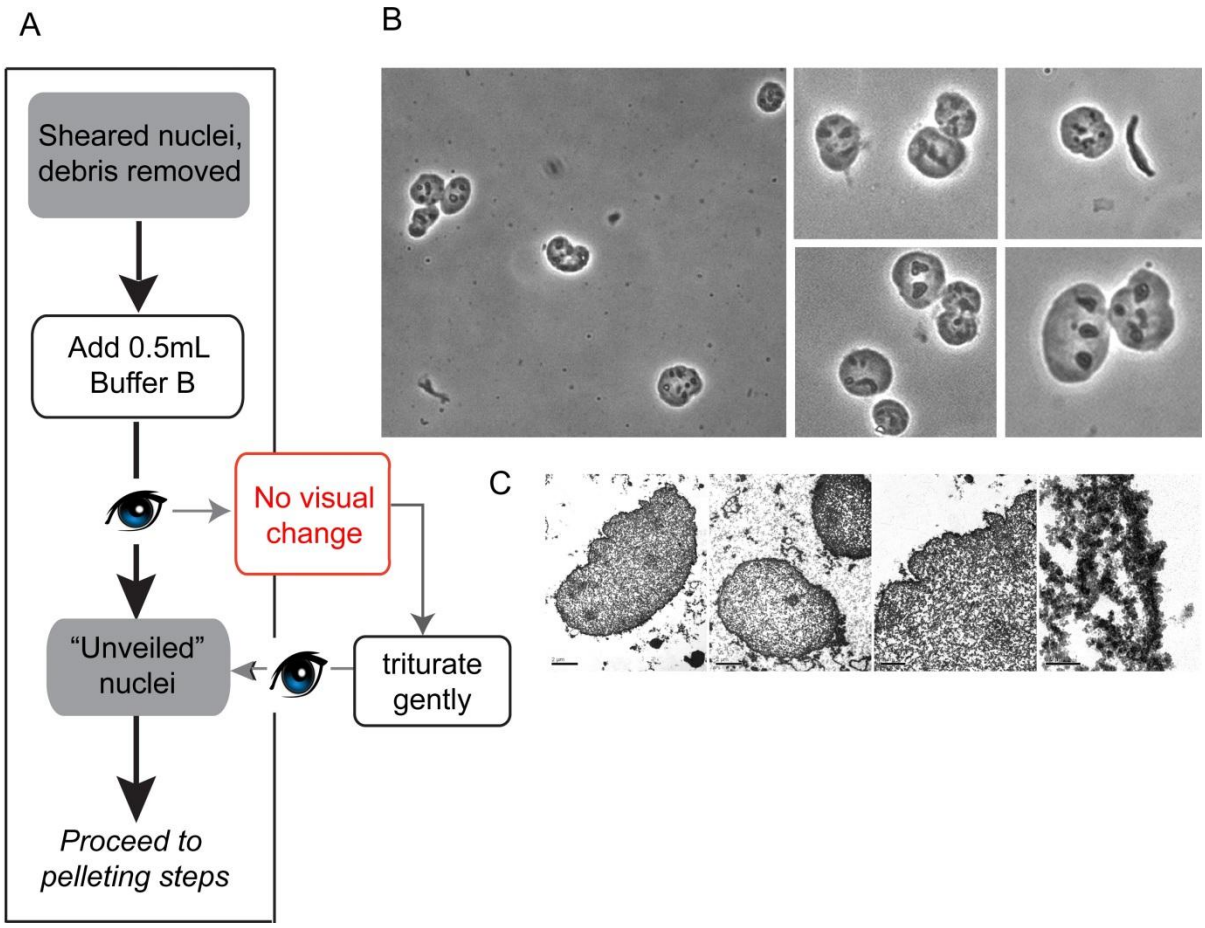

Figure 3. Unveiling of sheared nuclei. (A) Diagram of pre-pelleting purification steps. (B) Phase contrast images of nuclei following addition of Buffer B. Images were taken using a 40x objective. Portions of images at this magnification were digitally enlarged and are shown to the right. At this stage, nuclear particles show increased contrast and nucleoli become visible. (C) Electron micrographs of nuclei, fixed immediately after addition of buffer B. In the two leftmost panels, intact nuclei are observed with no attached debris at low magnification. High magnification images of nuclear borders (two rightmost panels) demonstrate removal of the nuclear envelope at this stage.

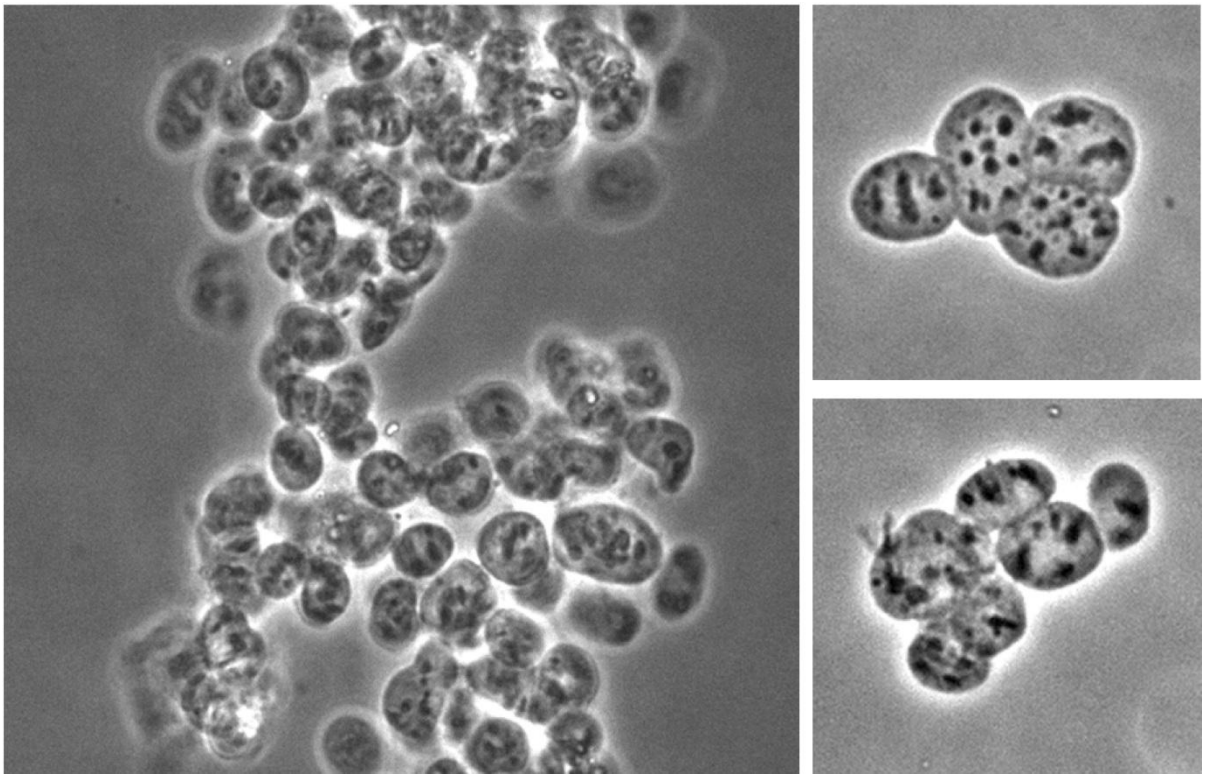

Figure 4. Morphology of purified nuclei. Purified envelope-free nuclear fractions were imaged by phase contrast using a 40x objective. (A) Nuclear particles are prone to aggregation after envelope removal. (B) Inspection of smaller groups of purified nuclear particles confirms that individual particles do not change shape or appearance during the final centrifugation steps of the purification process.

3.4.3 Criteria for Successful Membrane Removal from Purified Envelope-Free Nuclei

Visualization of envelope-stripped nuclei by EM directly interrogates the membrane content of nuclear preparations. Low-magnification (<2000x) electron micrographs of purified, envelope-free nuclei (Figure 5B) demonstrate efficient removal of extraneous material, as contaminating organelles or other heterogeneous membrane debris are not apparent.

When inspected at higher magnification (>10,000x) by EM, the peripheries of individual nuclear particles present a fuzzy border and no membrane bilayer structures are visible at these peripheries (Figures 5D and 5F). However, the high resolution EM analyses detect two classes of impurities that commonly evade detection by lower magnification EM – i.e., the types of analyses typically presented as evidence for the envelope-free status of purified nuclear particles [17]. First, small co-purifying membrane-like strands, attached to the isolated nuclear particles, are occasionally observed (Figure 5H). Secondly, these structures are also occasionally observed in the absence of an attached nucleus, and these are recorded as well (Figure 5G). Typically, 2 strands are recorded per 100 nuclei, and 1 small patch (average length ~ 500nm) is identified per 34 nuclei (Table 1). We find this low level of potential contamination to be unavoidable.

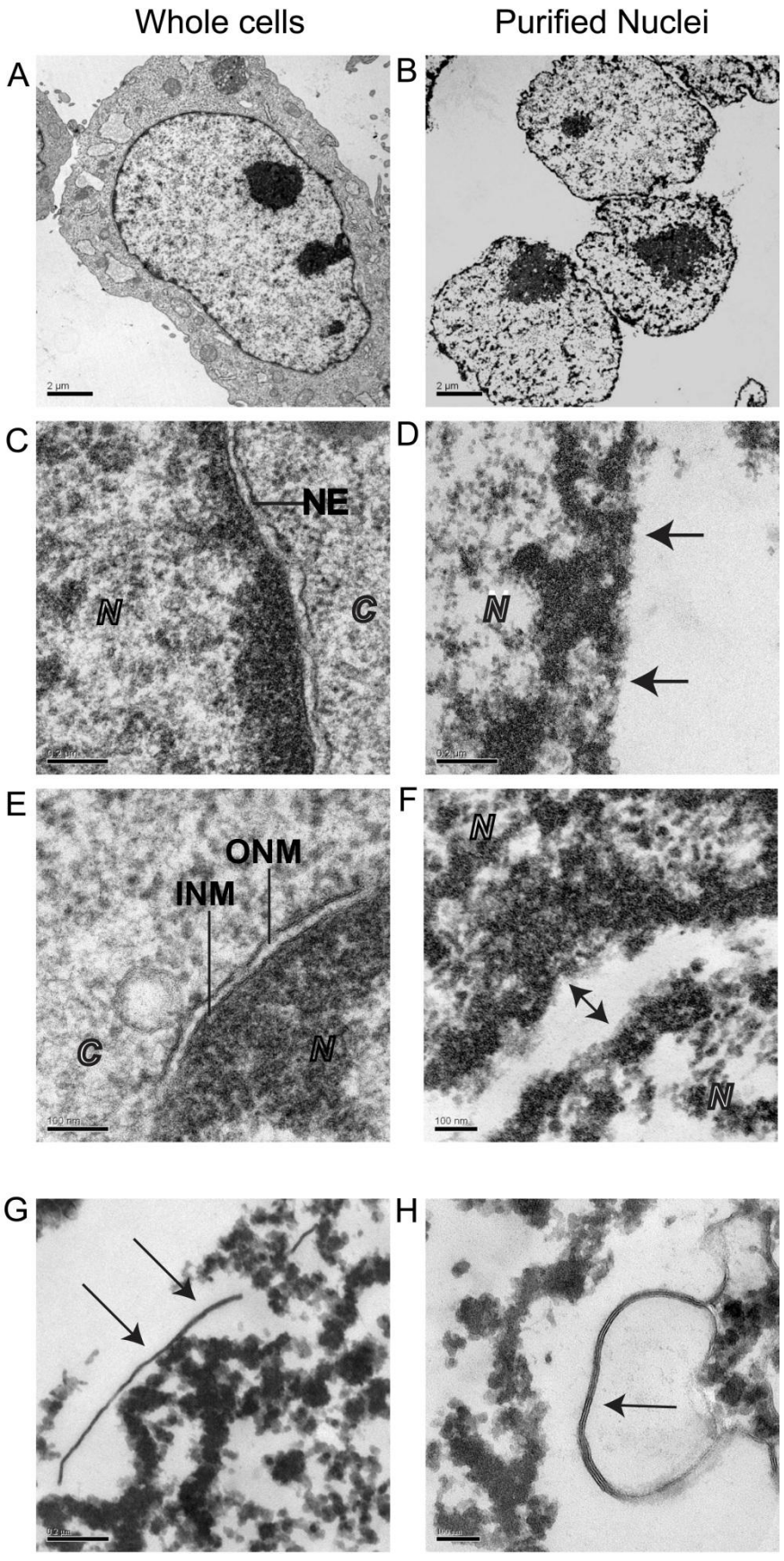
Whole cells
Purified Nuclei
A
B
2 µm
2 µm
C
D
NE
N
C
N
E
F
ONM
INM
C
N
N
N
100 nm
100 nm
G
H

Figure 5. Electron microscopic analysis of envelope-free nuclear preparations. (A) Whole iMEF cell. Nucleus is centered. (1100x magnification, scale bar = 2µm.) (B) Three purified nuclear particles at 1100x magnification. Nuclei are free of membrane and cellular debris as evidenced by the clear background. (scale bar = 2 µm). (C) Nucleocytoplasmic boundary in whole iMEF cells. The nuclear envelope (NE) and its inner and outer leaflets are observed at 11,000x magnification, separating the nuclear contents (N) from the cytosolic portion of the cell (C). (Scale bar = 0.2 µm). (D) Nuclear boundary after envelope removal. At magnifications greater than 10,000x, envelope-stripped borders of nuclei appear dark and fuzzy (arrows). This is due to the osmophilic nature of the lamin boundary and condensed chromatin at the nuclear periphery, which is no longer attached to the nuclear envelope. (E) High magnification images of nuclear boundary in an intact iMEF cell. At 30,000x magnification, the outer nuclear envelope (ONM) sits above the inner nuclear envelope (INM), which is bound tightly to the underlying lamin border. (Scale bar = 0.1µm) (F) High magnification image (30,000x) of two juxtaposed nuclei. Bidirectional arrow directs attention to the borders of the two purified nuclei, which lack discernable traces of bilayer (scale bar = 0.1 µm). (G-H) Identifying membrane contaminants. Membrane strands are indicated by arrows. (G) Scanning nuclear peripheries for membrane contaminants at magnifications higher than 10,000x enables detection of free membrane strands. (15,000x magnification, scale bar = 0.2µm). (H) High magnification (42,000x) micrograph of two juxtaposed nuclei and a contaminating membrane patch (arrow). (Scale bar = 50 nm.) In quality preparations, no nuclei retain patches of membrane greater than 2 µm in length and contaminating membrane is most commonly a very small patch -- on average 500 nm in length.

Table 1. Quantification of contaminants in envelope-free nuclear preparations. Highly purified nuclear fractions (n=9) were examined by electron microscopy. Borders of approximately 100 nuclei were examined at greater than 10,000x magnification for membrane patches or strands (see Figures 5G, H for descriptions).

Sample	*# nuclei examined*	*% w/o membrane*	*% w/ 1 membrane patch*	*% w/ > 1 membrane patch*	*# of membrane strands*
1	114	96.5	2.6	0.9	2
2	85	87.1	4.7	9.4	8
3	93	95.7	4.3	0.0	1
4	105	97.1	2.9	0.0	2
5	104	99.0	1.0	0.0	0
6	104	90.4	7.7	1.9	0
7	97	99.0	1.0	0.0	1
8	103	97.1	1.9	1.0	0
9	102	98.0	1.0	0.0	1
AVG	**101**	**95.5**	**3.0**	**1.5**	**2**

3.4.4 Biochemical Criteria for Purified Envelope-Free Nuclei

The accepted biochemical standard for envelope-free nuclei is the absence of the abundant cytosolic protein β-tubulin in the most purified fractions [17, 21, 51, 67]. This criterion does not adequately interrogate the preparation for contamination by the nuclear envelope – a membrane system physically contiguous with the highly abundant ER. To control for these primary sources of contaminating membranes, we monitored membrane-free nuclear preparations for abundant integral membrane proteins of the ER and nuclear envelope. Endonuclear fractions purified by the protocol described herein exhibited undetectable levels of the abundant integral ER membrane protein, calnexin, and the inner nuclear envelope integral membrane protein, NURIM, in addition to undetectable levels of β-tubulin (Figure 6A). We define the threshold for acceptable nuclear matrix purity as lack of detectable calnexin immunoreactivity in a sample of 2.4×10^5 nuclei in ECL immunoblotting experiments. Odyssey immunoblotting experiments indicate that less than 0.3% of cellular calnexin remains in nuclear preparations (Figure 6B) – indicating a greater than 300-fold enrichment of nuclear particles from contaminating ER membranes.

The endonuclear fractions were, however, highly enriched for the nuclear matrix constituent lamin A (Figure 6A). We also examined the nucleolar protein fibrillarin as a marker for enrichment. Fibrillarin is localized in the nucleoplasm as well as in nucleoli [68], and thus serves as a marker for loss of both nucleoplasm and nucleoli. Based on quantitative immunoblotting data, we estimate a 100-250 fold purification of nuclear matrix components (i.e.,, fibrillarin) over contaminating ER membrane protein (i.e., calnexin).

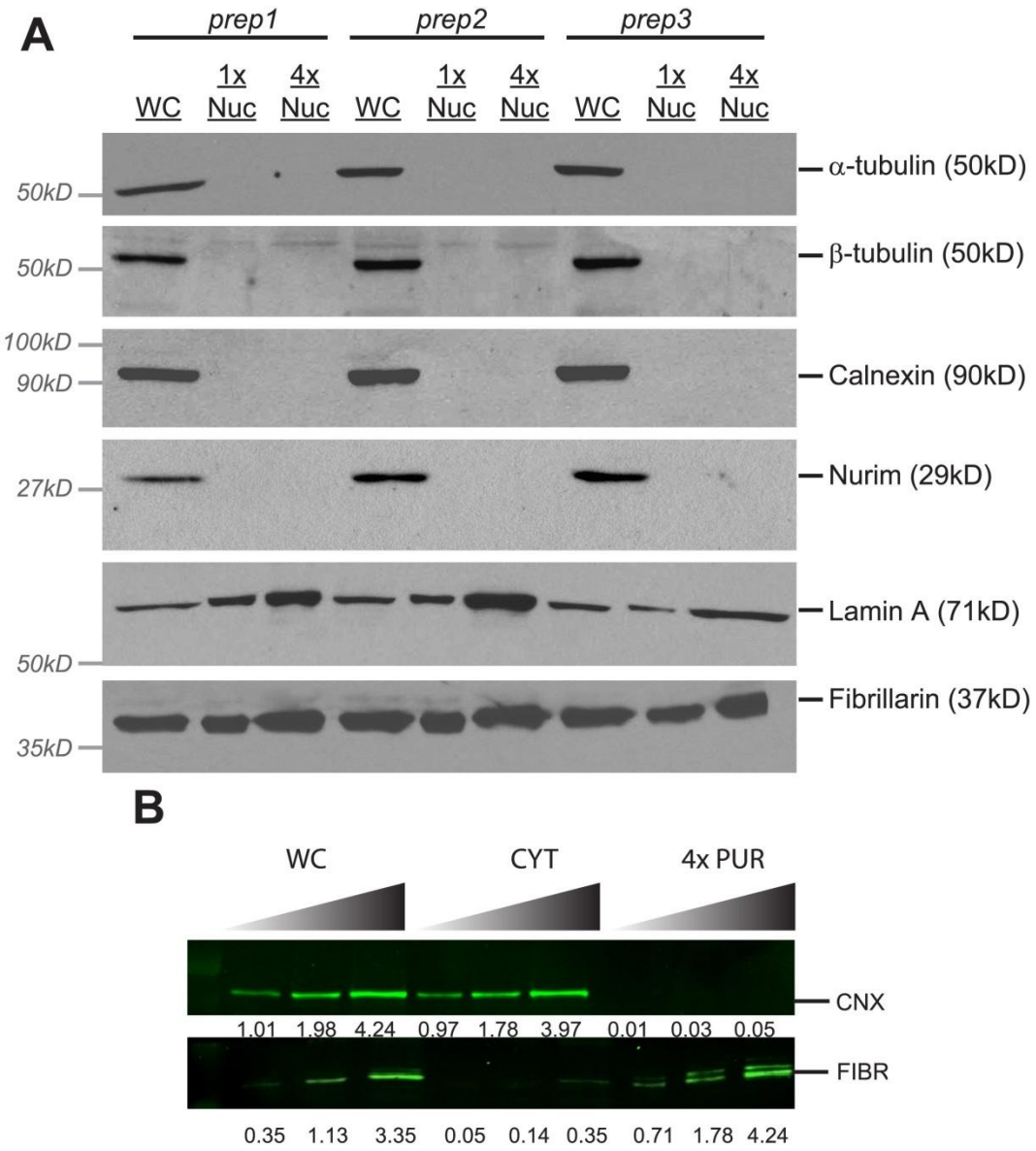

Figure 6. Immunoblot analyses of nuclear fractions. (A) Enhanced chemiluminenscence immunoblot analysis of whole cell (WC) and purified nuclear fractions (PUR). Fractions collected from 3 separate nuclear preparations were prepared for gel electrophoresis as described in Materials and Methods. Gels were loaded by cell equivalents (CEs) based on the amount of whole cell lysate needed for blotting in the linear range. Comparison to a four-fold excess of purified nuclei (PUR 4x) highlights the absence / enrichment of cellular proteins in nuclear fractions. (B) Odyssey Immunoblot analysis of calnexin and fibrillarin content in whole cell, cytosolic, and 4x nuclear fractions from a single preparation. Each sample was loaded in triplicate. Gels were loaded with 15,000, 30,000, and 60,000 cell equivalents of both whole cell and cytosolic protein fractions, whereas 60,000, 120,000, and 240,000 cell equivalents of purified nuclear protein were loaded for analysis. Relative intensity of each individual band was quantified using the Odyssey 2.0 software. These values are listed below the image underneath the corresponding bands.

3.4.5 Total Phospholipid in Cells and Nuclei

The resident GPLs were quantified and their compositions profiled in purified endonuclear compartments. Based on a signal-to-noise ratio of >3 as limit of detection threshold, we find the nuclear matrix to be a GPL-poor compartment. While PtdCho, phosphatidylethanolamine (PtdEtn), phosphatidylserine (PtdSer), phosphatidylinositol (PtdIns), phosphatidic acid (PtdOH), and phosphatidylglycerol (PtdGro) were all detected in the endonuclear compartment, in rank order of mass abundance, the quantities were small relative to whole cell amounts. The total GPL mass measured per unit endonuclear compartment (0.077 ± 0.0075 nmol/10^6 cells) was almost 2-orders of magnitude less than that measured per unit iMEF cell (5.1 ± 0.43 nmol/10^6 cells). That is, the total endonuclear GPL pool represents ca. 1.4% of total cellular GPL.

3.4.6 Lipidomic Profiling of the Major Endonuclear Phospholipids

With regard to composition, the bulk iMEF phospholipidome presents a diverse signature, with the leading GPL classes (by mass) represented by PtdCho, PtdEtn, and PtdSer molecular species, respectively. We note that 38:4 PtdIns was also represented within the 10 most abundant bulk GPL species.

By contrast, the endonuclear phospholipidome exhibited a simpler profile. The most abundant GPLs by mass in iMEF nuclei are represented by PtdCho, PtdEtn and PtdSer molecular species. PtdIns, PtdOH and PtdGro were poorly represented in endonuclear compartments. Interestingly, and as discussed in greater detail below, the differences in fractional representation of these minor PLs in bulk membranes vs. the endonuclear compartment were highly significant ($p<0.001$). By contrast, the PtdCho/PtdEtn ratio between these two systems was similar (ca. 1.85).

PtdCho is the most abundant endonuclear PL class – represented by 9 of the top 10 most abundant molecular species (Table 1). Greater than half of the endonuclear GPL mass is accounted for by PtdCho species (53.1% ± 2.8%). The proportion of the PtdCho pool represented by saturated molecular species is only modestly increased in nuclei relative to whole cells. In that regard, the 32:0 and 30:0 forms were the only saturated PtdCho molecular species with sufficient abundance to quantify in the endonuclear fractions. Reciprocally, the polyunsaturated PtdCho species were modestly reduced in abundance in the nuclear matrix relative to their representation in bulk GPL. The relative representation of monounsaturated PtdCho species did not significantly differ in the endonuclear compartments versus bulk cell material (Figure 7B, middle row).

These profiling data do not indicate strong enrichment of saturated PtdCho molecular species in the envelope-free nuclear preparations. Indeed, unsaturated PtdCho molecular species compromise 79% of the total endonuclear PtdCho mass (Figure 7). This pattern is observed across the other GPL classes as well. Inspection of the rank order of the 42 most abundant endonuclear GPLs indicates a general paucity in both diversity and mass abundance of saturated species (Table 2). For example, only 30% of the PtdSer mass is represented by saturated molecular species, and this fraction is much larger than for any other quantifiable endonuclear GPL class. PtdSer represents the third most abundant nuclear GPL class, comprising some 15% of the total endonuclear GPL mass. The preponderance of unsaturated GPLs was encouraging given the legitimate concern that detergent-mediated stripping of the nuclear envelope could generate artifactual detergent-insoluble lipid domains expected to be enriched in saturated GPL molecular species and sphingolipids. In that regard, sphingomyelin (SM) was at the limit of detection in endonuclear fractions – indicating this

sphingolipid class is a very minor constituent, at best, of the iMEF endonuclear PL pool (data not shown).

PtdEtn, the second most abundant GPL in the nuclear matrix, accounts for some 28% of total endonuclear GPL mass. We observed interesting distinctions between non-nuclear and nuclear PtdEtn species. Ether-linked PtdEtn was substantially reduced in endonuclear fractions when evaluated as a percentage of the overall PtdEtn pool. From a fractional representation of 40.4% ± 1.0% of bulk iMEF PtdEtn molecular species, only 27.7% ± 1.5% of the mass of endonuclear PtdEtn species was ether-linked (Figure 7C, bottom row). The PtdCho/PtdEtn mass ratio, however, remains similar in endonuclear compartments as compared to bulk iMEF GPL – further confirming ether-linked PtdEtn species are genuinely segregated from the nuclear matrix.

Table 2. Ranking of GPL by abundance in whole iMEFs and nuclei (pmol/million cells or pmol/million nuclei, mean and standard error; n=9)

whole MEFs			
species	mean	sem	rank
PS(36:1)	301.5	44.7	1
PC(36:2)	250.1	17.5	2
PC(32:1)	195.0	12.8	3
PE(38:4)	146.4	14.8	4
PC(34:1)	142.1	8.1	5
PS(34:1)	122.2	10.0	6
PC(38:6)	108.7	14.5	7
PC(36:1)	102.5	25.8	8
PI(38:4)	97.8	18.3	9
PE(38:0)/PE(40:7e)/PE(40:6p)	90.4	16.1	10
PC(38:4)	89.5	10.7	11
PE(38:5e)/PE(38:4p)	89.1	5.4	12
PC(30:1)	86.5	32.8	13
PE(38:5)	84.0	11.2	14
PC(32:0)	83.5	6.0	15
PS(36:2)	82.7	7.4	16
PS(40:5)	82.7	14.7	17
PC(30:0)	81.7	5.1	18
PE(36:2)	81.0	3.8	19
PS(40:6)	80.9	13.0	20
PS(38:4)	78.2	9.6	21
PE(40:6e)/PE(40:5p)	77.6	8.4	22
PE(38:3)	77.2	11.2	23
PC(38:5)	75.2	11.7	24
PC(40:6)	75.2	10.0	25
PE(40:5e)/PE(40:4p)	74.2	11.6	26
PE(36:1)	67.4	4.4	27
PC(38:3)	67.1	8.9	28
PC(34:2)	66.4	4.6	29
PE(34:1)	64.6	5.8	30
PC(38:0)	62.6	15.8	31
PG(36:2)	60.8	18.3	32
PS(38:3)	58.5	12.8	33
PE(40:4e)/PE(40:3p)	58.4	12.1	34
PC(36:3)	56.5	4.4	35
PS(40:4)	56.2	11.4	36
PC(38:6e)/PC(38:5p)	55.9	21.1	37
PC(34:1e)	52.7	10.5	38
PG(40:7)	52.4	15.9	39
PC(36:0)	52.1	7.7	40
PC(38:2)	48.9	6.4	41
PC(38:5e)/PC(38:4p)	46.8	10.5	42
PG(34:1)	46.7	4.6	43
PS(36:0)	45.2	15.8	44
PE(40:6)	44.3	7.7	45
PE(36:5e)/PE(36:4p)	43.4	3.9	46
PE(38:1)	42.7	4.6	47
PC(32:2)	42.3	3.2	48
PI(38:3)	41.7	9.3	49
PI(36:2)	39.9	6.3	50
PC(36:4)	39.3	5.0	51
PE(40:5)	39.2	6.8	52

MEF nuclei			
species	mean	sem	rank
PC(36:2)	5.2	0.7	1
PC(32:1)	5.1	0.5	2
PC(32:0)	5.0	0.5	3
PC(38:6)	4.9	0.5	4
PC(34:1)	4.3	0.5	5
PC(36:1)	4.1	0.5	6
PC(36:4)	3.8	0.6	7
PE(38:4)	3.7	0.5	8
PC(30:0)	3.5	0.4	9
PC(38:4)	3.2	0.7	10
PS(36:1)	2.8	0.7	11
PC(34:2)	2.5	0.5	12
PE(36:1)	2.2	0.2	13
PE(36:2)	2.0	0.3	14
PE(38:5e)/PE(38:4p)	1.6	0.2	15
PE(34:1)	1.6	0.3	16
PE(38:5)	1.5	0.3	17
PS(38:4)	1.5	0.6	18
PS(36:0)	1.3	0.1	19
PS(38:0)	1.3	0.1	20
PS(34:1)	1.2	0.2	21
PE(34:2e)/PE(34:1p)	1.2	0.1	22
PE(36:5e)/PE(36:4p)	1.1	0.1	23
PE(38:6)	1.0	0.2	24
PE(38:0)/PE(40:7e)/PE(40:6p)	1.0	0.1	25
PE(38:3)	1.0	0.2	26
PE(40:6)	0.9	0.1	27
PE(40:6e)/PE(40:5p)	0.9	0.1	28
PA(36:2)	0.9	0.1	29
PS(38:5)	0.8	0.1	30
PI(38:4)	0.8	0.2	31
PS(36:2)	0.8	0.1	32
PE(40:5)	0.7	0.1	33
PS(40:6)	0.7	0.1	34
PS(38:3)	0.7	0.1	35
PG(34:1)	0.7	0.2	36
PS(40:5)	0.6	0.1	37
PS(40:4)	0.6	0.1	38
PE(40:7)	0.6	0.1	39
PE(40:4)	0.5	0.1	40
PI(38:5)	0.3	0.0	41
PI(38:3)	0.2	0.0	42

Table 2, continued. Ranking of phospholipids by abundance in whole iMEFs and nuclei (pmol/million cells or pmol/million nuclei, mean and standard error; n=9).

PI(38:5)	37.8	6.7	53
PG(38:6)	37.1	23.4	54
PG(38:4)	34.4	9.3	55
PC(36:2e)/PC(36:1p)	33.4	5.4	56
PE(36:3e)/PE(36:2p)	32.2	2.4	57
PG(40:6)	31.6	12.3	58
PA(34:1)	31.1	4.6	59
PG(38:3)	30.0	8.4	60
PE(40:4)	29.2	5.0	61
PE(34:2e)/PE(34:1p)	28.6	2.4	62
PS(40:3)	28.0	8.2	63
PS(32:1)	27.6	4.2	64
PA(36:1)	26.3	4.0	65
PC(38:1)	25.9	2.9	66
PG(36:3)	25.7	5.2	67
PE(38:2)	24.2	4.8	68
PS(38:2)	22.6	3.9	69
PG(40:5)	22.2	7.3	70
PG(38:5)	22.0	5.3	71
PG(36:1)	21.7	3.6	72
PS(34:2)	21.4	2.7	73
PE(40:7)	21.4	1.8	74
PA(32:1)	19.7	3.6	75
PA(36:2)	17.3	3.1	76
PC(34:2e)/PC(34:1p)	15.6	3.3	77
PS(34:0)	15.2	4.7	78
PG(34:2)	15.0	2.2	79
PS(36:4)	14.7	1.5	80
PI(36:4)	14.5	1.6	81
PI(36:1)	13.9	3.0	82
PI(36:3)	13.8	2.2	83
PI(34:2)	13.6	1.9	84
PA(32:0)	13.0	2.4	85
PS(36:3)	12.8	1.8	86
PS(42:1)	12.8	2.6	87
PG(42:8)	12.7	4.1	88
PI(34:1)	12.6	1.7	89
PC(36:5)	12.4	0.2	90
PS(40:1)	12.3	2.0	91
PG(40:4)	12.2	3.9	92
PS(40:2)	12.0	2.4	93
PA(40:5)	11.9	2.0	94
PG(38:2)	11.9	3.4	95
PG(42:9)	10.6	3.4	96
PA(40:4)	10.5	2.3	97
PG(42:7)	10.2	3.4	98
PA(34:0)	8.9	1.9	99
PA(38:4)	8.3	1.7	100
PA(40:6)	8.0	2.5	101
PG(40:8)	7.7	2.2	102
PG(42:10)	7.7	2.4	103
PA(34:2)	7.6	1.9	104
PC(36:5e)/PC(36:4p)	7.4	0.9	105
PA(38:3)	6.9	1.3	106
PI(40:5)	6.9	1.5	107
PI(40:6)	5.4	1.2	108
PI(38:2)	5.3	1.1	109
PI(40:4)	4.9	0.8	110
PG(32:1)	3.8	0.3	111

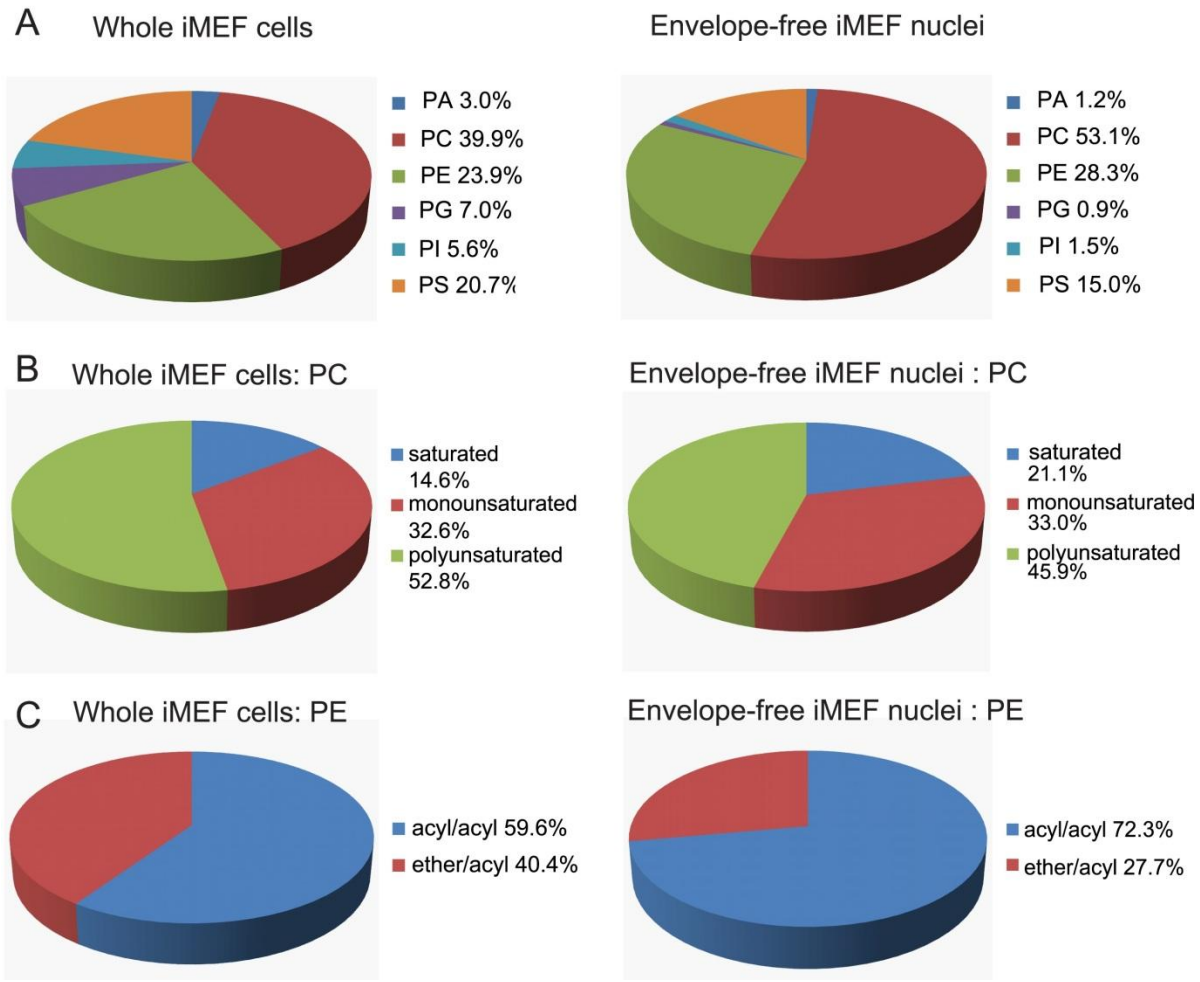

Figure 7. Composition of iMEF nuclei in comparison to whole cells. (A) GPL composition of iMEF cells and purified envelope free nuclei. Top row: GPL distribution by class for whole iMEFs and envelope-free iMEF nuclei (mean of n=9 shown). The difference in composition between whole cells and nuclei for PtdOH, PtdGro, and PtdIns is highly significant ($p<0.001$), while the PtdCho/PtdEtn ratio is ~1.85 for both whole cells and nuclei, with no significant difference. (B) Percent contributions of saturated, mono-, and poly-unsaturated species to PtdCho pool. The proportions of polyunsaturated and saturated PtdCho differ somewhat ($p<0.01$) between whole iMEFs and nuclei. (C) The relative mass contribution of ether-linked PtdEtn species to the PtdEtn pool is substantially greater in whole iMEFs than in nuclei ($p<0.001$).

3.4.7 Lipidomic Profiling of the Minor Endonuclear Phospholipids

While PtdCho and PtdEtn are highly represented in the endonuclear phospholipid profile, this compartment is relatively deprived of other GPL species. For example, there is little PtdIns found in the envelope-free nuclear fractions (1.5% ± 0.2% of the nuclear GPL) as compared to the whole iMEFs (5.6% ± 0.6% of bulk cellular GPL). The distribution by headgroup class (Figure 7, top row) shows that the minor GPL classes (PtdOH, PtdIns, PtdGro) were all significantly reduced (in terms of fractional representation) in the most purified endonuclear fractions relative to PtdCho and PtdEtn. For purposes of comparison, endonuclear PtdCho, PtdEtn, and PtdSer species accounted for 1.63%, 1.77%, and 1.13% of the corresponding total cellular pools. By contrast, PtdGro was particularly sparse -- only 0.02% of the total iMEF pool was recovered in the nuclear matrix. Endonuclear PtdOH and PtdIns comprised only 0.53% and 0.42% of the corresponding total cellular pools. Interestingly, whereas the most abundant endonuclear PtdIns was the 38:4 molecular species, the only detectable PtdOH in this compartment was the 36:2 molecular species. In that regard, none of the three acyl chain configurations identified for endonuclear PtdIns were of the 36:2 variety.

3.5 Discussion

Herein, we describe a facile and reliable method for purifying quality envelope-free nuclei from iMEFs. The choice of cell model is driven by the wealth of MEF lines that can be derived from mutant mouse lines. The method incorporates an expanded repertoire of quality controls and defined criteria for purity. Particular attention is paid to the abundant integral membrane constituents of the membranes that constitute the greatest reservoirs for

contamination (e.g., endoplasmic reticulum and nuclear envelope). This method reproducibly yields purified nuclear particles that have the dual properties of a reasonable preserved ultrastructure and are demonstrably envelope-free. Quantitative phospholipidomics of the iMEF endonuclear compartment leads us to three basic conclusions: First, in agreement with previous reports [17, 28, 59], the composition of the endonuclear GPL pool is distinct from that of bulk cell GPL. Second, the nucleoplasm is a PL-deprived environment. Third, the endonuclear GPL pool is not substantially enriched in saturated molecular species relative to the saturated/unsaturated GPL-composition of the bulk cellular pool. These latter two conclusions are incongruent with prevailing views regarding the fundamental properties of the mammalian endonuclear phospholipidome.

3.5.1 A GPL-Deprived Nucleoplasm

Mass measurements of the 42 detectable endonuclear GPL species demonstrate the nuclear matrix to be a PL-poor environment with an estimated load of ca. 5.9×10^7 GPL molecules per nuclear particle. Thus, the endonuclear phospholipidome accounts for 1.4% of the total cellular GPL mass. Based on this value, we calculate the GPL component occupies < 0.1% of the iMEF nucleoplasm.

Strict interpretations of these values are subject to several obvious, and unavoidable, caveats. First, removal of the nuclear envelope demands detergent extraction, and it is not clear how much of the endonuclear GPL is lost during that obligate step. Second, we consistently detect, by high resolution EM, trace amounts of membrane-like material in the most purified nuclear particle fractions. If these represent membrane remnants, such contaminants will contribute to the GPL mass measured in the purified endonuclear fractions.

We also note that our analyses cannot determine the extent to which the matrix leaflet of the inner nuclear envelope is removed. Since the lipids of this leaflet contact lamins and other abundant proteins of the nuclear periphery, this lipid pool is likely resistant to stripping. The morphological state such remnants would assume during the preparation of envelope-free nuclei is unclear. These may represent the membrane remnants we discuss above, or we may fail to recognize such contamination altogether. Thus, the values reported herein, although low, may yet overestimate endonuclear GPL mass. However, we are encouraged with the reproducibility of the quantitative measurements.

The values we measure for endonuclear GPL load diverge from those reported for the IMR-32 neuroblastoma cell line. A load of ca. 4 nmol PtdCho/10^6 nuclei was reported for these cells, along with an estimate that PtdCho alone occupies 12-16% of the IMR-32 nuclear volume [17]. Why this large discrepancy between the two analyses? One formal possibility is that different cell lines exhibit variable endonuclear GPL loads. While cell line-specific variations will almost certainly prove to be the case, we consider it unlikely that such variations could fully account the ca. 50-fold range that separates the two measurements. Rather, as ER/nuclear envelope remnants were not systematically monitored in that study [17], we suspect membrane contamination from this system contributed to the GPL mass and compositional measurements which were attributed to strictly endonuclear GPL pools. Such contamination would lead to large overestimates of endonuclear GPL mass if the nucleoplasm is a PL-poor environment – as we contend is the case.

3.5.2 Implications for Organization of Nuclear GPLs

The reported abundance of endonuclear GPL, particularly saturated PtdCho, raises the central question of how such a large PL load is organized within the nuclear matrix.

Standard solutions to the 'PL-accomodation' problem, such as incorporation into membrane bilayers, are untenable. While invaginations of the nuclear envelope do extend into the nuclear interior, these structures are topologically distinct from the nuclear matrix itself [30, 31]. Indeed, a hallmark feature of the nucleus is that it does not contain internal membrane-bound sub-compartments, despite the presence of morphologically and functionally distinct endonuclear domains [reviewed in 69].

Alternatively, it is speculated that the large nuclear PL-load provokes assembly of endonuclear PL into large aggregates or liquid crystalline phases [reviewed in 18, 19]. In that regard, there are reports of endonuclear PL 'rafts' [15, 70-72]. If protein binding is a primary mechanism for nuclear PL-organization, then the reported high nuclear abundance of PL demands that a large fraction of nuclear protein be PL-associated. All of these general ideas lead to speculations that PtdCho and other PLs may play significant structural roles in the nuclear matrix [17, 34].

The complicated issues surrounding mechanisms of PL-accommodation largely evaporate if the nuclear matrix proves to be a PL-poor compartment – as our data indicate it to be. With the stoichiometries we measure, GPL-binding to resident proteins alone could potentially satisfy the PL-accommodation problem without the need for occupying the major fraction of nuclear protein with bound GPL. A PL-deprived nuclear matrix also dismisses issues associated with a global gel-like physical environment formed by an abundance of saturated GPL. Indeed, several studies describe the nucleoplasm as a highly dynamic environment where presumably naive molecules (e.g., GFP) exhibit comparable diffusion coefficients in the cytoplasm and nuclear matrix [reviewed in 34]. While involvements of GPLs in structural or organizational functions within the nuclear matrix remain tenable, our

data indicate any such involvements must be highly constrained and of a small scale. Indeed, the purported nuclear rafts are seen only in heavily processed nuclei [15, 70-72], and their identity as such has not been directly confirmed. In our opinion, the weight of present evidence favors the view that the nucleoplasm is a PL-poor environment.

3.5.3 Endonuclear PL Molecular Species

In our hands, iMEF endonuclear GPL are predominantly of the unsaturated variety with few saturated molecular species. Indeed, of the major endonuclear PL classes (PtdCho, PtdEtn, PtdSer), >70% of the total PL mass is represented by unsaturated molecular species. Most of these are of the polyunsaturated variety. While the relative contributions of unsaturated molecular species to the total pool are modestly reduced for iMEF nucleoplasmic GPLs (as compared to bulk GPLs), the collective data are at odds with a previous conclusion that saturated PtdCho dominates the endonuclear phospholipidome [17]. Our results indicate that a nuclear matrix rich in saturated GPL is not a general (nor perhaps even an authentic) property of mammalian cells.

3.5.4 Implications for Nuclear PL Signaling

There is an abundance of evidence demonstrating the nucleus as an active compartment of lipid signaling. The nucleus contains the necessary components of a complete phosphoinositide cycle [41, 57, 61], PtdOH and DAG metabolism [24, 33, 46], phosphoinositide-dependent enzymatic activities that require the intact PL as a co-factor [20, 25, 73], and SM-dependent sphingolipid signaling pathways [28, 57, 74-80]. The barren landscape of the endonuclear phospholipidome, at least under steady-state conditions, holds interesting implications for nucleoplasmic signaling in iMEFs. First, the data suggest nuclear

signaling in these cells may involve only a small number of GPL molecules. Execution of such pico-scale signaling implies either an intimate channeling between signaling PLs (or their products) and effector, or that PL action is mediated by direct association with a catalytic activity which efficiently amplifies signaling. One example of the latter scenario is the STAR-PAP poly-A RNA polymerase that uses PtdIns-4,5-P_2 as essential co-factor [20, 62].

Second, if the signaling scheme consumes many GPL molecules, then the bulk of the endonuclear GPL-driven signaling events likely occur on the nucleoplasmic surface of the inner nuclear envelope. It also remains a formal possibility that in situ GPL synthesis fuels high flux endonuclear pathways, and the nucleus is demonstrated to house isoforms of the PtdCho-biosynthetic enzymes of the CDP-choline pathway [17, 60].

Robust pathways for GPL import into the nucleoplasm may also exist. PtdIns-driven signaling pathways are outstanding candidates for this type of supply mechanism, as it is largely accepted that PtdIns synthase activity is excluded from the nuclear compartment [17]. Similarly, the paucity of SM in iMEF nucleoplasm implies a requirement for active import pathways if these cells genuinely execute endonuclear SM-signaling pathways.

No matter the scale, consumption of signaling lipids is essential for proper regulation of both the gain and the persistence of any lipid signaling response. Perhaps downregulation is a primary rationale for why lipid metabolic enzymes are found in the nucleoplasm – i.e., to consume signaling lipids by channeling these into production of more inert molecular species. Our identification of 38:4 PtdIns as by far the most abundant endonuclear PtdIns molecular species, when only 36:2 PtdOH is detected in this same compartment in an essentially 1:1 stoichiometry, is interesting from this perspective. A simple nucleoplasmic

phospholipase C-DAG kinase pathway will yield endonuclear 38:4 PtdOH. Perhaps this PtdOH is generated, but is rapidly and quantitatively remodeled to 36:2 PtdOH in the nucleoplasm. Such a remodeling could occur via an endonuclear Lands cycle which employs the sequential actions of phospholipase A_2 and lyso-PtdOH acyltransferase [76]. Alternatively, 38:4 PtdOH may be channeled into 38:4 PtdCho or 38:4 PtdEtn synthesis by nuclear isoforms of enzymes of the CDP-choline and CDP-ethanolamine pathways [17, 60]. In either case, the physical context for how such enzymes register their substrates in the GPL-depleted nucleoplasm remains an open question. How (or whether) the corresponding biosynthetic products are exported from the nucleoplasm also remains to be established.

3.5.5 Endonuclear Lipid Dynamics and Metabolism

The open questions regarding scale and nature of PL signaling and metabolism in the nucleus, and how (or whether) PLs shuttle into and out of the nucleoplasm, are difficult ones to experimentally address. As non-invasive methods with which to investigate these issues do not exist, the most tractable experimental approaches demand reliable methods to rapidly and effectively purify envelope-stripped nuclear particles. These methods must yield endonuclear fractions with consistent properties, and the analytical platforms must be chaperoned by rigorously defined sets of quality controls. Herein, we describe one such method. We find this particular protocol does not translate seamlessly to other cell types, and therefore requires modification as a function of the specific application. The method does, however, provide a useful platform, and a useful set of quality control parameters, for development of nuclear matrix purification regimes suited for cell lines of interest to individual researchers.

CHAPTER 4

ENDONUCLEAR PHOSPHOINOSITIDE SIGNALING: A PUTATIVE ROLE FOR A PHOSPHATIDYLINOSITOL TRANSFER PROTEIN IN NUCLEAR IMPORT OF PHOSPHATIDYLINOSITOL

4.1 Summary

Phosphoinositide signaling in the endonuclear compartment is robust. Numerous phosphoinositides and their metabolic enzymes have been described in the nuclear compartment. Despite this, PtdIns cannot be synthesized *in situ*. Instead, it must be imported into the nuclear matrix via a currently unknown mechanism. Our profiling studies of endonuclear PtdIns mass in iMEF cells, indicates that the endonuclear compartment is sparsely populated with GPLs. Because of this, we have proposed that a lipid-binding and transfer protein is ideally suited to import PtdIns to discrete sites in the nuclear matrix. If the candidate (the Phosphatidylinositol Transfer protein alpha, PITPα) is responsible for this activity, then cells lacking this protein are likely to be deficient in the endonuclear PtdIns load. We have used pulse labeling and dynamic lipidomics analyses to determine whether the rate of incorporation is affected negatively in cells lacking PITPα. Our current findings, although preliminary, suggest that PITPα is not necessary for steady state maintenance or flux of endonuclear PtdIns levels.

4.2 Introduction

Endonuclear compartments of eukaryotic cells are now recognized as sites of lipid metabolism and signaling. Nuclear isoforms of phosphatidylcholine (PtdCho), phosphatidic acid (PtdOH), phosphatidylethanolamine (PtdEtn), and phosphatidylserine (PtdSer) biosynthetic enzymes have been described [17, 80] and have been demonstrated as active in the nuclear compartment. Consistent with such an idea, the endonuclear compartment is reported to hold a surprisingly large amount of phospholipid (PL). PtdCho alone is estimated to occupy some 10-16% of the total endonuclear volume [17] – an astonishing number given the lack of obvious membrane bilayers within that compartment. This is clearly not a universal phenomenon, as our quantitative lipidomic analysis of mouse embryonic fibroblast nuclei in Chapter 3 indicates that the nucleus is a phospholipid poor environment. Regardless of the quantity, phospholipid is routinely detected within nuclear fractions, and it has been shown to play roles in liver regeneration, DNA damage pathways, apoptosis, the oxidative stress response and cell cycle progression.

Several cell essential pathways rely on production of endonuclear phosphoinositides for proper function. Given the apparent proclivity of the nuclear matrix to synthesize (or otherwise metabolize) PLs, nuclear isoforms of phosphatidylinositol (PtdIns) synthase (the enzyme that condenses Ins and CDP-diacylglycerol to generate PtdIns) are conspicuous in their absence. In spite of this, considerable evidence supports the existence of PtdIns-directed metabolic machinery within the nuclear matrix. Nuclei possess PtdIns kinases and phospholipases C (PLC) that generate and consume phosphoinositides (PIPs), respectively [41, 42, 24]. Moreover, PIPs (e.g., phosphatidylinositol-4,5-bisphosphate; PIP_2) reside within the nuclear matrix, and endonuclear PIP_2 is required for proper 3'-polyadenylation of

a specific subset of mRNAs [20]. In addition, endonuclear PLC (either β1, δ, or γ isoforms) generates Ins-1,4,5-P_3 (IP_3) and 1,2-diacylglycerol at the expense of PIP_2 in that compartment [reviewed in 81]. IP_3 is an obligate precursor in the synthesis of inositol polyphosphates that are themselves known to regulate endonuclear activities, such as transcription, mRNA splicing, mRNA export, and non-homologous end joining [reviewed in 54].

How is the mammalian nucleus supplied with PtdIns in the face of its inability to synthesize this PL in situ? Recent attention has focused on phosphatidylinositol transfer protein alpha (PITPα) as carrier. PITPα is a soluble 35kd protein that is found in most mammalian cell types and is able to mobilize PtdIns and PtdCho monomers between membrane bilayers in vitro. Whether PITPα (and PITPs in general) truly function in mobilization of PLs in cells, or whether these represent nanoreactors that directly influence the catalytic mechanism of lipid kinases, is a matter of debate [82, 83]. Nonetheless, using the principal tenets of a transfer mechanism, de Vries et al. [84] proposed a PITPα-driven cycle of PtdIns/PtdCho exchange from the nuclear matrix that functions to supply the nuclear matrix with PtdIns at the expense of nuclear PtdCho. The essential features of this hypothesis are outlined in Figure 1.

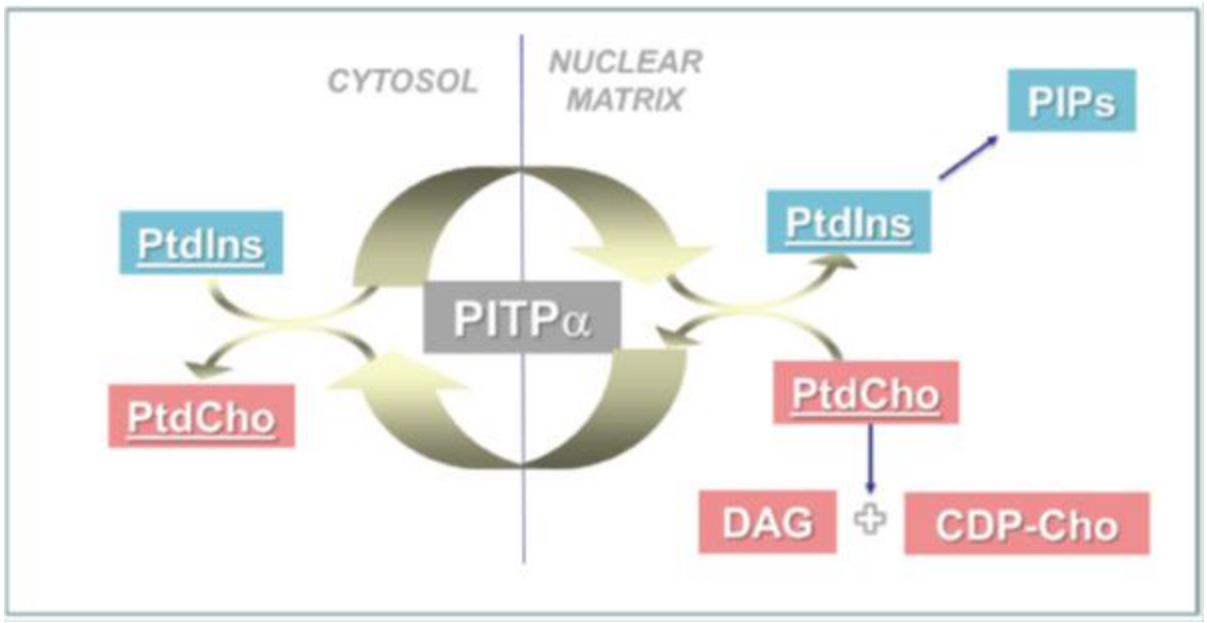

Figure 1. PITPα-centric model for nuclear import of PtdIns.

PITPα::PtdIns is imported into the nucleus where it deposits PtdIns for a molecule of nuclear PtdCho. The resultant PITPα::PtdCho complex is then recycled to the cytoplasmic compartment where a heterotypic PtdCho/PtdIns exchange reaction recharges the PITPα with PtdIns for another round of nuclear import. Three lines of evidence form the primary basis for such a proposal. First, PITPα exhibits the proper PL binding activities to support such an import mechanism. Second, this protein exhibits the proper localization. Experiments where fluorescently-labeled protein is microinjected into mammalian cells, or where PITPα is expressed as an EGFP-tagged chimera, consistently indicate PITPα resides in both the cytosol and nuclear matrix [84, 86, 82]. Third, the presence of nuclear isoforms of PtdCho biosynthetic enzymes, when coupled with reports of surprising quantities of PtdCho in the nuclear matrix [17], argue that the nuclear PtdCho load is sufficient to sustain such a cycle. However, how a PL exchange reaction might occur in a compartment devoid of identifiable bilayer structures is not addressed by this model. We also note that none of these three lines of evidence directly address the basic validity of the PITPα-import conjecture.

Herein, we report the results of quantitative assessments of central precepts of the PITPα-import conjecture. These include: (i) PITPα must shuttle between the cytoplasmic compartment and the nuclear matrix, (ii) nuclear import competence of PITPα is influenced by its ligand-bound state – i.e., whether it is bound to PtdIns or PtdCho, and (iii) dynamic endonuclear PtdIns lipidomics are altered upon functional ablation of PITPα. The experimental tests of the model take advantage of a facile new method, described in Chapter 2 and Chapter 3, for purifying nuclear matrix free of contamination by ER membranes and nuclear envelope from murine embryonic fibroblasts (MEFs) of defined PITPα genotype. The collective data from a combination of mass-shift labeling experiments and lipidomic

profiling experiments demonstrate that PITPα is not a primary contributor to the PtdIns endonuclear supply pathway(s). These findings hold significant implications for ongoing discussions regarding the dynamic lipidomics of the mammalian nuclear matrix and the physical requirements of housing PL molecules in this bilayer-free endonuclear compartment.

4.3 Materials and Methods

4.3.1 Reagents and Antibodies

Dulbecco's Modified Eagle Medium (DMEM) and antibiotics were obtained from Mediatech (Herndon, VA). The mass labels *myo*-^{6}*d*-inositol and ^{9}*d*-choline were obtained from C/D/N isotopes (Pont-Claire, Quebec, Canada) and Sigma-Aldrich (Poole, Dorset, UK), respectively. Other biochemicals used in this study were purchased from Sigma-Aldrich or Fisher Scientific (Fair Lawn, NJ) and were of reagent grade. Organic solvents and supplies used to prepare samples for electron microscopy were obtained from EMD Biosciences (San Diego, CA).

Monoclonal antibodies directed against the HA-epitope (anti-HA, Covance Research Chemicals, Alice, TX) were employed as primary antibodies in immunofluorescence experiments. In both cases, the primary antibodies were decorated with Alexa fluor 488-labeled secondary goat-anti-mouse antibodies for purposes of visualization (Molecular Probes, Eugene, OR). Other primary antibodies used in these studies included: monoclonal anti-β-tubulin antibody (Sigma-Aldrich), rabbit polyclonal anti-Calnexin antibodies (Nventa Biotechnologies, San Diego, CA), and rabbit polyclonal anti-acetylated Histone H3 antibodies (Calbiochem, San Diego, CA). In those cases, goat-anti-mouse or goat-anti-rabbit

horseradish peroxidase (HRP)-conjugated secondary antibodies from Jackson ImmunoResearch (West Grove, PA) were used for development.

A mouse IgM primary antibody directed against $PI(4,5)P_2$ (Echelon Biosciences) was used in detection of endonuclear PIP2. An Alexa-fluor 488-labeled secondary goat anti-IgM antibody (also purchased from Molecular Probes) was used for visualization. Confirmation of the speckle localization was confirmed using a Sigma mouse monoclonal IgG Speckle marker antibody.

4.3.2 Fluorescence Recovery After Photobleaching

HeLa tissue culture cells were transiently transfected with EGFP-N1 or PITPα-EGFP in EGFP-N1 plasmids. Sixteen hours post transfection, transfected cells were identified on an Olympus IX81 FV1000 laser scanning confocal inverted microscope equipped with an Argon ion 488 laser. Nuclear or cytoplasmic regions in transfected cells were selected and a 0.2µm spot was pulse photobleached at full power for 0.2s. Recovery scans were performed using 1% laser power with 0.2s intervals on tornado scan mode. Data was analyzed using MatLab software as described by Gordon et al. [87].

4.3.3 Molecular Biological Techniques and Site-directed Mutagenesis

Rat *PITPα* cDNA was amplified by PCR and subcloned as a 0.85 kb *Hind*III-*Bam*HI fragment into the multiple cloning site (MCS) of pEGFP-N1 (Clontech, Palo Alto, CA). An HA epitope-tagged rat *PITPα* cDNA (tag at C-terminus) was generated by amplification of the rat *PITPα* cDNA and insertion of the 0.85kb product into the unique *BamH*I-*Not*I sites of pEF3HA, a derivative of pEF4 (Invitrogen, Carlsbad, CA) as described in [88]. This

construct contains an HA epitope that was incorporated into that construct as an *Xba*I-*Pme*I cassette (DNA sequence 5'-TATCCTTACGACGTTCCAGACTATGCA-3').

Site-directed mutagenesis primers used in this study were from Fisher Scientific, and rat PITPα cDNAs were mutagenized according to Quickchange mutagenesis kit specifications (Stratagene, La Jolla, CA). All mutant constructs were confirmed by nucleotide sequence analysis.

4.3.4 Mammalian Cell Culture and Transfections

Mouse embryonic fibroblasts (MEFs) were derived from E16 *PITPα*$^{+/+}$ and *PITPα*$^{0/0}$ embryos, and immortalized lines of each were generated by SV40 Large T-antigen method. Unless otherwise specified, all primary and immortalized cell lines were cultured in complete Dulbecco's Modified Eagle Medium containing 4.5 g/L glucose, and media were supplemented with 10% FBS, 1U/mL penicillin G, and 100μg/mL streptomycin (complete DMEM). All cell culture was performed at 37°C in a 10% CO_2 incubator.

Immortalized cell lines were transfected using the FuGene transfection reagent (Roche, Indianapolis, IN). Briefly, Cos 7 cells or immortalized MEF (iMEF) lines were seeded onto plastic dishes in complete DMEM 24hrs prior to transfection. Once cells settled on the plastic surface, the medium was exchanged for antibiotic-free DMEM. 1μg *PITPα-GFP* constructs were incubated in 100μL Opti-MEM (Invitrogen, Carlsbad, CA) pre-mixed with 3μLtransfection reagent according to the manufacturer's instructions. The complete transfection cocktail was incubated at room temperature for 1hr before distribution to the medium. At 12hrs post-transfection, cells were split onto coverslips and cultured in complete DMEM. In experiments involving epitope-tagged versions of PITPα, the protocol was modified in that cells were seeded directly onto coverslips prior to transfection.

4.3.5 Immunocytochemistry

Cells cultured on glass coverslips were transiently transfected with the appropriate PITPα-GFP or epitope-tagged PITPα expression plasmids, incubated for an additional 24hrs, then fixed in 4% paraformaldehyde in PBS. After permeabilization in 0.2% Triton-X 100, fixed cells were counterstained with DAPI (Molecular Probes) for 1min. Cells transfected with epitope-tagged PITPα were fixed by the same protocol, but were permeabilized 16-18hrs after transfection and incubated for 1hr at room temperature in blocking buffer (2% BSA in PBS). Primary antibodies (1:4000 dilution in blocking buffer) were incubated with the cells for 12-15hrs at 4°C. Cells were serially washed three times for 10mins in 1%BSA in PBS. Secondary antibodies (1:8000 in blocking buffer) were applied, fixed cells were incubated at 4°C for 5-8hrs, and after several washes (1%BSA in PBS), the cells were counterstained with DAPI. Coverslips were mounted on glass slides, imaged on a Leica SP2 scanning laser confocal microscope, and images were processed using Adobe Photoshop 6.0.

4.3.6 Labeling of MEFs with Deuterated Phospholipid Precursors

Early passage (p3-p5), primary $PITP\alpha^{+/+}$ or $Pitp\alpha^{0/0}$ MEFs were seeded in complete DMEM and grown to a subconfluent (~70%) density. Cells were washed twice in PBS and labeled for the desired time periods with 80ug/mL d_9-choline and/or *myo*-d_6-inositol as described previously [17]. For bulk phospholipid determinations, $PITP\alpha^{+/+}$ or $Pitp\alpha^{0/0}$ MEFs pooled from three p150 tissue culture plate cultures were isolated and resuspended in 800μL PBS for analysis by ESI MS/MS. In experiments involving purified nuclei stripped of membranes, 10^7 cells were pelleted and washed in PBS prior to detergent-mediated removal of the nuclear envelope.

4.3.7 Isolation of Membrane-stripped MEF Nuclei and Quality Control Analyses

Envelope stripping of both *PITP*$\alpha^{+/+}$ or *Pitp*$\alpha^{0/0}$ nuclei was performed as described in *Chapter 2* (*pp. 23-51*). Quality control analyses were performed as described in the *Methods and Materials* section of *Chapter 2 (pp. 68-70)*.

4.3.8 RNA Isolation and qPCR Analyses

To induce oxidative stress, *PITP*$\alpha^{+/+}$ and *Pitp*$\alpha^{0/0}$ cells were grown to 85-90% confluence and treated for 4 hours with either >0.1% DMSO (vehicle) or with 100μM t-butylhydroquinone (tBHQ). Total cellular RNA was then extracted using TRI reagent (Sigma Aldrich) according to the manufacturer's protocol. cDNA was then generated from the mRNA using the Stratagene RT-PCR kit. cDNAs were diluted to a concentration of 5ng/μL and analyzed by qPCR in triplicate for Heme-oxidase-1 cDNA content as described in [20]. Results were normalized to β2M expression levels.

4.3.9 IP_6 Analyses

PITP$\alpha^{+/+}$ and *Pitp*$\alpha^{0/0}$ MEFs were seeded and grown overnight to 25% confluency in 6-well charged tissue dishes. Inositol-labeling media was prepared without inositol using the inositol-labeling media kit (Cell & Molecular Technologies, Phillipsburg, NJ) and supplemented with 10% dialyzed FBS (Gemini Bio-sciences, Woodland, CA) and antibiotic. 24 hours after plating, cells were washed twice in inositol-labeling media and incubated in inositol labeling media containing 100mCi/mL H^3-*myo*-inositol (American Radiolabeled Chemicals, Inc., St. Louis, MO). 72 hours post-treatment, the medium was removed and cells were washed once in PBS. Cells were incubated for 5 minutes in 1mL 0.5N HCl and

subsequently scraped into Eppendorf tubes. Lysates were centrifuged for 10 minutes at 13,200 x *g* to remove cell debris. Following filtration through a 0.45μm syringe filter, samples were frozen at -80°C prior to HPLC analysis of inositol phosphates. Inositol polyphosphates were then separated by HPLC on a Partisphere strong-anion exchange column as reported [93]. IP_6 peaks were identified on the basis of co-elution with known standards.

4.4 Results

4.4.1 PITPα Shuttles Between Cytoplasmic and Nuclear Compartments

PITPα is identified as a cytosolic and nuclear matrix protein by experiments where fluorescently-labeled protein is microinjected into mammalian cells or expressed as an EGFP-tagged chimera [82, 84, 86]. Both approaches are prone to artifact, and nuclear localization of EGFP-tagged reporters is particularly problematic as EGFP itself accumulates in the nucleus of living cells, and PITPα-EGFP chimeras are prone to cleavage events that liberate the EGFP domain (our unpublished data). These issues inject considerable uncertainty into the interpretations of such imaging experiments. To minimize noise caused by undesirable cleavage events, a PITPα-EGFP chimera was generated with a 24 amino acid linker between the PITPα and EGFP domains, and whose integrity is well-maintained in mammalian cells (Figure 2A).

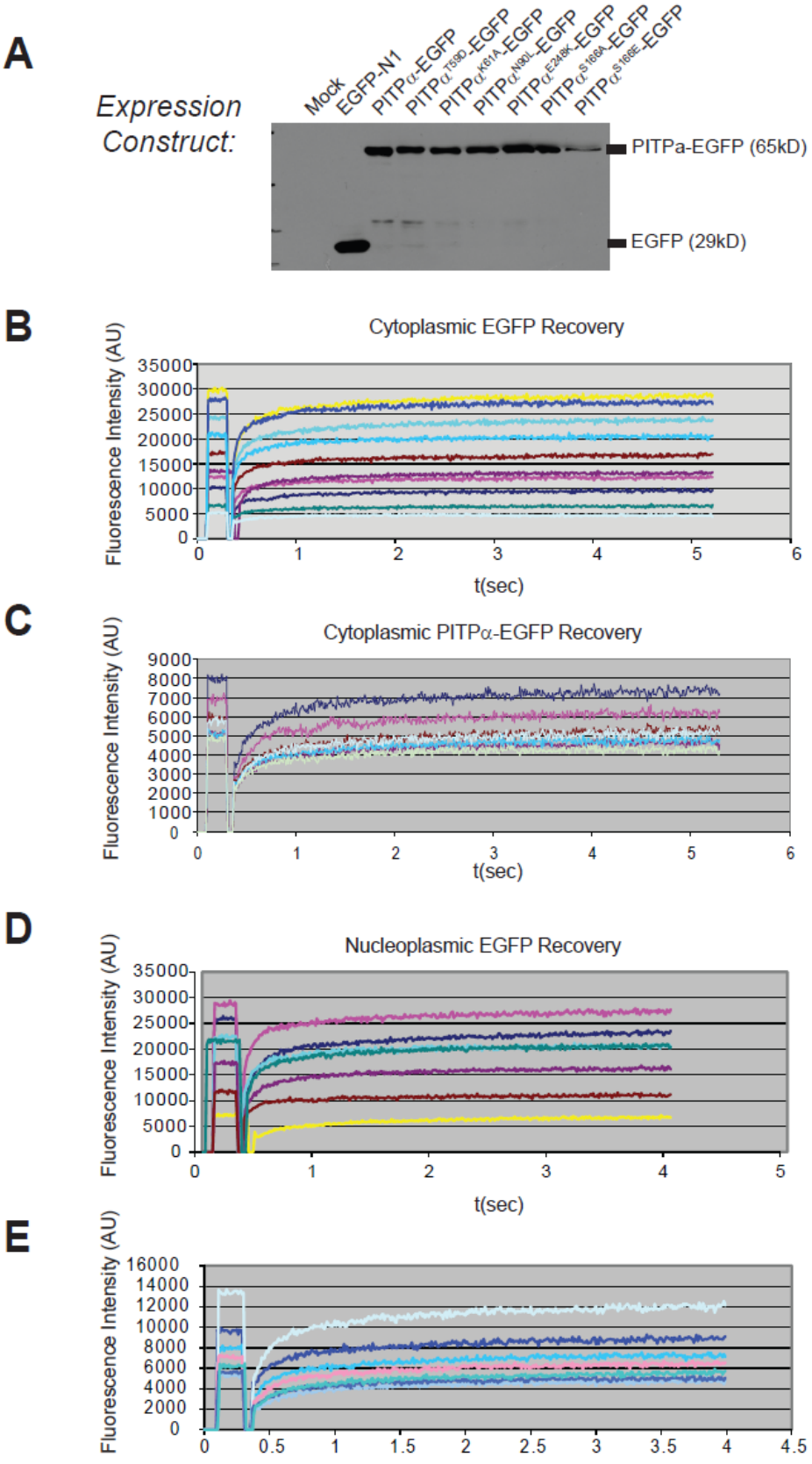
A
Expression Construct:
Mock
EGFP-N1
PITPα-EGFP
PITPα T59D-EGFP
PITPα K61A-EGFP
PITPα N90L-EGFP
PITPα E248K-EGFP
PITPα S166A-EGFP
PITPα S166E-EGFP
PITPa-EGFP (65kD)
EGFP (29kD)
B
Cytoplasmic EGFP Recovery
Fluorescence Intensity (AU)
t(sec)
C
Cytoplasmic PITPα-EGFP Recovery
Fluorescence Intensity (AU)
t(sec)
D
Nucleoplasmic EGFP Recovery
Fluorescence Intensity (AU)
t(sec)
E
Fluorescence Intensity (AU)

Figure 2. Mobility of transiently expressed PITPα-EGFP fusion proteins. (A) Cleavage analysis of transiently-expressed PITPα-EGFP fusion proteins by immunoblot. Cell lysates were analyzed for cleavage of the GFP tag 18 hours after transfection in HeLa cells. Cleavage of EGFP-tagged, point mutant constructs defective for lipid binding (Pitpα^{T59D}, Pitpα^{K61A}, Pitpα^{N90L}, Pitpα^{S166A}, Pitpα^{S166E} and Pitpα^{E248K} constructs) was analyzed alongside the wild-type PITPα-EGFP construct. (B-E) Point FRAP recovery curves of transiently expressed fluorescent protein. Five of 40 seconds of recovery are shown here. Bleach pulse in these experiments was 0.2 seconds. (B) Recovery curves of transiently overexpressed EGFP (n=10 cells). (C) Recovery curves of transiently overexpressed wild type PITPα-EGFP fusion proteins (n=6 cells). (D) Recovery curves of nucleoplasmic overexpressed EGFP (n=10 cells). (E) Recovery curves of nucleoplasmic PITPα-EGFP (n=7 cells).

The mobility of PITPα protein in the cytoplasm and nucleus is an essential characteristic of a nucleocytoplasmic PtdIns shuttle protein. We used Point fluorescence recovery after photobleaching (FRAP) of cells transiently expressing the PITPα-EGFP fusion protein. As a control for mobility we transiently expressed unconjugated EGFP and performed a parallel experiment. Transiently expressing cells were spot photobleached in either the cytoplasm or nuclear portion of the cell, and the recovery imaged at 0.1 second intervals. Recovery curves for cytoplasmic and nucleoplasmic PITPα-EGFP pools (Figure 2C and 2E) are demonstrated in comparison to those for cytoplasmic and nucleoplasmic EGFP pools (Figure 2B and 2D). Spot bleaching of cytoplasmic PITPα-EGFP protein pools is followed by a recovery on average > 94% over a 20 second time frame. Overexpressed cytoplasmic EGFP recovers only slightly better, at a > 97 % percent rate after 40 seconds. EGFP in the nucleus will 96% Nucleoplasmic PITPα-EGFP proteins are equally mobile with their cytoplasmic counterparts (greater than 90% recovery; Figure 2E). The recovery curves were used to calculate the diffusion coefficients of PITPα-EGFP vs. EGFP in the cytoplasm and nucleus. In the cytoplasm, the average diffusion coefficient for PITPα-EGFP is equal to $7.90 \pm 4.8 \times 10^{-9}$ m/s^2 vs. $4.38 \pm 1.38 \times 10^{-8}$ m/s^2 for EGFP. Nuclear diffusion coefficients for PITPα-EGFP and EGFP are $8.29 \pm 0.8 \times 10^{-8}$ m/s^2 and 5.26 ± 1.92 x 10-8 m/s^2, respectively.

4.4.2 Relationship between PtdIns-binding and PITPα-import into the Nucleus

We addressed whether the ability of PITPα to bind PtdIns is an obligate requirement for transport of this protein into the nuclear matrix. A previously published report suggested this is the case, but that report showed no quantitative assessment of the issue thereby

limiting interpretation [86]. Thus, we investigated the question in detail. A combination of genetic screens and structural studies identified a set of residues critical for coordination of the PtdIns headgroup in the PITPα binding pocket [89-91], and PtdIns-binding is an essential functional property for PITPα in mammalian cells [92]. Four mutant versions with specific defects in PtdIns-binding were employed in these experiments – Pitpα^{T59D}, Pitpα^{K61A}, Pitpα^{N90L}, and Pitpα^{E248K}. The corresponding missense substitutions were incorporated into the PITPα-EGFP reporter for transient expression in HeLa cells and imaged. These constructs are also stably expressed in cells as indicated in western blotting experiments (Figure 2A). Individual cells were scored as to whether the chimera localizes predominantly to the nucleus (as in the wild-type protein) or to the cytoplasm. This is judged by co-localization with DAPI staining. Only 2.1% of cells expressing the control PITPα-EGFP reporter demonstrated a strong cytosolic signal with little to no nuclear fluorescence (9/440; Figure 3). By contrast, 51.6% of cells (190/368) expressing Pitpα^{T59D}-EGFP construct displayed a nuclear localization defect. Similar results were scored for cells expressing PITPα^{E248K}-EGFP (61.4%, 189/308 cells). Milder, but nevertheless significant, nuclear localization defects were recorded for the Pitpα^{N90L}-EGFP and Pitpα^{K61A}-EGFP chimeras (17.7%, 57/322 and 10.8%, 40/370 of expressing cells, respectively). Yet, Pitpα^{S166A}-EGFP and Pitpα^{S166E}-EGFP chimeras (i.e., proteins defective in both PtdIns and PtdCho-transfer activity; [82] were fully competent for localization to the nucleus. Some 2.7% (11/404) and 1.9% (8/425) of the cells expressing these proteins scored as failing to present nuclear EGFP fluorescence, respectively. While these collective results were obtained in HeLa cells, similar data were collected when these various chimeras were evaluated in either *Pitpα$^{0/0}$* MEFs and in Cos7 cells (our unpublished data). Thus, PtdIns-binding influences the efficiency of

nuclear localization for PITPα-EGFP chimeras, but it does not appear to be an obligate requirement (results quantified in Figure 3).

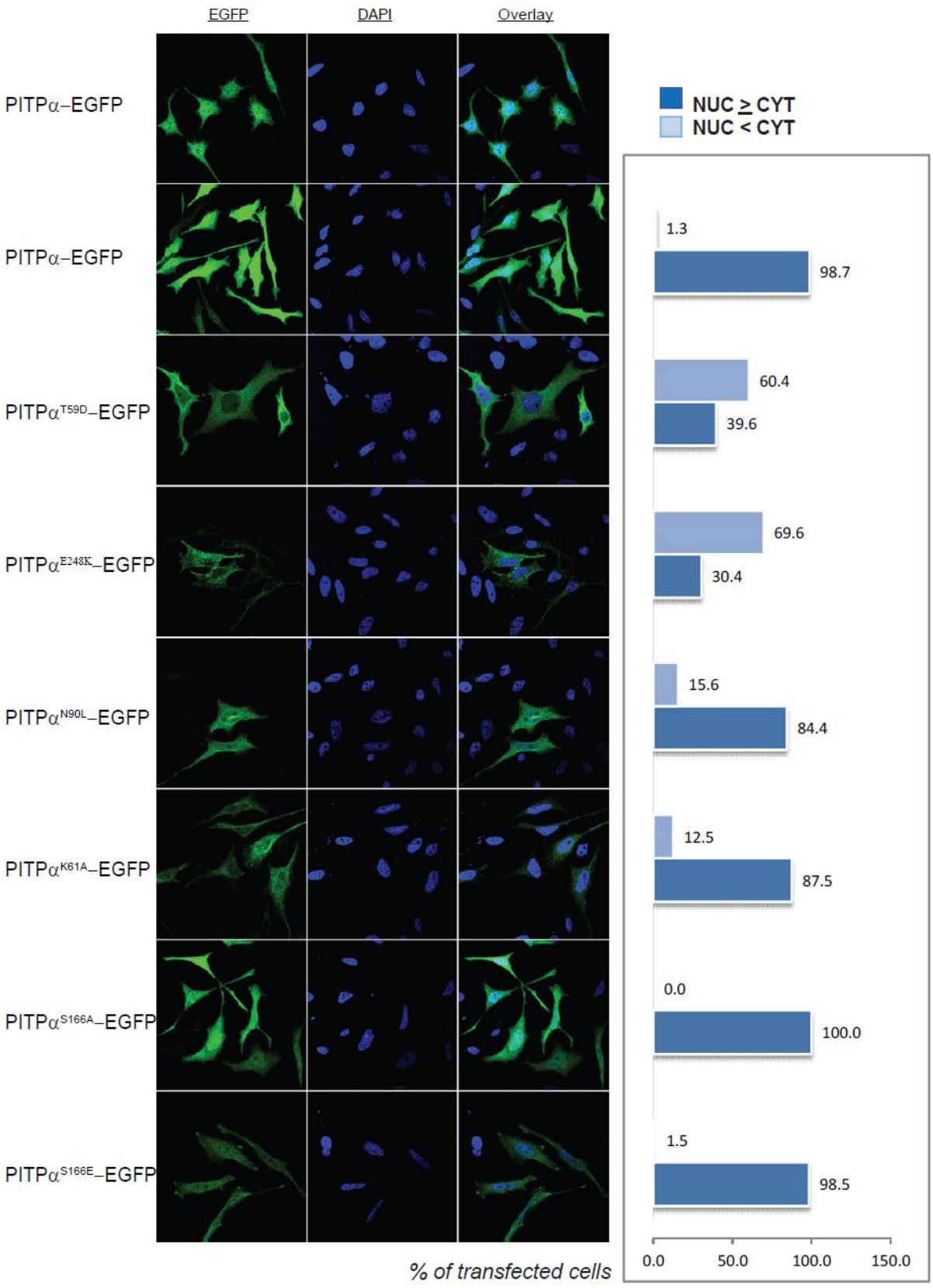
EGFP
DAPI
Overlay
PITPα–EGFP
PITPα–EGFP
PITPα^T59D–EGFP
PITPα^E248K–EGFP
PITPα^N90L–EGFP
PITPα^K61A–EGFP
PITPα^S166A–EGFP
PITPα^S166E–EGFP
NUC ≥ CYT
NUC < CYT
1.3
98.7
60.4
39.6
69.6
30.4
15.6
84.4
12.5
87.5
0.0
100.0
1.5
98.5
0.0
50.0
100.0
150.0
% of transfected cells

Figure 3. Nuclear localization patterns of PITPα-EGFP and lipid binding mutants transiently overexpressed in HeLa cells. (A) Confocal images of HeLa cells transiently expressing PITPα-EGFP and PITPα PL-binding and transfer mutants. Cells were grown on coverslips, transfected, and fixed 18 hours post-transfection. Cells are counterstained with 4',6-diamidino-2-phenylindole (DAPI) to examine nuclear localization of mutant constructs. Wt constructs produce nuclear fluorescence which is greater than or equivalent to cytoplasmic fluorescence in the vast majority of expressing cells. PtdIns-binding defective point mutants, Pitpα^{T59D}, Pitpα^{K61A}, Pitpα^{N90L} Pitpα^{E248K} and the PtdIns/PtdCho-binding defective point mutants Pitpα^{S166A} and Pitpα^{S166E} were scored for the relative strength of nuclear signal vs. cytoplasmic fluorescence, as judged by coincidence with nuclear DAPI stain. (B) Quantitation of nuclear localization defects in cells expressing PITPα-EGFP mutant constructs. Minimally 200 cells were scored for Nuclear signal ≥ Cytoplasmic signal (nuc ≥ cyt) or if Nuclear signal < Cytoplasmic signal (nuc<cyt).

The effects of the various missense substitutions on PITPα localization profiles were not dependent on the EGFP tag. HA-Epitope-tagged versions of PITPα, Pitpα^{T59D}, Pitpα^{K61A}, Pitpα^{N90L}, and Pitpα^{E248K} were individually expressed in HeLa cells. The cells were fixed, permeabilized, and HA-PITPα localization was visualized by indirect immunofluorescence. Quantified results (shown in Figure 4B) echoed those observed with our PITPα-EGFP tagged construct. The nuclear signal dominates the cytoplasmic signal in cells expressing the wild-type PITPα-HA fusion protein, and this localization pattern was observed in 97.6% of transfected cells (980/1004; Figure 4A, top two panels). Predominantly cytosolic phenotypes were observed for the Pitpα^{T59D}-HA (78.3%; 548/700), and Pitpα^{E248K}-HA expressing cells. In over 78% of cells expressing the Pitpα^{T59D}-HA fusion protein, the fluorescence signal was strongest in the cytosol (Figure 4A; 3rd panel from the top). We observed the nuclear localization defect approximately 95.1% of cells transiently expressing the Pitpα^{E248K}-HA fusion proteins (448/471 cells; Figure 4A, 4th panel from top). Nuclear localization defects are less frequent in cells expressing the Pitpα^{K61A}-HA fusion protein, with only 15.6% of cells demonstrating a nuclear localization defect (Figure 4A; second panel from bottom). We will note, however, that the nuclear signal in cells expressing Pitpα^{K61A}-HA, although commonly equal to the cytoplasmic signal, is rarely dominant to the cytoplasmic signal, as is seen in cells expressing the wild-type protein. Nuclear localization defects are also observed in 24.8% of cells expressing the PtdIns *and* PtdCho binding mutant, Pitpα^{S166E}-HA (34/137; Figure 4A bottom panels). Although not an obligate requirement, lipid-binding is required for wild-type nuclear accumulation of PITPα proteins. These findings are also consistent with its proposed role in import of nuclear PtdIns.

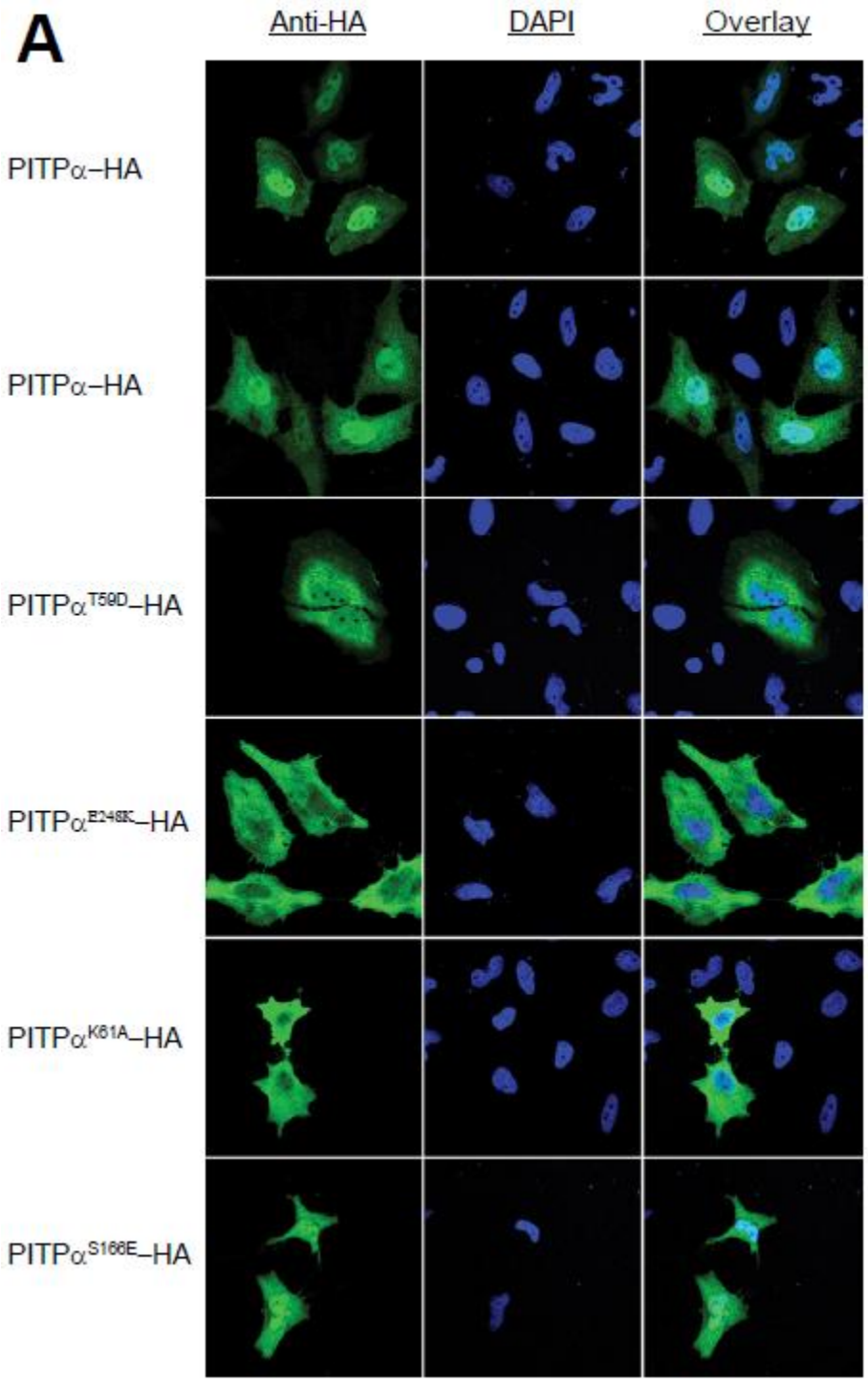
A
Anti-HA
DAPI
Overlay
PITPα–HA
PITPα–HA
PITPα^{T59D}–HA
PITPα^{E248K}–HA
PITPα^{K61A}–HA
PITPα^{S166E}–HA

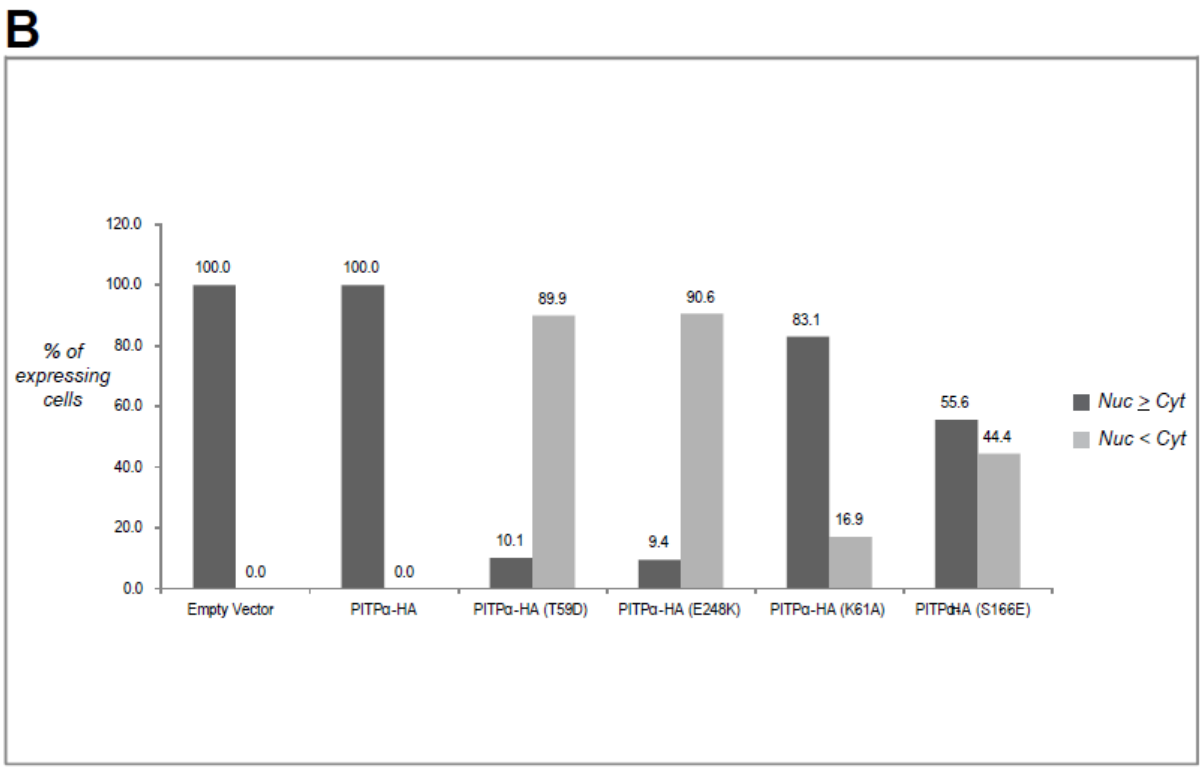

Figure 4. Nuclear localization patterns of epitope-tagged PITPα and lipid-binding mutants transiently overexpressed in HeLa cells. Confocal images of HeLa cells expressing PITPα-HA and PITPα point mutants defective in PL-binding and transfer. Cells are fixed and stained with anti-HA primary antibodies 16-18 hours after transfection. Cells are counterstained with 4',6-diamidino-2-phenylindole (DAPI) to facilitate examination mutant constructs nuclear localization. Wt constructs produce nuclear fluorescence which is greater than or equivalent to cytoplasmic fluorescence in the vast majority of expressing cells. PtdIns-binding defective point mutants, Pitpα^{T59D}, Pitpα^{K61A}, Pitpα^{E248K} and the PtdIns/PtdCho-binding defective point mutants and Pitpα^{S166E} were scored for the relative strength of nuclear signal vs. cytoplasmic fluorescence, as judged by coincidence with nuclear DAPI stain. (B) Quantitation of nuclear localization defects in cells expressing PITPα-EGFP mutant constructs. Minimally 200 cells were scored for Nuclear signal ≥ Cytoplasmic signal (nuc ≥ cyt) or if Nuclear signal < Cytoplasmic signal (nuc<cyt).

4.4.3 Purification of Envelope-free Nuclei from *PITPα*$^{+/+}$ and *Pitpα*$^{0/0}$ MEFs

Comparisons of steady-state nuclear matrix PtdIns content, and of the rates of PITPα-mediated PtdIns import into the nuclear matrix, define the acid tests of the PITPα-import conjecture. Accurate quantification of endonuclear lipids is primarily confounded by two technical challenges. First, such analyses require the complete removal of nuclear envelope, which is contiguous with the ER, from the endonuclear fractions. Even minor contamination by ER/nuclear envelope potentially leads to significant overestimates of endonuclear lipid mass. Second, removal of nuclear envelope requires use of detergents, and such extraction methods themselves introduce variables. Incomplete extraction, or inappropriately vigorous extraction, results in opposing, but nonetheless undesirable, influences on accuracy of measurement. Thus, optimal methods for preparation of envelope-free nuclei must negotiate the delicate balance between sufficient rigor so as to remove the nuclear envelope, and yet minimize the errors introduced by over-extraction. One final, and important, factor is the cell-type being used as suitable purification methods will necessarily vary between cell-types. To this end, we have devised a reproducible scheme for purifying envelope-free nuclei from MEFs – i.e., cell-types that most easily permit application of gene ablation methods to the study of endonuclear lipid homeostasis. This protocol is discussed in methodological detail in Chapters 2 and 3. Here, we use this technique to demonstrate that the envelope-stripping of *Pitpα*$^{0/0}$ nuclei is attainable to a similar degree of purity. The primary method by which purity is assessed is immunoblot for markers of nuclear membrane contaminants. The scheme for purification is demonstrated in Figure 2 of Chapter 2. In Figure 5A of this chapter, we demonstrate the absence of the commonly-used outer nuclear envelope marker, β-tubulin, from both *PITPα*$^{+/+}$ and *Pitpα*$^{0/0}$ nuclei purified using this

protocol. More notably, purified *Pitpα*$^{0/0}$ nuclear fractions are equally devoid of an abundant ER transmembrane protein, calnexin (CNX), which is a more stringent test of purity. The nuclear fractions also contain DNA-deposited Histone H3, as indicated by antigenicity of the purified fractions for Histone H3 acetylated at Lys9.

EM was used as an independent means to assess the quality of purified nuclear matrix fractions. As shown in Figure 5B, morphologically intact nuclei were obtained from *Pitpα*$^{0/0}$ iMEF as well as from wild type cells. In both cases, the nuclei were effectively stripped of nuclear envelope and were free of contaminating membranes – as evidenced by the lack of membrane bilayers at the electron-dense lamin borders of the stripped nuclei and the lack of co-purifying membrane vesicles in the background. These features are apparent even when the nuclear borders are examined at higher magnifications (Figure 5C).

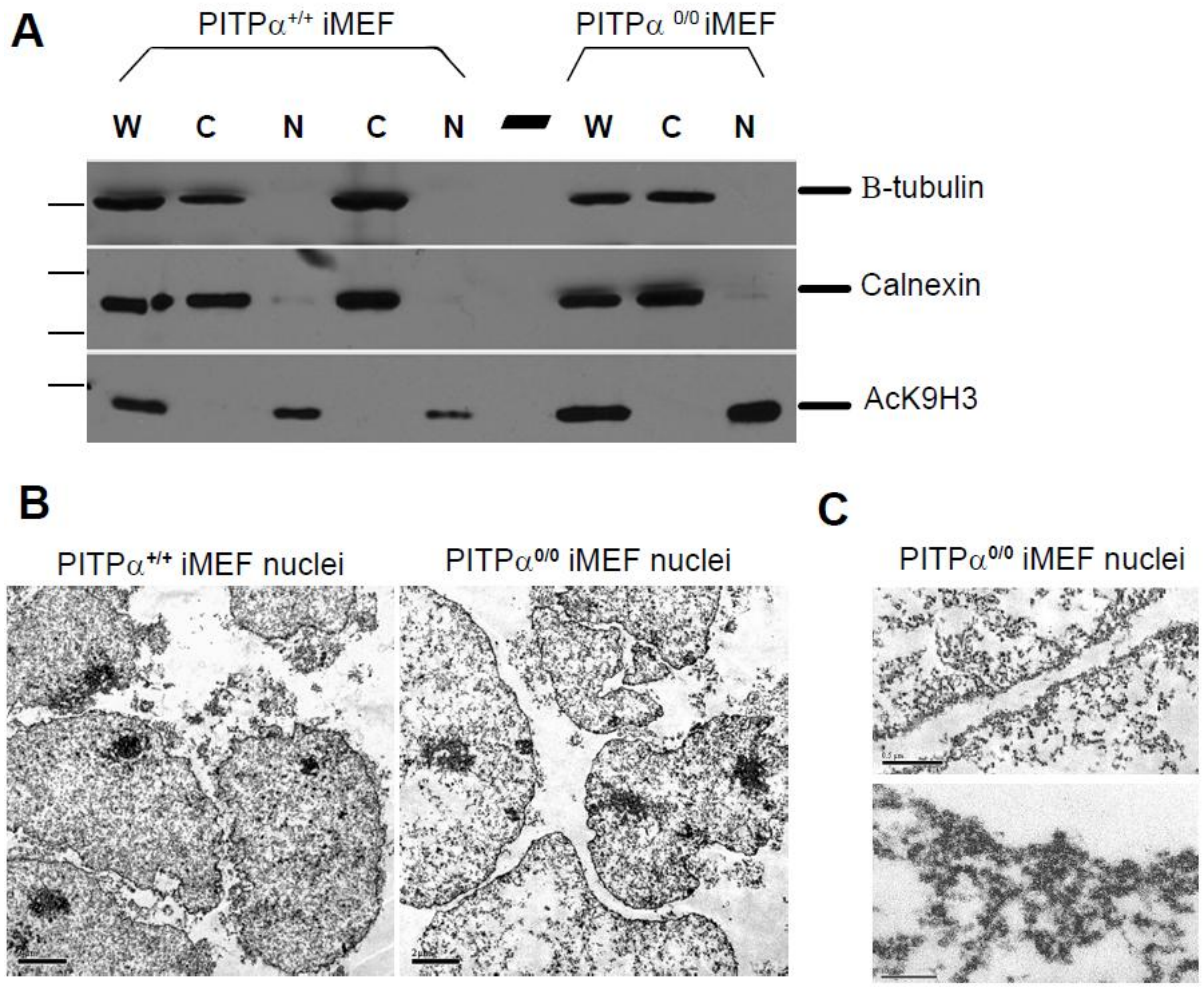

Figure 5. Quality control analysis of envelope-stripped *Pitpα*$^{0/0}$ nuclei. (A) Western blot analysis of *PITPα*$^{+/+}$ (left) and *Pitpα*$^{0/0}$ iMEF nuclear fractions. SDS-PAGE gels were loaded by cell equivalents with whole cell (W), cytosolic (C), and envelope-free nuclear (N) fractions generated during envelope free nuclear preparations from *PITPα*$^{+/+}$ and *Pitpα*$^{0/0}$ iMEF cells. Anti-Calnexin (90kD) and anti-β-tubulin (50kD) antibodies do not detect substrate in 30,000 cell equivalents worth of nuclear protein, but detect substrate in W and C fractions. Conversely, an anti-acetyl lys9 Histone H3 antibody recognizes substrate in W and N fractions but not in cytosolic fractions. (B) Low magnification (1100x) electron micrographs of envelope-devoid, individual *PITPα*$^{+/+}$ (left) and *Pitpα*$^{0/0}$ iMEF (right) nuclei. Our purification method produces intact nuclei with minimal debris. (C) High magnification images of *Pitpα*$^{0/0}$ nuclei. *Upper:* 6500x magnification of 2 opposing nuclei and their borders. Borders appear intact and fuzzy. White space between nuclei indicates a lack of extraneous debris / membranes. Scale bar = 0.5µm *Lower:* 15000x magnification of the nuclear border. Borders lack observable membrane traces. Scale bar is 100µm.

4.4.4 Comparative and Quantitative Lipidomic Profiling of *PITPα*$^{+/+}$ and *Pitpα*$^{0/0}$ Nuclei

The availability of highly purified envelope-free nuclei allows application of lipidomic strategies to comparatively profile the diversity of PL species in endonuclear compartments, and to compare the relative steady-state amounts of identifiable endonuclear PL species in *PITPα*$^{+/+}$ vs. *Pitpα*$^{0/0}$ iMEFs. Lipid extracts of 9 x 10^7 wild-type and *Pitpα*$^{0/0}$ iMEF purified nuclear pellets were separated and profiled as described in [65]. These analyses were also performed on 1 x 10^7 *PITPα*$^{+/+}$ or *Pitpα*$^{0/0}$ whole iMEF cell pellets for comparison. Our previously described analyses of envelope-free iMEF nuclei and whole cells indicate that endonuclear GPL pool is several orders of magnitude less than previously [17]. Molecular species profiling results and quantitation are shown in Tables 1 through 3 in terms of pmol/mg nuclear protein. Total endonuclear GPL load (averaged from 3 independent measurements) was 1.44 ± 0.11 x 10^8 PLs / *PITPα*$^{+/+}$ nucleus vs.1.28 ± 0.23 x 10^8 PLs / *Pitpα*$^{0/0}$ nucleus. Although PL profiles from experiment to experiment were not identical, PL classes were similarly represented in the *PITPα*$^{+/+}$ and *Pitpα*$^{0/0}$ endonuclear profiles (Figure 6B). The predominant PL class in nuclei is PtdCho (8 of the top 10 molecular species), comprising over 50% of endonuclear mass. While endonuclear PL species are predominantly of the PtdCho class, PtdSer and PtdEtn molecular species also contribute heavily to endonuclear phospholipid pools. Very minor contributions from PtdIns, PtdOH, and PtdGro phospholipids are also detected in *Pitpα*$^{0/0}$ nuclei. Whole cell PL profiles were similar to wild type contain all phospholipid types (shown in Figure 6A). When comparing quantitative profiling data from in *PITPα*$^{+/+}$ or *Pitpα*$^{0/0}$ iMEF whole cells,

no dramatic differences in PL mass or in the relative amounts of PL molecular species were noted (data not shown).

Table 1. Ranking of GPL by abundance in 7.5 x 10^7 wild type nuclei and PITPα nuclei (SET 1) (pmol/million cells or pmol/million nuclei, mean and standard error; n=9).

wt NUC		ko NUC	
	pmol / mg protein		pmol / mg protein
PS(36:1)	396.5	PS(36:1)	244.55
PC(38:6)	218.84	PC(32:0)	118.9
PC(32:0)	189.18	PC(38:6)	107.94
PC(36:2)	140.67	PC(34:1)	97.49
PS(34:1)	138.19	PS(34:1)	85.43
PC(38:5)	128.99	PC(32:1)	74.11
PC(32:1)	122.94	PE(38:4)	73.92
PE(38:4)	111.77	PC(30:0)	71.77
PC(30:0)	109.23	PC(38:5)	69.73
PS(38:4)	93.29	PC(36:2)	61.19
PE(36:1)	88.19	PS(38:4)	55.92
PC(40:6)	87.51	PC(40:6)	49.73
PS(36:0)	87.37	PS(36:0)	49.02
PC(36:5)	81.19	PC(36:5)	42.3
PC(34:1e)	80.42	PC(36:0)	41.71
PC(36:0)	60.87	PC(38:4)	38.13
PE(38:3)	58.81	PS(40:5)	37.48
PE(36:2)	55.6	PC(34:1e)	37.42
PC(38:4)	54.99	PE(38:3)	34.36
PE(34:1)	53.79	PE(36:1)	31.11
PS(40:6)	49.2	PS(40:6)	29.99
PS(36:2)	45.92	PE(34:1)	26.19
PS(40:5)	45.35	PS(36:2)	25.64
PE(40:6e)/PE(40:5p)	39.13	PI(38:4)	25.56
PS(38:3)	38.65	PC(36:4)	25.07
PC(36:4)	38.48	PS(38:3)	24.97
PE(38:5)	35.01	PA(36:1)	22
PA(36:1)	34.48	PC(38:3)	20.04
PE(40:5e)/PE(40:4p)	34.37	PE(36:2)	19.75
PE(38:0)/PE(40:6p)	33.47	PS(40:4)	19.63
PE(38:5e)/PE(38:4p)	32.41	PA(32:0)	19.24
PC(38:3)	31.4	PA(34:1)	16.94
PC(34:2)	30.71	PS(32:1)	16.25
PI(38:4)	28.86	PE(40:4e)/PE(40:3p)	16.14
PC(36:3)	27.66	PE(38:5e)/PE(38:4p)	14.27
PA(32:0)	26	PC(34:2)	14.17
PE(40:4e)/PE(40:3p)	23.47	PC(36:3)	13.95
PA(34:1)	22.79	PC(30:1)	13.77
PS(36:4)	22.02	PS(42:1)	13.46
PC(38:2)	21.67	PC(38:2)	13.31
PS(32:1)	20.88	PE(38:5)	13.12
PC(34:1)	20.61	PE(40:5e)/PE(40:4p)	12.88
PC(38:1)	19.9	PE(40:6e)/PE(40:5p)	12.31
PC(30:1)	19.26	PS(36:4)	12.05
PS(34:0)	18.36	PC(38:1)	11.01
PE(38:2)	17.87	PA(40:6)	10.19
PE(38:1)	16.74	PI(38:5)	9.72

PC(36:2e)/PC(36:1p)	16.63	PS(34:0)	9.72
PS(40:4)	15.49	PS(40:1)	9.3
PA(40:6)	14.11	PA(34:0)	8.98
PA(34:0)	13.77	PI(34:2)	8.53
PC(38:5e)/PC(38:4p)	13.72	PC(36:2e)/PC(36:1p)	7.95
PC(38:0)	13.53	PE(38:0)/PE(40:6p)	7.89
PI(36:2)	12.94	PE(38:2)	7.82
PS(38:2)	11.89	PC(38:6e)/PC(38:5p)	7.64
PG(36:1)	11.86	PA(40:5)	7.37
PS(40:1)	11.8	PI(38:3)	7.15
PA(40:5)	11.36	PA(36:2)	7.08
PC(38:6e)/PC(38:5p)	10.9	PC(38:0)	7
PI(38:3)	10.74	PI(36:2)	6.96
PG(36:2)	10.69	PS(38:2)	6.75
PC(32:2)	10.24	PC(38:5e)/PC(38:4p)	6.31
PS(36:3)	10.22	PC(32:2)	6.25
PI(38:5)	10.13	PA(32:1)	5.68
PA(36:2)	9.97	PS(40:3)	5.67
PG(34:1)	9.37	PE(38:1)	5.12
PI(36:1)	8.84	PS(34:2)	4.96
PS(34:2)	8.64	PI(36:4)	4.73
PG(42:10)	8.15	PA(38:4)	4.7
PA(32:1)	7.83	PG(34:1)	4.61
PA(38:3)	7.43	PA(38:3)	4.51
PS(40:3)	7.26	PI(36:1)	4.45
PG(36:3)	7.09	PS(40:2)	4.12
PA(38:4)	6.92	PI(34:1)	4.08
PC(34:2e)/PC(34:1p)	6.57	PS(36:3)	4.07
PI(34:2)	6.36	PG(42:10)	4.01
PI(34:1)	5.6	PG(36:3)	3.49
PG(42:9)	5.26	PG(36:2)	3.04
PS(40:2)	4.98	PI(36:3)	2.92
PI(36:4)	4.16	PC(34:2e)/PC(34:1p)	2.89
PI(36:3)	3.66	PG(42:9)	2.15
PI(38:2)	2.02	PI(40:5)	1.31
PI(40:5)	1.85	PG(36:1)	1.13
PI(40:6)	1.44	PI(40:6)	1.1
PI(40:4)	0.83	PI(38:2)	0.83
PA(34:2)		PI(40:4)	0.62

Table 2. Ranking of GPL by abundance in 7.5 x 10^7 wild type nuclei and PITPα nuclei (SET 2) (pmol/million cells or pmol/million nuclei, mean and standard error; n=9).

wt NUC		ko NUC	
	pmol / mg protein		pmol / mg protein
PC(34:1)	89.7	PC(32:0)	102.6
PS(36:1)	88.9	PC(36:1)	96.8
PC(38:2)	86.7	PS(36:1)	96.1
PC(32:0)	86.3	PC(34:1)	81.6
PC(36:1)	80.9	PC(36:5e)/PC(36:4p)	80.1
PC(32:1)	75.3	PC(38:2)	70.3

PC(36:5e)/PC(36:4p)	61.2	PC(32:1)	63.5
PC(38:6)	58.5	PC(38:6)	54.4
PC(36:2)	51.4	PC(36:2)	39.2
PS(34:1)	33.5	PE(38:4)	30.4
PE(36:1)	23.8	PC(38:4)	26.2
PC(38:1)	22.4	PS(34:1)	25.2
PC(40:6)	21.8	PA(32:0)	23.1
PE(34:1)	20.9	PC(38:1)	21.1
PC(38:3)	20.7	PC(40:6)	20.5
PE(38:4)	19.4	PS(38:4)	18.8
PC(38:0)	16.7	PE(36:1)	17.8
PE(36:2)	15.7	PG(36:5)	17.7
PC(34:2)	14.2	PA(34:0)	17.0
PS(38:4)	14.1	PE(34:1)	16.2
PE(38:5e)/PE(38:4p)	13.1	PC(38:3)	15.0
PS(36:2)	11.9	PS(40:5)	14.3
PE(38:6e)/PE(38:5p)	11.6	PA(34:1)	13.7
PE(38:0)	11.5	PE(38:5e)/PE(38:4p)	13.5
PE(36:0)	11.4	PC(38:0)	12.6
PG(36:5)	11.0	PI(38:4)	12.6
PA(32:0)	10.4	PE(38:0)	12.5
PC(38:4)	10.0	PE(38:6e)/PE(38:5p)	11.9
PC(36:3)	9.8	PS(40:6)	11.6
PE(36:2e)/PE(36:1p)	9.2	PA(36:1)	11.4
PI(38:4)	8.8	PC(28:0)	11.2
PS(36:0)	8.4	PC(34:2)	11.2
PA(36:1)	8.3	PE(36:0)	10.8
PS(40:5)	8.2	PE(38:5)	10.5
PS(40:6)	7.9	PS(36:2)	10.2
PE(36:5e)/PE(36:4p)	7.7	PC(36:0)	9.9
PE(36:1e)/PE(36:0p)	7.5	PE(36:2)	9.6
PS(38:3)	7.4	PS(36:0)	9.1
PA(34:1)	7.3	PC(36:3)	9.1
PE(38:5)	7.3	PE(36:4)	8.3
PC(28:0)	6.8	PE(40:6)	8.2
PE(40:6)	6.5	PS(38:3)	7.2
PG(34:2)	6.2	PE(38:6)	6.9
PE(36:4)	6.0	PS(40:4)	6.7
PE(38:3e)/PE(38:2p)	5.9	PE(36:5e)/PE(36:4p)	5.4
PE(38:6)	5.7	PG(34:1)	5.4
PC(36:0)	5.6	PS(32:0)	5.3
PE(38:3)	5.6	PS(34:0)	5.3
PI(36:2)	5.5	PE(40:5)	5.0
PE(34:2)	5.2	PE(38:3e)/PE(38:2p)	4.4
PS(32:1)	5.1	PS(32:1)	4.4
PE(32:1)	4.9	PG(34:2)	4.3
PG(34:3)	4.7	PE(36:1e)/PE(36:0p)	3.9
PI(36:1)	4.6	PS(36:4)	3.8
PA(34:0)	4.5	PE(32:1)	3.7
PS(36:4)	4.4	PA(36:0)	3.5
PE(40:5)	4.2	PA(32:1)	3.5
PE(36:3)	4.0	PI(34:0)	3.5
PE(36:3e)/PE(36:2p)	3.8	PE(38:3)	3.4

PS(32:0)	3.7	PS(38:1)	3.2
PS(34:0)	3.7	PI(34:1)	3.1
PG(36:2)	3.5	PI(38:5)	3.0
PE(36:4e)/PE(36:3p)	3.4	PE(34:2)	3.0
PE(38:1)	3.4	PE(36:2e)/PE(36:1p)	3.0
PS(38:1)	3.2	PE(38:1)	3.0
PG(38:6)	2.9	PA(36:2)	3.0
PE(36:5)	2.9	PE(36:5)	2.9
PI(38:5)	2.7	PE(36:3)	2.9
PI(38:3)	2.7	PG(36:1)	2.7
PA(36:2)	2.6	PG(38:6)	2.7
PG(36:4)	2.6	PG(34:3)	2.6
PE(34:0)	2.5	PI(38:3)	2.6
PS(38:2)	2.5	PA(38:3)	2.4
PS(40:4)	2.4	PG(36:2)	2.3
PA(32:1)	2.4	PA(38:4)	2.3
PG(36:1)	2.3	PS(38:0)	2.3
PI(34:1)	2.2	PI(36:2)	2.2
PG(34:1)	2.2	PE(40:3)	2.2
PS(38:0)	2.1	PE(36:4e)/PE(36:3p)	2.0
PI(34:0)	2.1	PE(40:4)	1.8
PE(40:4)	2.0	PI(36:1)	1.8
PA(38:3)	1.9	PE(32:0)	1.4
PA(36:0)	1.7	PS(38:2)	1.3
PA(38:4)	1.6	PE(36:3e)/PE(36:2p)	1.3
PE(38:2)	1.5	PE(34:0)	1.3
PE(32:0)	1.3	PG(36:4)	1.1
PE(40:3)	1.3	PA(38:1)	1.0
PI(36:3)	1.1	PS(40:3)	0.9
PS(40:3)	1.0	PI(36:3)	0.8
PG(32:1)	0.7	PI(40:5)	0.7
PA(38:1)	0.6	PI(40:6)	0.6
PI(40:5)	0.6	PG(32:1)	0.6
PI(38:2)	0.6	PE(38:2)	0.4
PI(36:0)	0.5	PI(40:4)	0.4
PI(40:6)	0.5	PI(38:6)	0.4
PI(36:5)	0.3	PI(36:0)	0.3
PI(38:6)	0.3	PI(36:5)	0.3
PI(40:4)	0.3	PI(40:7)	0.2
PI(38:1)	0.2	PI(38:0)	0.1
PI(40:7)	0.2	PI(38:2)	0.1
PI(38:0)	0.1	PI(40:3)	0.1
PI(40:3)	0.1	PI(38:1)	0.0

Table 3. Ranking of GPL by abundance in 7.5 x 10^7 wild type nuclei and PITPα nuclei (SET 3) (pmol/million cells or pmol/million nuclei, mean and standard error; n=9).

wt NUC		ko NUC	
	pmol / mg protein		pmol / mg protein
PC(32:0)	68.5	PC(32:0)	75.1
PC(36:1)	54.8	PC(34:1)	60.9
PS(36:1)	54.7	PC(36:1)	59.4

PC(34:1)	51.9	PS(36:1)	58.9
PC(36:5e)/PC(36:4p)	50.4	PC(38:2)	56.9
PC(32:1)	43.6	PC(32:1)	49.3
PC(38:2)	40.5	PC(36:5e)/PC(36:4p)	47.3
PC(38:6)	35.4	PC(38:6)	42.0
PC(36:2)	24.2	PC(36:2)	35.5
PE(38:4)	19.8	PS(34:1)	23.2
PC(40:6)	18.4	PC(38:1)	19.5
PC(38:4)	18.0	PE(36:1)	19.3
PA(32:0)	17.5	PE(38:4)	17.7
PS(34:1)	16.8	PC(40:6)	17.2
PC(38:3)	14.0	PE(34:1)	15.1
PC(38:1)	13.9	PG(36:5)	11.1
PG(36:5)	13.6	PC(38:3)	11.1
PE(36:1)	13.3	PC(38:4)	9.9
PE(34:1)	12.7	PE(36:2)	9.8
PA(34:0)	10.1	PC(38:0)	9.6
PC(28:0)	9.6	PC(34:2)	9.3
PA(36:1)	9.1	PS(36:0)	8.0
PS(38:4)	8.7	PS(38:4)	7.9
PA(34:1)	8.6	PA(32:0)	7.7
PE(36:2)	7.6	PS(36:2)	7.4
PI(38:4)	7.4	PI(38:4)	6.3
PC(34:2)	7.3	PA(36:1)	6.3
PS(36:0)	7.2	PC(28:0)	6.0
PC(38:0)	7.1	PE(38:5e)/PE(38:4p)	5.8
PS(40:5)	6.8	PE(40:6)	5.4
PE(38:5e)/PE(38:4p)	6.6	PG(34:2)	5.4
PS(36:2)	6.3	PS(40:5)	5.3
PE(38:5)	6.1	PE(38:5)	5.2
PS(40:6)	6.0	PS(40:6)	5.1
PE(36:4)	5.8	PA(34:1)	5.1
PE(40:6)	5.2	PE(36:4)	5.0
PE(38:0)	5.1	PS(38:3)	4.7
PC(36:0)	4.9	PS(32:1)	4.3
PS(32:0)	4.5	PE(36:1e)/PE(36:0p)	4.3
PE(36:0)	4.4	PE(36:0)	4.1
PS(38:3)	4.2	PE(38:3e)/PE(38:2p)	4.1
PE(38:3e)/PE(38:2p)	4.1	PE(38:3)	3.9
PA(32:1)	3.9	PE(40:5)	3.8
PE(38:6e)/PE(38:5p)	3.8	PC(36:0)	3.8
PE(38:6)	3.5	PE(32:1)	3.7
PG(34:2)	3.5	PS(34:0)	3.6
PE(38:3)	3.2	PG(34:3)	3.6
PG(34:1)	3.2	PE(38:0)	3.5
PE(36:1e)/PE(36:0p)	3.2	PA(34:0)	3.5
PS(34:0)	3.2	PS(32:0)	3.4
PE(36:5e)/PE(36:4p)	3.1	PI(36:2)	3.4
PE(40:5)	3.1	PE(38:6)	3.3
PA(36:0)	2.8	PE(38:6e)/PE(38:5p)	3.3
PS(40:4)	2.7	PE(34:2)	3.2
PE(32:1)	2.7	PI(36:1)	3.2
PE(36:2e)/PE(36:1p)	2.7	PS(40:4)	3.1

PE(34:2)	2.6	PE(36:2e)/PE(36:1p)	3.1
PG(34:3)	2.4	PG(34:1)	3.0
PG(38:6)	2.3	PS(36:4)	2.8
PA(38:3)	2.0	PG(38:6)	2.8
PA(36:2)	1.8	PE(36:5e)/PE(36:4p)	2.4
PI(34:1)	1.8	PE(36:3)	2.4
PI(38:5)	1.7	PG(36:1)	2.0
PE(36:3)	1.7	PS(38:1)	2.0
PI(34:0)	1.6	PS(38:2)	1.8
PA(38:4)	1.6	PA(32:1)	1.8
PI(36:2)	1.5	PG(36:2)	1.7
PE(38:1)	1.3	PA(36:2)	1.7
PS(38:2)	1.3	PE(40:4)	1.7
PA(38:1)	1.3	PI(38:5)	1.7
PG(36:1)	1.2	PG(36:4)	1.6
PI(36:1)	1.2	PE(34:0)	1.5
PE(36:4e)/PE(36:3p)	1.1	PI(38:3)	1.5
PE(32:0)	1.0	PS(38:0)	1.5
PI(38:3)	0.9	PE(38:2)	1.3
PE(34:0)	0.9	PI(34:0)	1.3
PG(36:4)	0.8	PE(40:3)	1.3
PI(40:5)	0.6	PE(36:3e)/PE(36:2p)	1.2
PE(38:2)	0.4	PE(36:4e)/PE(36:3p)	1.2
PI(38:0)	0.2	PA(38:3)	1.1
PI(38:2)	0.2	PI(34:1)	1.1
PI(40:7)	0.1	PA(36:0)	1.1
PC(36:3)		PA(38:4)	1.0
PE(36:3e)/PE(36:2p)		PE(32:0)	1.0
PE(36:5)		PI(36:3)	0.8
PE(40:4)		PS(40:3)	0.6
PE(40:3)		PG(32:1)	0.5
PG(32:1)		PI(40:5)	0.4
PG(36:2)		PI(38:2)	0.4
PI(36:5)		PI(36:0)	0.3
PI(36:3)		PI(40:6)	0.3
PI(36:0)		PI(40:4)	0.3
PI(38:6)		PI(36:5)	0.2
PI(38:1)		PI(38:6)	0.2
PI(40:6)		PI(40:7)	0.1
PI(40:4)		PI(38:1)	0.1
PI(40:3)		PI(38:0)	0.1
PS(32:1)		PA(38:1)	
PS(36:4)		PC(36:3)	
PS(38:1)		PE(36:5)	
PS(38:0)		PE(38:1)	
PS(40:3)		PI(40:3)	

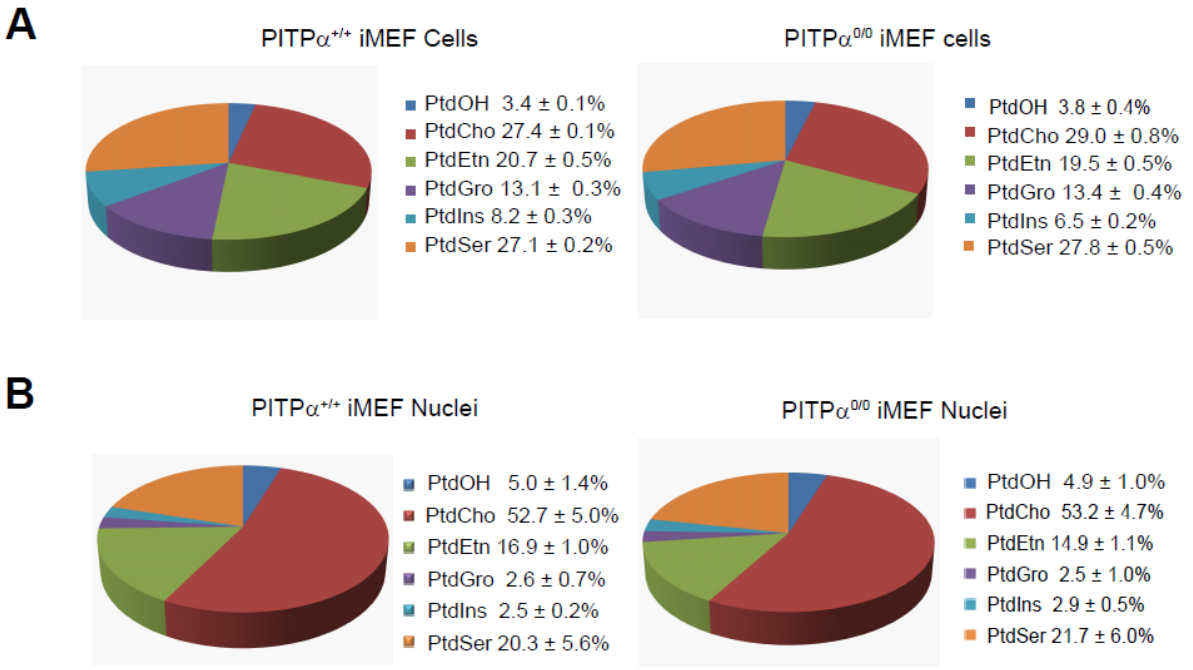

Figure 6. PL Composition of *Pitpα*$^{0/0}$ cells and nuclei in comparison to wild type. (A) Percent composition of the different phospholipid classes in *PITPα*$^{+/+}$ (left) and *Pitpα*$^{0/0}$ iMEF (right) whole cells. Percentages were averaged between 3 independent experiments for both genotypes. (B) Percent composition of the different phospholipid classes in *PITPα*$^{+/+}$ (left) and *Pitpα*$^{0/0}$ iMEF (right) envelope-stripped nuclei. Percentages were averaged between 3 independent experiments for both genotypes.

4.4.5 Incorporation of Newly Synthesized PtdIns and PtdCho into *PITPα*$^{+/+}$ and *Pitpα*$^{0/0}$ Nuclei

The low steady-state mass quantities of PL (particularly PtdIns) in the nuclear matrix indicate the plausibility of endonuclear supply by a shuttling carrier protein such as PITPα. Moreover, when coupled with the excess of endonuclear PtdCho to PtdIns mass in the nuclear matrix, the PtdIns/PtdCho balance is consistent with the base precepts of the PITPα-import model. An acid test of the model requires kinetic analysis of the process in the presence and absence of PITPα. To this end, standard pulse-chase strategies were modified to investigate endonuclear dynamics of PtdIns and PtdCho lipidomics in *PITPα*$^{+/+}$ or *Pitpα*$^{0/0}$ MEFs. Deuterated PL precursors (Cho-d_9 and Ins-d_6) were used to label newly synthesized iMEF PtdCho and PtdIns in a defined pulse and precursor scan ESI-MS was used as readout to analyze the data. The ESI-MS analyses were conducted on whole cell lipid extracts as bulk control, and on purified envelope-free nuclei as specific test case. Precursor scan of the Cho headgroup-derived m/z 184$^+$ and m/z 193$^+$ fragments over the mass range of 600-920 amu identified endogenous (i.e., pre-existing) and newly synthesized PtdCho and sphingomyelin (SM) species, respectively. Similarly, precursor scan of the Ins headgroup-derived m/z 241$^-$ and m/z 247$^-$ fragments over the mass range of 600-1000 amu identified pre-existing and newly synthesized PtdIns species, respectively. The light (pre-existing) species in each case represent a steady-state baseline for these measurements.

Fractional rates of incorporation of newly synthesized PtdIns in endonuclear compartments were delayed relative to that of newly synthesized PtdCho in both *PITPα*$^{+/+}$ and *Pitpα*$^{0/0}$ MEFs (Figure 7B vs. 7A). Very little newly synthesized PtdIns was recovered from *PITPα*$^{+/+}$ or *Pitpα*$^{0/0}$ endonuclear compartments during a 1hr pulse. Significant

fractional incorporation required a pulse of 2 hours. Thus, import of PtdIns is not rapid. We interpret these data to reflect the intrinsic PtdCho biosynthetic capacity of endonuclear compartments, while PtdIns must be imported rather slowly from extranuclear sources. We also note that rates of fractional incorporation of newly synthesized PtdIns into *Pitp*$\alpha^{0/0}$ MEF endonuclear compartments were not substantially reduced relative to those measured for stripped *PITP*$\alpha^{+/+}$ MEF nuclei (Figure 7B) although there is a delay in incorporation of PtdIns (2-4 hour time points). These data indicate PITPα is not an obligatory contributor to the pathway(s) that supply endonuclear compartments with PtdIns.

A

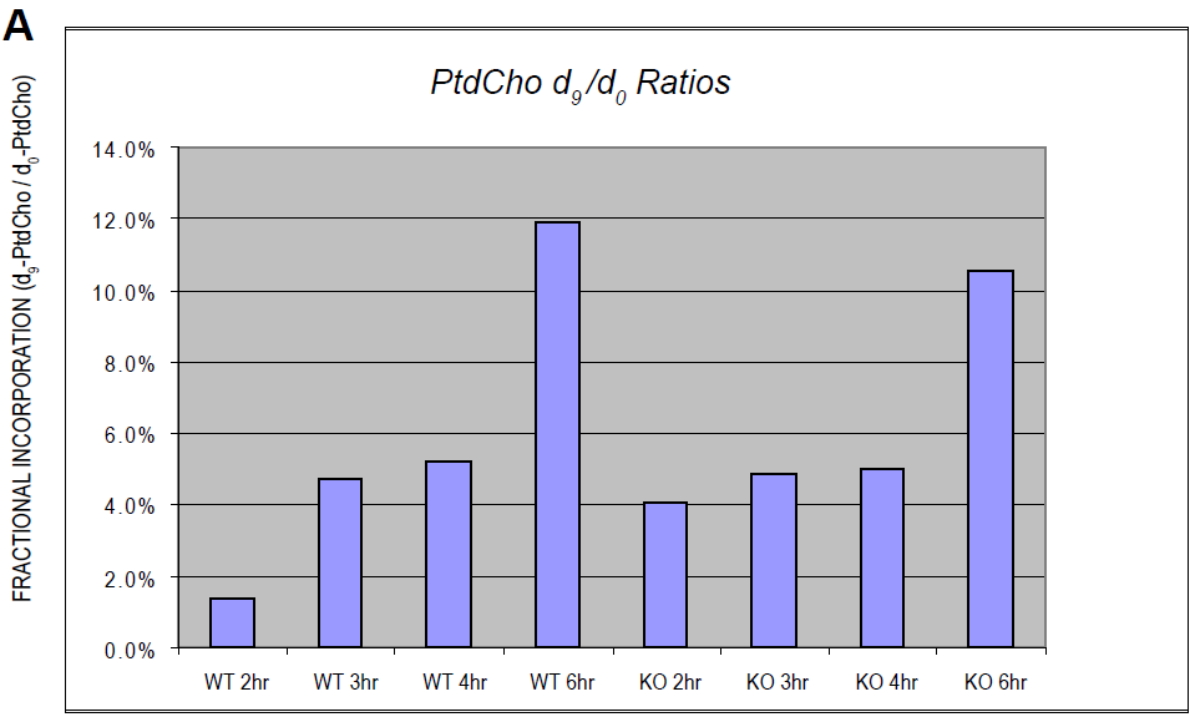
PtdCho d_9/d_0 Ratios
FRACTIONAL INCORPORATION (d_9-PtdCho / d_0-PtdCho)
14.0%
12.0%
10.0%
8.0%
6.0%
4.0%
2.0%
0.0%
WT 2hr
WT 3hr
WT 4hr
WT 6hr
KO 2hr
KO 3hr
KO 4hr
KO 6hr

B

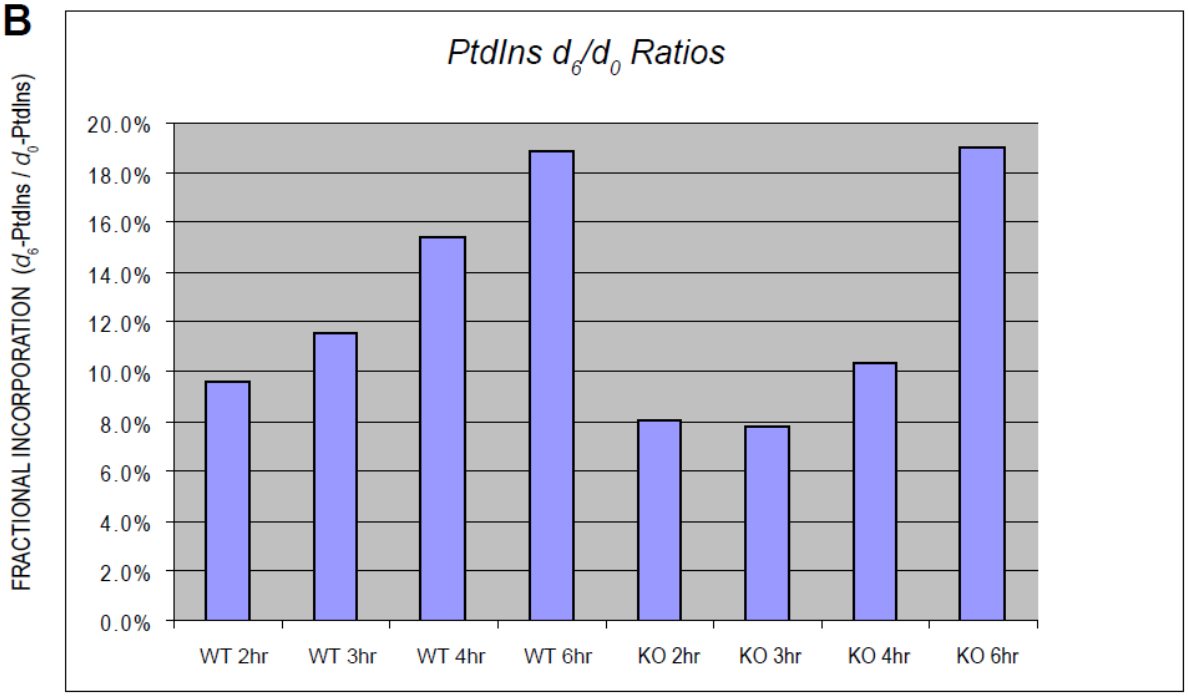
PtdIns d_6/d_0 Ratios
FRACTIONAL INCORPORATION (d_6-PtdIns / d_0-PtdIns)
20.0%
18.0%
16.0%
14.0%
12.0%
10.0%
8.0%
6.0%
4.0%
2.0%
0.0%
WT 2hr
WT 3hr
WT 4hr
WT 6hr
KO 2hr
KO 3hr
KO 4hr
KO 6hr

Figure 7: PtdIns and PtdCho flux into *PITPα*$^{+/+}$ and *Pitpα*$^{0/0}$ iMEF nuclei. (A) Incorporation of d_9-PtdCho species into the endonuclear compartment as a function of time. The d_9-choline headgroup (m/z = +193) from all PtdCho species was quantified in *PITP*$\alpha^{+/+}$ (left) and *Pitp*$\alpha^{0/0}$ iMEF (right) purified envelope-free nuclear fractions after 2, 3, 4, and 6 hours of labeling with 80µg/mL d_9-choline (n=1). Results are reported as a fraction of the unlabeled headgroup (m/z = +184). (B) Incorporation of d_6-PtdIns species into the endonuclear compartment as a function of time. The *myo*-d_6-inositol headgroup (*m/z* = -247) from all PtdIns species was quantified in *PITP*$\alpha^{+/+}$ (left) and *Pitp*$\alpha^{0/0}$ iMEF (right) purified envelope-free nuclear fractions after 2, 3, 4, and 6 hours of labeling with 50µg/mL *myo*-d_6-inositol. Results are reported of a fraction of the unlabeled PtdIns headgroup (Inositol; *m/z* = -241).

4.4.6 Phosphoinositide Status of *PITPα*$^{+/+}$ and *Pitpα*$^{0/0}$ Nuclei

An alternative function for PITPα in the nuclear matrix is stimulation of PIP (PtdIns-4-phosphate and PIP_2) synthesis by endonuclear PtdIns- and PtdIns-4-P kinases. Attempts to accurately quantify endonuclear PIPs were not successful. Using ESI-MS as readout, we found measurable amounts of PIP and PIP_2 in purified envelope-free nuclei, but these quantities were uncomfortably near the level of detection – even when 10^8 MEF cells were used as starting material in these analyses (our unpublished data). We conclude endonuclear PIPs are present at level so low as to preclude confident comparisons of the PIP loads of *PITPα*$^{+/+}$ vs. *Pitpα*$^{0/0}$ MEF nuclei. Two indirect lines of experimentation suggest PIP_2 is not significantly reduced in *Pitpα*$^{0/0}$ vs. *PITPα*$^{+/+}$ nuclear matrix. First, we readily detect the characteristic punctate endonuclear staining when fixed and permeabilized *PITPα*$^{+/+}$ and *Pitpα*$^{0/0}$ MEFs are stained with anti-PIP_2 antibodies (Figure 8A). No significant differences in presumptive PIP_2 speckle number or morphology were apparent in *PITPα*$^{+/+}$ vs. *Pitpα*$^{0/0}$ endonuclear compartments. In agreement with previous reports [24], these presumptive PIP_2 speckles colocalize with the commercial nuclear speckle marker (Figure 8A). We notice two PIP2 speckling patterns in stained nuclei: (1) uniformly distributed speckles (Figure 8A); (2) asymmetrically distributed speckles which cluster toward one side of the nucleus (Figure 8A). Both phenotypes are observed in stained *Pitpα*$^{0/0}$ and *PITPα*$^{+/+}$ nuclei. We do observe an increased frequency of the asymmetrical speckling pattern in *Pitpα*$^{0/0}$ nuclei in comparison to wild type, but the significance of this finding is unknown (Figure 8B).

As speckles also harbor the endonuclear PtdIns-4-P 5-OH kinase [24], and the product of this enzyme (PIP_2) is required for STAR-PAP-mediated poly-adenylation and maturation of specific mRNAs (e.g., Heme Oxidase-1) induced in response to oxidative

stress (100µM tBHQ; 20), we tested whether STAR-PAP activity was affected in *Pitpα*$^{0/0}$ MEFs. Quantitative RT-PCR analyses *Pitpα*$^{0/0}$ MEFs (immortalized or primary) in induced levels of the HO-1 mRNA in response to oxidant challenge (Figure 8C). We also indicate that oxidant challenge produces no visible change in the appearance or quantity of the PIP_2 foci.

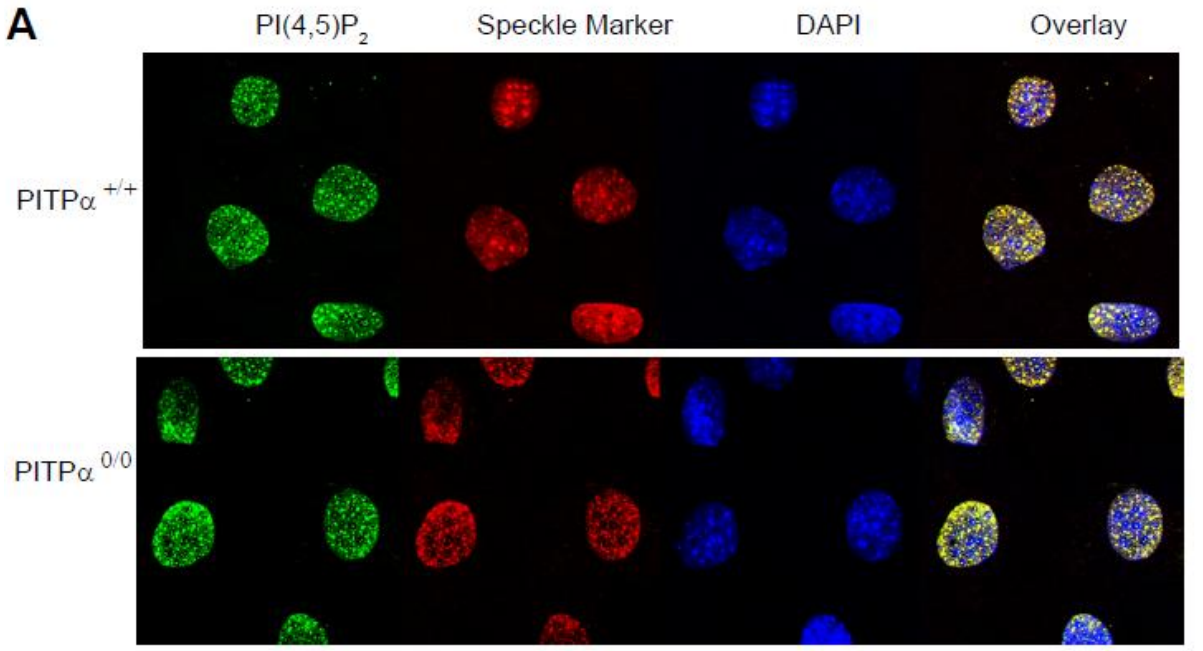
A
PI(4,5)P2
Speckle Marker
DAPI
Overlay
PITPα +/+
PITPα 0/0

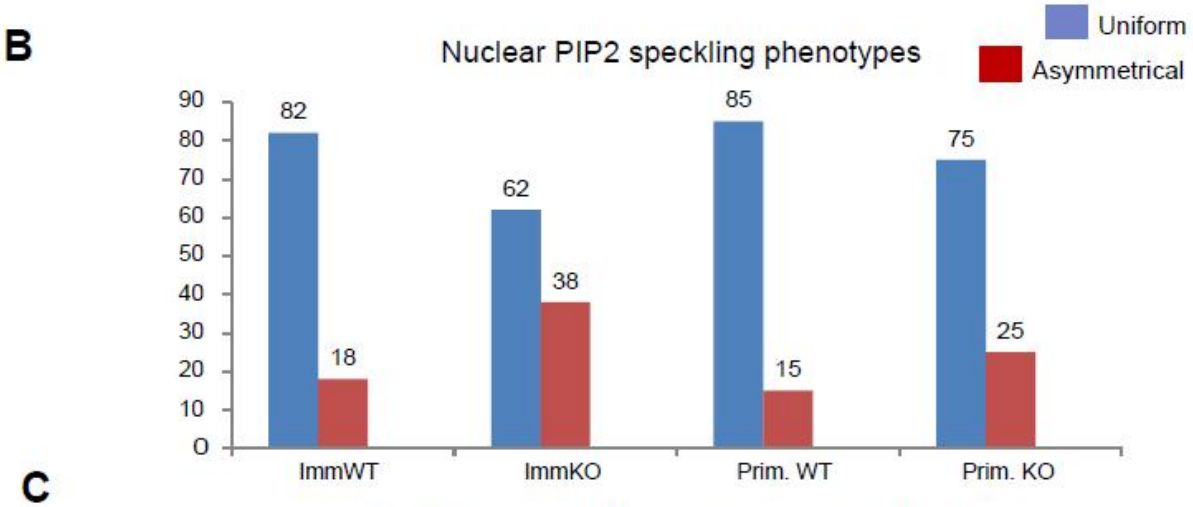
B
Nuclear PIP2 speckling phenotypes
Uniform
Asymmetrical
90
80
70
60
50
40
30
20
10
0
82
18
62
38
85
15
75
25
ImmWT
ImmKO
Prim. WT
Prim. KO

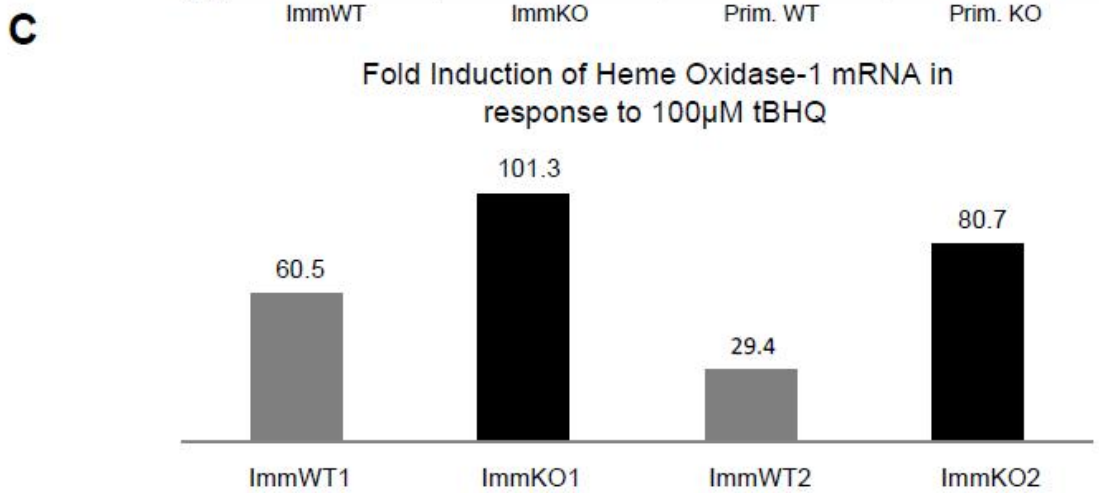
C
Fold Induction of Heme Oxidase-1 mRNA in response to 100μM tBHQ
60.5
101.3
29.4
80.7
ImmWT1
ImmKO1
ImmWT2
ImmKO2

Figure 8: Steady state levels of PI(4,5)P_2 are normal in *PITP*$\alpha^{0/0}$ nuclei in comparison to wild-type. (A) Immunofluorescence staining of PI(4.5)P_2 foci in fixed and permeabilized *PITP*$\alpha^{+/+}$ and *Pitp*$\alpha^{0/0}$ iMEF cell nuclei using an antibody specific to PI(4,5)P_2. Fluorescent foci colocalize with a commercially available speckle marker. The predominantly observed speckling pattern for PIP_2 foci is a uniform distribution throughout the nucleoplasm (the two uppermost nuclei in the panel exemplify this). Also observed, but less frequently, is an asymmetrical staining pattern to PIP_2 foci (exemplified by two leftmost nuclei in *Pitp*$\alpha^{0/0}$ panel). (B) Quantitation of uniform vs. asymmetrical nuclear speckling phenotypes in *PITP*$\alpha^{+/+}$ and *Pitp*$\alpha^{0/0}$ primary and immortalized MEF nuclei. 100 cells/genotype/cell lines were examined.

Finally, as mentioned above, Ins polyphosphates regulate gene transcription and mRNA export in eukaryotic cells. A defect in nuclear PIPs could conceivably result in diminished Ins-polyphosphates given PIP_2 is the obligate metabolic precursor of these molecules. To this end, we measured cellular levels of the major product of this pathway – Ins hexakisphosphate (IP_6; [93]). MEFs were cultured in Ins-free medium supplemented with [^{3}H]-Ins for 72 hours, disrupted in mild acid, and individual Ins-polyphosphate species were resolved and quantified. Steady-state IP_6 levels are not depleted in *Pitpα*$^{0/0}$ iMEFs relative to wild type (Figures 9A and 9B), nor are they depleted in a transgenic iMEF line expressing the Pitpα^{T59D} PtdIns-binding mutant (Figure 9C). We note that the wild-type IP_6:IP_5 ratio is reduced from 3:1 to 2:1 both in the *Pitpα*$^{0/0}$ and in the *Pitpα*^{T59D} knock-in iMEF cells (Figure 9C). This finding is of unknown significance. Taken together, these data contraindicate an obligate role for PITPα in stimulating synthesis of endonuclear PIP or Ins polyphosphate pools in MEFs.

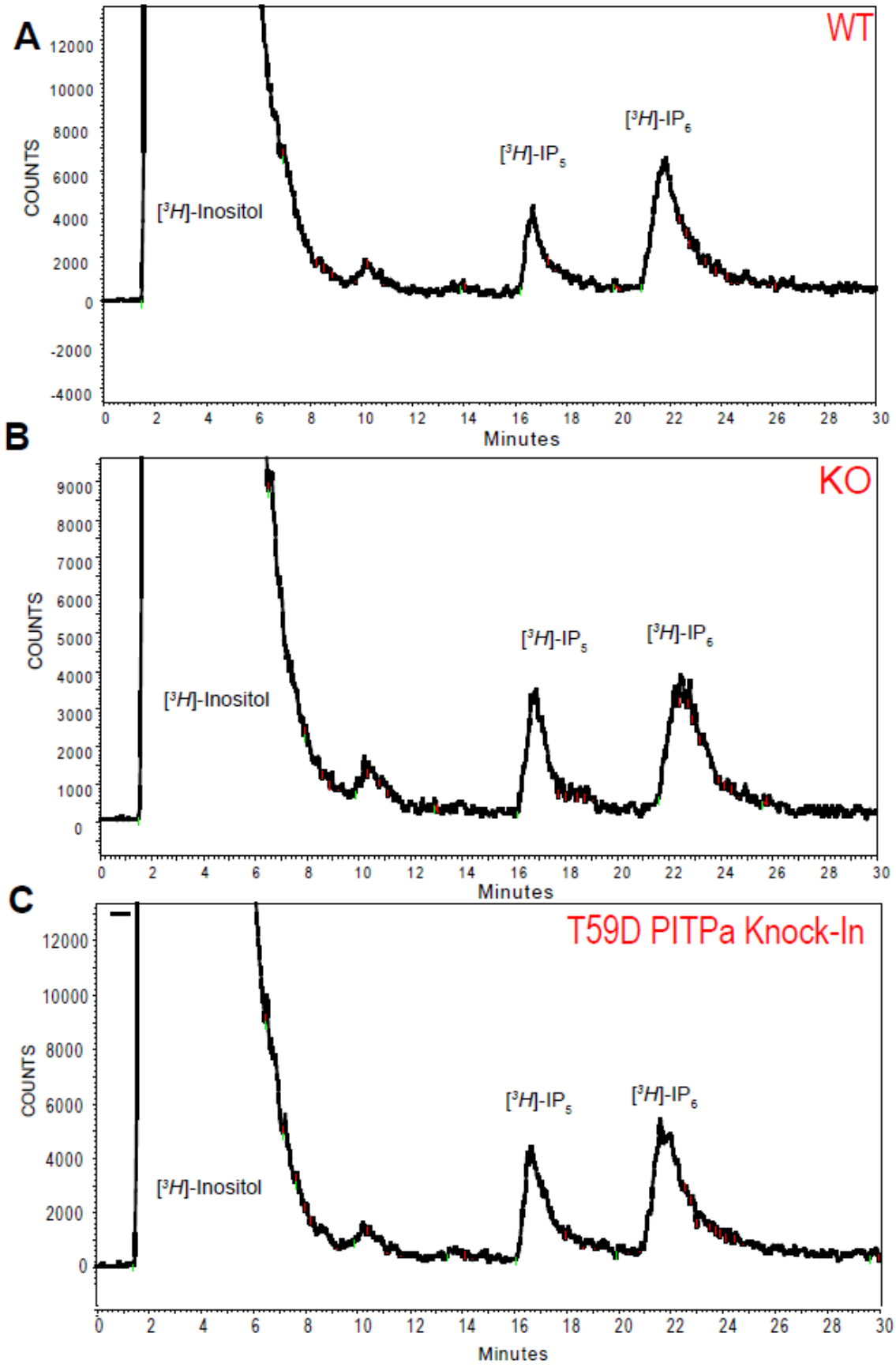
A
WT
COUNTS
[3H]-Inositol
[3H]-IP5
[3H]-IP6
Minutes
B
KO
COUNTS
[3H]-Inositol
[3H]-IP5
[3H]-IP6
Minutes
C
T59D PITPa Knock-In
COUNTS
[3H]-Inositol
[3H]-IP5
[3H]-IP6
Minutes

Figure 9. Inositol Phosphate levels in *PITPα*$^{+/+}$ and *Pitpα*$^{0/0}$ iMEF cells. Strong anion exchange HPLC chromatograph of tritiated inositol phosphate pools acid-extracted from *PITPα*$^{+/+}$ (A) and *Pitpα*$^{0/0}$ (B) iMEF cells after 72 hours of labeling with 100μM [^{3}H]-inositol. IP_5 and IP_6 peaks are labeled.

4.5 Discussion

The PITPα-import conjecture for nuclear PtdIns supply makes several important and testable predictions. These include: (i) PITPα must shuttle between the cytoplasmic compartment and the nuclear matrix, (ii) nuclear import competence of PITPα is influenced by its ligand-bound state – i.e., whether it is bound to PtdIns or PtdCho, (iii) either the steady-state levels of PtdIns or PIPs in the nuclear matrix, or the rate of PtdIns import into the nucleus, will be reduced upon functional ablation of PITPα. In this study, we subject these predictions to the experimental test.

Our results are summarized as follows. First, consistent with the prediction of the PITPα-import conjecture, we find PITPα is mobile in the cytoplasmic and endonuclear compartments. Second, some (but not all) PITPα variants with specific defects in PtdIns-binding exhibit deficiencies in nuclear localization. These results are provisionally consistent with the PITPα-import conjecture. However, two additional lines of experimental evidence yielded results in direct contradiction to that hypothesis. Lipidomic profiling experiments report no significant qualitative or quantitative differences between PL content or composition in endonuclear compartments derived from *PITPα*$^{+/+}$ and *Pitpα*$^{0/0}$i MEFs. Moreover, mass-shift pulse-labeling experiments indicate rates of PtdIns import into the MEF nuclear matrix are not affected by functional ablation of PITPα. These collective lipidomic data argue PITPα is not a primary contributor to the PtdIns endonuclear supply pathway(s) – at least not under the conditions employed. Finally, a direct outcome of the quantitative lipidomics experiments is a measurement of iMEF endonuclear PL load. The data indicate that *PITPα*$^{0/0}$ iMEFs, like their wild-type counterparts, harbor several orders of magnitude less endonuclear PL mass than reported for other cell types [17]. These findings

hold significant implications for ongoing discussions regarding the dynamic lipidomics of the mammalian nuclear matrix and the physical requirements of housing PL molecules in this bilayer-free endonuclear compartment.

4.5.1 Mechanisms of Nuclear PtdIns Import

The work within this chapter has tested whether PITPα imports PtdIns to the nuclear matrix. Although our data would suggest that PITPα is not acting in this context, PITPα is only one of many PtdIns/PtdCho lipid-transport proteins found in mammalian cells. PITPα has been considered the prime candidate for a nuclear PtdIns importer because of its specific localization, but in its absence another lipid transport protein may serve in its place.
Our measurements of endonuclear PtdIns mass are most consistent with a protein assisted PtdIns-import mechanism. By our calculations, (Chapter 3) fewer than 1,000,000 PtdIns molecules are present in the iMEF nucleus, and this number corresponds to approx. 1.5% of endonuclear lipid mass. These low numbers are consistent with the absence of obvious bilayer structures in the nuclear compartment and make lipid-transport proteins ideally suited to deliver PtdIns to discrete endonuclear sites. Although this seems the obvious choice for an import mechanism, non-protein mediated import mechanisms of import are also feasible. The massive reorganization of membrane structures around the Mitotic phase of the cell cycle could be responsible for internalization of small bilayer remnants. Alternatively, inner nuclear envelope invaginations could deposit PtdIns, or its metabolites within the nuclear interior [30, 31]. However, the most rapid and likely responsive mechanism of PtdIns delivery is via a shuttle protein.

PtdIns within the endonuclear compartment is consumed, not regenerated, and thus deficiencies in PtdIns can be monitored by monitoring the production of or steady-state

levels of its metabolites. PIP and IP flux measurements are necessary to conclusively exclude PITPα as a non-essential component in the generation of endonuclear PtdIns metabolites.

4.5.2 Nuclear Activities for PITPα

We are gaining new insights into the nuclear functions of PITPα. That PtdIns-binding mutations decrease the nucleoplasmic localization of the protein would suggest that the protein requires this activity to cross the nuclear envelope. However, not all PtdIns-binding mutations we tested behave similarly in cells. This is likely due to the residue selection in mutagenesis and the impact the endpoint residue has upon the lipid binding cavity. For instance, our selection of Ala in mutation of Lys61 creates more space in the lipid binding cavity, while mutation of Thr 59 to Asp decreases space in the lipid binding cavity. It will be interesting to see if less conservative amino acid substitutions produce more dramatic results.

The photobleaching data indicate that the PITPα-EGFP construct is highly mobile in both the nuclear and cytoplasmic compartments. Other nuclear dynamics studies suggest that biologically active proteins are most frequently bound within the nucleoplasm: does the EGFP tag interfere with function? The available test for function is the ability to rescue a lethal loss of function in the cell-essential yeast PITP, Sec14. In these complementation assays, the PITPα-EGFP construct rescues growth of a temperature sensitive Sec14 strain at the restrictive temperature (our unpublished data). What avenues we have for investigations have huge technical limitations, and improvements in methods for detection of Phosphoinositides, Inositol phosphates, and their flux, must be improved to permit further study.

CHAPTER 5

SUMMARY AND DISCUSSION

5.1 Summary

The work we have presented here is motivated by a desire to clarify important details about endonuclear phospholipids. Initially, we hypothesized that with the appropriate quality control measures and careful analysis of nuclei during envelope-free nuclear purification would improve the accuracy of and *lower* measurements of endonuclear lipid mass. We have devised a facile new method for purification of envelope-free nuclei from MEF cells, which meets accepted and an expanded set of quality control criteria. When this protocol and the quality control steps are properly implemented, we obtain a different picture of GPL mass in the nuclear matrix. We find that the amount of lipid in the nucleus is lower by several orders of magnitude than measurements performed in the IMR-32 nuclei. Overall, Chapter 2, Chapter 3, and Chapter 4 offer proof of our thesis. We show that we were able:

1. To generate a nuclear preparation method for embryonic fibroblasts that is well documented in description and is more quantitative in practice (Chapter 2).
2. To apply this method to the biological problem of endonuclear GPL mass (Chapter 3).
3. To disprove the hypothesis that PITPα supplies the nucleus with PtdIns for endonuclear PIP signaling (Chapter 4).

These informative results raise new questions about nuclear metabolism and organization. In this chapter, we outline our results thus far and discuss future approaches.

5.2 A Step by Step Analysis of Nuclei During Purification and Envelope Removal

Our protocol for creation of envelope-stripped nuclei from MEF cells details step-by-step removal of cellular debris and the nuclear envelope. Visual analysis of the nuclei produced via this method ensures the loss of visible debris. This is confirmed by TEM analyses which confirm that greater than 95% of the purified nuclei contain no traces of bilayer. Odyssey Western blotting indicates a 100 to 250 fold purification of nuclear components over cytosolic membrane components. Even those nuclei with contaminant patches have relatively little attached lipid in contrast to the surface area of the nuclear particle. The purified material is compatible with LC/MS/MS analyses of the lipid content and is highly repeatable.

The protocol in current use (Chapter 2) went through several rounds of development. Although we do not detail the majority of failed experiments in this document, there were several lessons learned from these failures regarding the important elements of nuclear preparations. What became clear is that the fibroblast nuclei require the application of substantial force to be separated from nuclear components. This cannot be compensated for with additional detergents or increases in extraction time. Methods that only wash nuclei in detergent and do not require mechanical shearing steps will not effectively remove the nuclear envelope. Some justify the lack of forceful manipulations with the use of differential centrifugation of nuclei through a sucrose cushion. In our experience, this does not prevent co-sedimentation of incompletely

removed lipid debris. Thus, an effective shearing step is an essential component of the envelope-removal process.

The most challenging aspect of nuclear preparations is the assessment of the membrane-free status of purified nuclei. Amidst the time constraints of preparation, sampling an adequate number of nuclei to represent the entire population is challenging. Our assessment of purity is reliant upon a quick examination of a fraction of a very large number of purified nuclei, of various shapes and states of intactness. In addition, phase contrast microscopy is very helpful in normalizing preparations, but will only obviate large morphological changes in the nuclear particle. Smaller contaminants could be missed. Even the more probative assays for membranes (EM) may fail to obviate non-bilayer structures which may or may not be detergent artifact. Given all of these possibilities, can we conclude that nuclear preparations contain mostly endonuclear lipid? There are several experimental lines of evidence that we can: (1) The nuclei purified according to these standards have very low quantities of lipid associated with them. If there are contaminants associated with the purified nuclei, there aren't many of them. (2) This low quantity of lipid is reproducibly observed in purified nuclear fractions. (3) The saturated and monounsaturated GPL molecular species detected in nuclear fractions are not overrepresented in comparison to polyunsaturated GPLs. This is commonly associated with detergent artifacts.

With the removal of the nuclear envelope and use of detergents, certain losses in nuclear material are expected. In fact, the more completely the envelope is removed, the greater the loss in nuclear yield. In terms of yield, we regularly retrieve about 25% of cellular DNA in nuclear preparations and between 10-15% of total cellular RNA (our unpublished data). We have conducted a few preliminary experiments using RNase inhibitors, and they show a slight increase the yield of RNA in the final pellet to ~20%. This does not have a visible effect on nuclei during

the purification or in the size of the final pellet, but more careful analyses of DNA and protein yields are needed before making a definitive statement on the effect of RNase inhibitors in nuclear preparations. However, measurements of nucleic acids are not measures of nuclear intactness on all levels. The best we can do is compare DNA, RNA and protein analyses to generate a complete picture of how intact the purified nuclei are. An interesting test of nuclear intactness after the purification procedure would be to analyze purified nuclei by scanning electron microscopy. We do know, however, that our nuclear preparations frequently retain a large portion of the Histone pool, that what we obtain in DNA yield is matched by RNA yield, and that the purified particles maintain their integrity in the absence of envelope. This indicates that what is in our final pellet is largely intact, and that we are not collecting partially damaged nuclei for analysis.

There comes a point when the disadvantage caused by loss of the endonuclear material exceeds the benefit of membrane removal. With additional applied force during the shearing step, we can decrease the frequency with which contaminants appear to within 1-2% on a consistent basis. However, this results in less than 100µg of nuclear protein in the purified pellet of a 1x preparation (in comparison to the normal average of ~300µg nuclear protein). Also, the nuclei are deformed and often destroyed by the additional physical stress of shearing, and the purified nuclei aggregate to the point that they behave as a single particle. This is one aspect that we want to improve in the future, and we recognize that this may require significant changes to the protocol.

Published protocols for envelope-free nuclear preparations are available, but have neglected to offer the details needed to troubleshoot these protocols. While the base components of our protocol are similar to another that was recently published for fibroblast cell lines, the

protocols lack the kinds of detail that make protocols for generation of envelope-free nuclei reproducible and beginner friendly [13]. This is important, and thus the focus of our envelope-free nuclear preparation method is the detail that we show in step by step preparation and in quality controls. Also, in the above mentioned protocol that bears similarity to ours, the authors claim to remove only the outer envelop.

5.3 The Nuclear Matrix of iMEF Cells is a GPL Poor Environment

Our LC/MS/MS analysis of global phospholipid species in purified envelope free iMEF nuclei indicates that the nuclear matrix is only sparsely populated with GPLs. This is highly contrary to previous findings published for IMR-32 neuroblastoma nuclei, and is more consistent with findings generated from Hepatocyte nuclei [27, 28]. We find that there are ~5.5 x 10^7 phospholipids per nucleus, and in accordance with other published materials, the majority of these species are PtdCho species. Over half of the GPL analyzed were PtdCho species, with major contributions from the PtdSer and PtdEtn species, and only minimal contributions from a few PtdIns, PtdGro, and PtdOH species. There did not appear to be an enrichment of saturated or monounsaturated acyl chain constituents in the PtdCho species or in any of the GPLs analyzed, also in contrast to reports regarding IMR-32 neuroblastoma nuclei.

Based on published values of HeLa cell nuclear volume and estimates of phospholipid volumes from measurements of egg PtdCho bilayers, we estimate that the GPL within the nucleus of iMEFs occupies 0.02% of endonuclear lipid volume. When we factor in the yield of nuclear material (based on fibrillarin recovery, which is at the least 20%), this leaves us with a volume estimate that is maximally~0.1% of the nuclear space. We acknowledge that we need to repeat the volumetric measurements in the iMEF nuclei, but we also know that HeLa nuclei are

smaller than iMEF nuclei, and thus the value that we use to estimate nuclear volume is likely lower than in actuality.

It is interesting that many of the phospholipids that would be involved in the same metabolic pathways do not have similar acyl chain profiles. For instance, we observe equal quantities of saturated / monounsaturated PtdCho species and polyunsaturated species. We also see PtdIns species which are polyunsaturated (4 double bonds). The only PtdOH species (metabolites of both PtdCho and PtdIns species) have two double bonds, and therefore look like neither of the lipid species from which they would be derived. It is possible that these acyl chains could rapidly be remodeled within the nuclear space. It is also concerning that PtdCho is so abundant within the nucleus and PtdOH is such a small percentage of the nuclear space. The most interesting lipids to examine next would be the Diacylglycerol phospholipid species as they are metabolites of PtdIns, PtdCho, and PtdOH.

The constant concerns when measuring a substance in purified cellular material is overestimation/underestimation of the measured substance. As discussed in the previous section, the use of detergents in nuclear preparations is unavoidable. On the analysis front, the method of MS analysis also influences what is detected in nuclear preparations. Our analyses use HPLC prior to ESI of the lipid extract. This is a slightly less sensitive method than a direct injection analysis, but again, the use of detergents prohibits direct injection for mechanical reasons. However, this can be advantageous in that GPLs which do go undetected do not significantly contribute to the endonuclear GPL pool. Thus, noise is eliminated from these experiments.

5.4 PITPα does not participate in the endonuclear import of PtdIns

Several lines of evidence indicated that the mammalian PtdIns/PtdCho transfer protein, PITPα, was an ideal candidate to function in the supply of PtdIns to the nuclear matrix. PITPα is a nucleocytoplasmic protein whose nuclear localization is dependant upon PtdIns binding as seen in our transient expression studies. The wild-type is protein is highly mobile in the cytoplasm and even more so in the nuclear compartment. This is a necessary feature of a shuttle protein that rapidly moves individual PtdIns molecules from the cytosol to the nucleus. Lastly, the PITPα protein has transfer activity towards PtdIns that would allow extraction of single PtdIns monomers from a bilayer and move them to a new location.

If responsible for import of PtdIns into the nuclear matrix, one would expect that the rate of endonuclear PtdIns import is compromised in cells lacking PITPα. Our dynamic lipidomics strategy utilizing deuterated lipid precursors for pulse labeling enabled us to test this hypothesis. Neither steady state PtdIns levels nor the incorporation of PtdIns was negatively affected by the loss of PITPα. In addition, endonuclear PIP and IP metabolites of PtdIns were not decreased in the absence of PITPα. Thus, the collective data indicate that PITPα is not necessary for either PtdIns import or PIP synthesis to occur in the endonuclear compartment.

What would be the role of PITPα in the nuclear compartment? Does the protein even have a nuclear role? The current available reagents for localization studies of PITPα require fluorescent tagging of the protein. What effect this has on localization is unknown. It is possible that the fluorescent tag interferes with localization, or that overexpression of the protein causes accumulation of PITPα in atypical sites. It is unlikely this is the case because (1) nuclear phenotypes (PIP2 speckling patterns) would indicate that there is a role for PITPα in the nuclear compartment and (2) in Fluorescence loss in photobleaching experiments, continuous

photobleaching of the cytoplasm depletes nuclear PITPα-EGPF pools, indicating that there is continuity between the cytoplasmic and nuclear pools of PITPα-EGFP.

Many possible mechanisms could account for the origins of endonuclear PtdIns. Nuclear envelope invaginations, documented to have PIP_2 at the tips of the projection, could account for the origins of endonuclear PtdIns. However, this is likely to be a temporally insensitive and unresponsive mechanism for endonuclear PtdIns supply. Alternately, endonuclear GPLs including PtdIns could be deposited on decondensing chromatin after Mitosis. If endonuclear GPLs have an intended endonuclear function, as indicated by the sheer number of GPL metabolic enzymes in the nuclear compartment, then the random deposition of GPL within the chromatin seems inefficient and disorganized. However, if endonuclear GPLs are an unnecessary consequence of mitosis, and an undesired element of the nuclear matrix, then possibly export of PtdIns or even flux through the PIP signaling pathway would be a more informative area to investigate. One last possibility arises from another, poorly characterized, PITPα-domain containing protein functioning as a PtdIns importer. A myriad of PtdIns/PtdCho transfer proteins are found within metazoan cells that are still unstudied. This is the easiest hypothesis to test and should be explored in the future.

5.5 Conclusion and Future Directions

This document has been aimed at determining the best conditions for nuclear preparation that i) efficiently produce the most-membrane stripped iMEF nuclear particles with the best yield, ii) meet current and more quantitative quality control analyses, and iii) produce material compatible with mass spectrometry applications for phospholipid mass analysis. Having examined several methods for purifying envelope-stripped nuclei, we are of the opinion that the

method by which nuclei are purified is the most crucial element of accurate endonuclear phospholipid measurements. In addition, the best way to guarantee purification effectiveness and accuracy is from the use of properly employed quantitative controls. Also, as a small fraction of cellular membrane is not removed from purified nuclei, quantitative methods detailing the degree of purity are necessary to gauge the accuracy of endonuclear phospholipid measurements.

Currently, the standard quality control regime employed in envelope-free nuclear preparation is useful in several ways: 1) Western blot analyses probe the bulk purified material for markers of membrane contaminants, 2) TEM directly reports the presence or absence of contaminating membrane remnants in purified envelope-free nuclear preparations, and 3) EM and Western Blot analyses are basic laboratory techniques available to and practiced by the vast majority of scientists. While these approaches have their distinct benefits, they are not ideal for use in quality control assays for three reasons. First, the classical quality controls had not been updated to include more quantitative measures of contaminants. We have begun to address these measures with the work described within. Second, processing of the purified material for Western Blot and TEM is time-consuming. This is more of an issue for the TEM analyses, but of the two, it is the one that directly examines lipid structures in the purified material. Third, neither assay is sensitive to atypical lipid structures that may be present in nuclear fractions either because they are bona fide endonuclear lipid structures or because they are introduced / unmoved by the detergent extraction process.

Imaging of purified particles can be both rapidly accomplished and, with the use of the correct probes, informative as to the shape and location of lipid structures [52, 53]. The purified particles are stable for a few additional rounds of washing and can be imaged by dropping them

onto a slide; however, heat from imaging will eventually lead to the disintegration of the purified particles. In addition, unfixed purified nuclei will not withstand the several rounds of buffer exchange required for immunofluorescence. In Chapter 2, we demonstrate that the nuclei are able to be fixed and imaged quite readily. Many lipid dyes and fluorescently conjugated lipids are commercially available and can either be used to label lipids prior to the extraction procedure, during extraction, or quickly afterwards. Nuclei purified from Hela cells stably expressing a Histone H2b-GFP construct can be counterstained with both Hoescht and Nile Red to image phospholipids. We show the benefits of developing an imaging approach in Figure 8 of chapter 2.

The most overwhelming criticism of envelope-free nuclear preparations is that they invariably call for the heavy use of detergents in removing the envelope. A given detergent has higher affinities for some lipids than others, resulting in generation of an artifactual detergent-resistant lipid pool. The degree to which detergents would influence the lipid pool in the nucleus is not known. Currently, there are no alternatives for detergent use in nuclear preparations; however, there are those who have developed protocols for isolating enveloped nuclei in ways that do not involve detergents [94]. These methods involve isolation of nuclei by dounce homogenizing cells in buffers with high concentrations of inert macromolecules. These methods have been demonstrated to preserve the dynamics of nuclear components even in the absence of the rest of the cell. The inert macromolecule does not need to penetrate the nucleus to produce intact particles. For instance, 8kDa polyethylene glycol (PEG) is unable to penetrate the nuclear envelope but can be used to isolate enveloped nuclei. It can also be used to restore normal morphology in nuclei that have begun to disintegrate in experimentally-generated, hypotonic conditions [95].

While we are of the opinion that the major focus of any upcoming work should be on detergent-free methodologies for generating envelope stripped nuclei and discovering the physiological form assumed by endonuclear lipids, there are other analyses of endonuclear phospholipids that can be performed with the protocol. Firstly, our mass analyses are for the major phospholipid classes in their unmodified forms. We are interested in doing mass measurements of endonuclear PIPs. Although these molecules are far less abundant than unmodified PtdIns in the cytosolic portion of the cell, we know nothing of how the balance of PtdIns and its derivatives are regulated in the nucleus. It could very well be that we see so little PtdIns in steady state measurements because it is immediately captured by PtdIns kinases. We intend to measure PIPs in envelope stripped nuclei generated using our protocol. Measuring PIPs by mass spectrometry is very challenging because of the amount of material needed to see them and the behavior of the molecules (PIPs are very sticky). Instead, we opt to use *in vitro* purified PI and PIP kinases in a radiolabeling assay to measure endonuclear PIP mass [14].

It would also be useful to extend our experiments to primary cells. The protocol we describe works for both primary and immortalized MEF cells, but we have not repeated the endonuclear lipid measurements in the primary cells. The reason is that the use of immortalized cells in endonuclear phospholipid measurements enables us to generate large populations of cells quickly. Primary cells, on the other hand, grow slower in general and have a finite lifespan. Our current efforts are being applied to comparing the whole cell phospholipid profiles of primary and immortalized MEFs. Should these profiles be similar (we expect that they will be), a future experiment detailing the endonuclear phospholipid profiles of the primary cells would be an interesting comparison to the immortalized cell profile.

The results of Chapter 4 indicate that PITPα is highly unlikely to be the importer of PtdIns into the nuclear matrix. Currently, our analysis of PIPs has been limited to PIP_2. It is possible that direct mass measurements of multiple endonuclear PIPs will elucidate a deficiency in PtdIns metabolites. This can easily be accomplished by purifying $PITP\alpha^{+/+}$ and $Pitp\alpha^{0/0}$ nuclei, extracting GPLs, and performing mass analyses that utilize purified PIP kinases and radiolabeled phosphate to measure PIP mass alongside purified standards. Alternately, recent improvements in mass spectrometric methods for PIP detection and measurement will hopefully enable flux measurements through phosphoinositide pathways.

There is much to learn still of endonuclear phospholipids and their regulation. We know that the purification guidelines we have detailed here will be useful in generating quality iMEF nuclei for further research into endonuclear lipid metabolic pathways. We hope to develop additional assays in the future for quality control analysis that will better aid in assessing nuclear purity.

REFERENCES

1. Rose H.G., Frenster J.H. (1965) *Biochim. Biophys. Acta* **106**:577.

2. Chayen J., Gahan P.B., Lacour L.R. (1959) *Quart. J. Microscop. Sci.* **100:**270.

3. Rees K.R., Rowland G.F., Varcoe J.S. (1963) *Biochem. J.* **86:**130.

4. Manzoli F.A., Cocco L., Facchini A., Casali A.M., Maraldi N.M., Grossi C.E. (1976) *Mol. Cell. Biochem.* **12(2)**:67-71.

5. Frenster J.H. *The Handbook of Molecular Cytology* (1969) (A. LIMA-DE-FARIA, ed.) Elseveir Publ, Amsterdam:251-276.

6. Johnson E.M., Karn J., Allfrey V.G. (1974) *J. Biol. Chem.* **249**:4990-4999.

7. Hachmann H.J., Lezius A.G. (1975) *European J. Biochem.* **50**:357-366.

8. Manzoli F.A., Capitani S., Maraldi N.M., Cocco L., Barnabei O. (1978) *Adv. Enzyme Regul.* **17**:175-197.

9. Manzoli F.A., Muchmore G.H., Bonora B., Capitani S., Bartoli S. (1974) *Biochim. Biophys. Acta* **340(1)**:1-15.

10. Manzoli F.A., Maraldi N.M., Cocco L., Capitani S., Facchini A. (1977) *Cancer Res.* **37(3)**:843-849.

11. Neumann F.R., Nurse P. (2007) *J. Cell Biol.* **179(4)**:593-600.

12. Yang L., Guan T., Gerace L. (1997) *J. Cell Biol.* **139(5)**:1077-1087.

13. Fiume R., Teti G., Faenza I., Cocco L. (2010) *Methods Mol. Biol.* **645**:143-164.

14. Jones D.R., Bultsma Y., Keune W.J., Divecha N. (2009) *Methods Mol. Biol.* **462**:75-88.

15. Cascianelli G., Villani M., Tosti M. Marini F. Bartoccini E., Magni M.V., Albi E. (2008) *Mol. Biol. Cell.* **19(12)**:5289-5295.

16. Jones D.R., Divecha N. (2004) *Curr. Opin. Genet. Dev.* **14(2)**:196-202.

17. Hunt A.N., Clarke G.T., Attard G.S., Postle A.D. (2001) *J. Biol Chem.* **276(11):**8492-8499.

18. Hunt A.N. (2006) *Biochim. Biophys. Acta*.**1761:**577-587.

19. Irvine R.F. (2006) *Biochim. Biophys. Acta*. **1761(5-6):**505-508.

20. Mellman D.L., Gonzales M.L., Song C., Barlow C.A., Wang P., Kendziorski C., Anderson R.A. (2008) *Nature.* **451(7181)**: 1013-1017.

21. Topham M.K., Bunting M., Zimmerman G.A., McIntyre T.M., Blackshear P.J., Prescott S.M. (1998) *Nature.* **394:**697-700.

22. Freyberg Z., Sweeney D., Siddhanta A., Bourgoin S., Frohman M., Shields D. (2001) *Mol Biol Cell* **12:**943-955.

23. Evangelisti C., Riccio M., Feanza I., Zini N., Hozumi Y., Goto K., Cocco L., Martelli A.M. (2006) *J. Cell. Physiol.* **209(2)**:370-379.

24. Boronenkov I.G., Loijens J.C., Umeda M., Anderson R.A. (1998) *Mol. Biol. Cell* **9(12):**3547-3560.

25. Gozani O., Karuman P., Jones D.R., Ivanov D., Cha J., Lugovskoy A.A., Baird C.L., Zhu H., Field S.J., Lessnick S.L., Villasenor J., Mehrotra B., Chen J., Rao V.R., Brugge J.S., Ferguson C.G., Payrastre B., Myszka D.G., Cantley L.C., Wagner G., Divecha N., Prestwich G.D., Yuan J. (2003) *Cell.* **111:**99-111.

26. Barlow C.A., Laishram R.S., Anderson R.A. (2010) *Trends Cell Biol.* **20(1):**25-35.

27. Viola-Magni M.P., Gahan P.B., Albi E., Iapoce R., Gentilucci P.F. (1987) *Basic Appl. Histochem.* **31(3)**:355-364.

28. Viola-Magni M.P., Gahan P.B., Pacy J. (1985) *Cell Biochem. Funct.* **3(1)**:71-78.

29. Albi E., Micheli M., Viola-Magni M.P. (1996) *Cell Biol. Int.* **20(6)**:407-412.

30. Echevarria W., Leite M.F., Guerra M.T., Zipfel W.R., Nathanson M.H. (2003) *Nat. Cell Biol.* **5:**440-446.

31. Fricker M., Hollinshead M., White N., Vaux D. (1997) *J. Cell Biol.* **136(3):**531-544.

32. Raben, D.M., Tu-sekine, B. (2008) *Front Biosci*.**13**:590-597.

33. Jones D.R., D'Santos C.S., Merida I., Divecha N. (2002) *Int. J. Biochem. Cell Biol.* **34(2):**158-168.

34. Gorski S.A., Dundr M., Misteli T. (2006) *Cur. Opin. Cell Biol.* **18(3)**:284-290.

35. Strickfaden H., Zunhammer A., van Koningsbruggen S. Kohler D., Cremer T. (2010) *Nucleus* **1(3)**:284-297.

36. Chasserot-Golaz S., Coorssen J.R., Meunier F.A., Vitale N. (2010) *Cell Mol. Neurobiol.* **30(8)**:1335-1342.

37. Irvine R.F. (2005) *J. Physiol.* **566(2)**:295-300.

38. Gonzales M.L., Anderson R.A. (2006) *J. Cell Biochem.* **97(2)**:252-260.

39. Smith C.D., Wells W.W. (1983) J. Biol. Chem. 258(15): 9360-9367.

40. Smith C.D., Wells W.W. (1983) J. Biol. Chem. 258(15): 9368-9373.

41. Cocco L., Gilmour R.S., Ognibene A., Letcher A.J., Manzoli F.A., Irvine R.F. (1987) *Biochem. J.* **248:**765-770.

42. Divecha N., Banfic H., Irvine R.F. (1991) *EMBO J.* **10(11)**:3207-3214.

43. Marteli A.M., Tabellini G., Bortul R., Manzoli L., Bareggi R., Baldini G., Grill V., Zweyer M., Narducci P., Cocco L. (2000) *Cancer Res.* **60(4)**:815-821.

44. Marteli A.M., Manzoli L., Feanza I., Bortul R., Billi A., Cocco L. (2002) *Biochim. Biophys. Acta* **1603(1)**:11-17.

45. Kakuk A., Friedlander E., Vereb G. Jr., Lisboa D., Begossi P., Toth G., Gergely P., Vereb G. (2008) *Exp. Cell Res.* **314(13)**:2376-2388.

46. D'Santos C.S., Clarke J.H., Divecha N., Irvine R.F. (1999) *Cur. Biol.* **9(8)**:437-441.

47. Cocco L., Faenza I., Follo M.Y., Billi A.M., Ramazzotti G., Papa V., Marteli A.M., Manzoli L. (2009) *Adv. Enzyme Regul.* **49(1)**:2-10.

48. Hunt A.N., Alb J.G., Koster G., Postle A.D., Bainkaitis B.A. (2004) *Biochem. Soc. Trans.* **32(6)**:1063-1065.

49. Cocco L., Martelli A.M., Fiume R., Faenza I., Billi A.M., Manzoli F.A. (2006) *Advan. Enzyme Regul.* **46:**2-11.

50. Vann L.R., Wooding F.B., Irvine R.F., Divecha N. (1997) *Biochem. J.* **327(Part 2)**:569-576.

51. Rubbini S., Cocco L., Manzoli L., Lutterman J., Billi A.M., Matteucci A., Wirtz K.W.A. (1997) *Biochem. Biophys. Res. Commun.* **230:**302-305.

52. Ragnarson B., Bengtsson L., Haegerstrand A. (1991) *Histochem.* **97**:329-333.

53. Genicot G., Leroy J.L.M.R., Van Soon A., Donnay I. (2005) *Theriogen.* **63**:1181-1194.

54. Monserrate J.P., York J.D. (2010) *Curr. Opin. Cell. Biol.***22:**365-373.

55. Barlow C.A., Laishram R.S., Anderson R.A. (2010) *Trends Cell Biol.* **20(1):**25-35.

56. Albi E., Viola-Magni M.P. (2004) *Biol. Cell.* **96(8):**657-667.

57. Martelli A.M., Gilmour R.S., Bertagnolo V., Neri L.M., Manzoli L., Cocco L. (1992) *Nature*. **358(6383):**242-245.

58. Albi E., Viola Magni M. (1994) *Lipids*. **29(10):**715-719.

59. Divecha N., Letcher A.J., Banfic H.H., Rhee S.G., Irvine R.F. (1995) *Biochem. J.* **312(1):**63-67

60. Wang Y., Sweitzer T. D., Weinhold P. A., Kent C. (1993) *J. Biol. Chem.* **268:**5899–5904.

61. Divecha N., Rhee S.G., Lechter A.J., Irvine R.F. (1993) *Biochem. J.* **289:**617-620.

62. Gonzales M.L., Mellman D.L., Anderson R.A. (2008) *J Biol. Chem*. **283(18):**12665-12673.

63. Shay J.W., Wright W.E. (1989) *Exp. Cell Research.* **184(1):**109-118.

64. Bligh E.G., Dyer W.J. (1959) *Can. J. Biochem. Physiol.* **37:**911-917.

65. Ivanova, P.T., Milne S.B., Byrne M.O., Xiang Y., Brown H.A. (2007) *Meth. Enzymology.* **432:** 21-57.

66. Milne S., Ivanova P., Forrester J., Brown H.A. (2006) *Methods*. **39:**92-103.

67. Manzoli L., Billi A.M., Gilmour R.S., Martelli A.M., Matteucci A., Rubbini S., Weber G., Cocco L. (1995) *Cancer Res.* **55:**2978-2980.

68. Phair R.D., Misteli T. (2000) *Nature.* **404:**604-609.

69. Misteli T. (2005) *BioEssays.* **27:**477-487.

70. Rossi G., Magni M.V., Albi E. (2007). *Arch. Biochem. Biophys.* **459:**27-32.

71. Rossi G., Viola-Magni M., Albi E. (2007) *Arch. Biochem. Biophys.* **464:**138-143.

72. Albi E., Lazzarini R., Viola Magni M. (2008). *Biochem. J.* **410:**381-389.

73. Mortier E. Wuytens G. Leenaerts I., Hannes F., Heung M.Y., Degeest G., David G., Zimmermann P. (2005) *EMBO J.* 24(14):2556-2565.

74. Tamiya-Koizumi K., Umekawa H., Yoshida S., and Kojima K. (1989). *J. Biochem.* **103:**593-598.

75. Alessanko A., Chattergee S. (1995) *Mol. Cell.Biochem.***143(2)**:169-174.

76. Neitcheva, T. and Peeva, D. (1995). *Int. J. Biochem. Cell Biol.* **27:**995-1001.

77. Tsugane K., Tamiya-Koizumi K., Nagino M., Nimura Y., Yoshida S. (1999) *J. Hepatol.* **31(1):**8-17.

78. Albi, E. and Viola Magni, M. P. (1999). *FEBS letters.* **460:**369-372.

79. Mizutani Y, Tamiya-Koizumi K, Nakamura N, Kobayashi M, Hirabayashi Y, Yoshida S. (2001) *J. Cell Sci.* **114(20):**3727-36.

80. Albi, E., Pieroni, S., Viola Magni, M. P. and Sartori, C (2003) *J. Cell. Physiol.***196:**354-361.

81. Cocco L, Faenza I, Follo MY, Billi AM, Ramazzotti G, Papa V, Martelli AM, Manzoli L. (2009) *Adv Enzyme Regul*. **49**(1):2-10.

82. Ile KE, Schaaf G, Bankaitis VA (2006) *Nat Chem Biol* **2**(11):576-83.

83. Schaaf G, Ortlund EA, Tyeryar KR, Mousley CJ, Ile KE, Garrett TA, Ren J, Woolls MJ, Raetz CR, Redinbo MR, Bankaitis VA. Mol Cell. 2008 Feb 1;29(2):191-206.

84. De Vries KJ, Westerman J, Bastiaens PI, Jovin TM, Wirtz KW, Snoek GT.

Exp Cell Res. 1996 Aug 25;227(1):33-9.

85. Phillips SE, Ile KE, Boukhelifa M, Huijbregts RP, Bankaitis VA.Mol Biol Cell. 2006 Jun;17(6):2498-512

86. Morgan CP, Skippen A, Segui B, Ball A, Allen-Baume V, Larijani B, Murray-Rust J, McDonald N, Sapkota G, Morrice N, Cockcroft S. (2004) *J Biol Chem*. **279**(45):47159-71.

87. Gordon GW, Chazotte B, Wang XF, Herman B (1995) *Biophys J*. **68**(3):766-78

88. Von Willebrand M, Jascur T, Bonnefoy-Bérard N, Yano H, Altman A, Matsuda Y, Mustelin T. (1996) *Eur J Biochem*. **235**(3):828-35

89. Alb JG Jr, Gedvilaite A, Cartee RT, Skinner HB, Bankaitis VA.Proc Natl Acad Sci U S A. 1995 Sep 12;92(19):8826-30.

90. Yoder MD, Thomas LM, Tremblay JM, Oliver RL, Yarbrough LR, Helmkamp GM Jr. (2001) *J Biol Chem*. **276**(12):9246-52.

91. Tilley SJ, Skippen A, Murray-Rust J, Swigart PM, Stewart A, Morgan CP, Cockcroft S, McDonald NQ. (2004) *Structure*. **12**(2):317-26.

92. Alb JG Jr, Phillips SE, Wilfley LR, Philpot BD, Bankaitis VA. (2007) *J Lipid Res*. **48**(8):1857-72.

93. Stevenson-Paulik J, Chiou ST, Frederick JP, dela Cruz J, Seeds AM, Otto JC, York JD. (2006) *Methods*.**39**(2):112-21.

94. Hancock R., Hadj-Sahraoui Y. (2009) *PLoS One* **4(10)**:e7560.

95. Schnell S., Hancock R. (2008) *Methods Mol. Biol.* **463**:3-19.